NOTICE

The quality of this microform is heavily dependent upon the quality of the original thesis submitted for microfilming. Every effort has been made to ensure the highest quality of reproduction possible.

If pages are missing, contact the university which granted the degree.

Some pages may have indistinct print especially if the original pages were typed with a poor typewriter ribbon or if the university sent us an inferior photocopy.

Reproduction in full or in part of this microform is governed by the Canadian Copyright Act, R.S.C. 1970, c. C-30, and subsequent amendments.

AVIS

La qualité de cette microforme dépend grandement de la qualité de la thèse soumise au microfilmage. Nous avons tout fait pour assurer une qualité supérieure de reproduction.

S'il manque des pages, veuillez communiquer avec l'université qui a conféré le grade.

La qualité d'impression de certaines pages peut laisser à désirer, surtout si les pages originales ont été dactylographiées à l'aide d'un ruban usé ou si l'université nous a fait parvenir une photocopie de qualité inférieure.

La reproduction, même partielle, de cette microforme est soumise à la Loi canadienne sur le droit d'auteur, SRC 1970, c. C-30, et ses amendements subséquents.

UNIVERSITY OF ALBERTA

THE CYTOSKELETON AND A CELL ADHESION MOLECULE IN NEWT LENS REGENERATION

BY

YUEQING YANG

A THESIS

SUBMITTED TO THE FACULTY OF GRADUATE STUDIES AND RESEARCH IN PARTIAL FULFILLMENT OF THE REQUIREMENTS FOR THE DEGREE OF MASTER OF SCIENCE

DEPARTMENT OF ZOOLOGY

EDMONTON, ALBERTA. CANADA.
SPRING, 1992

ISBN 0-315-73106-0

UNIVERSITY OF ALBERTA

RELEASE FORM

NAME OF AUTHER: YANG YUE-QING

TITLE OF THESIS: THE CYTOSKELETON AND A CELL ADHESION MOLECULE IN NEWT LENS REGENERATION

DEGREE: MASTER OF SCIENCE

YEAR THIS DEGREE GRANTED: SPRING, 1992.

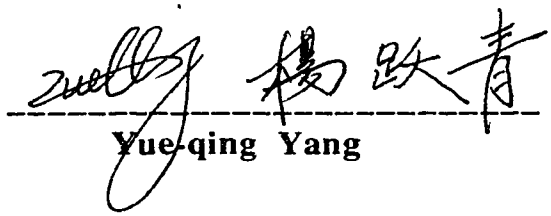

Yue-qing Yang

April 13, 1992.

UNIVERSITY OF ALBERTA

FACULTY OF GRADUATE STUDIES AND RESEARCH

The undersigned certify that they have read, and recommend to the Faculty of Graduate Studies and Research for acceptance, a thesis entitled THE CYTOSKELETON AND A CELL ADHESION MOLECULE IN NEWT LENS REGENERATION submitted by YUE-QING YANG in partial fulfillment of the requirements for the degree of MASTER OF SCIENCE in the FIELD OF DEVELOPMENTAL BIOLOGY.

Supervisor: Dr. SARA E. ZALIK

Committee Member:
Dr. ESMOND J. SANDERS

Committee Member:
Dr. WARREN GALLIN

Chairman and Examiner:
Dr. SUDARSHAN K. MALHOTRA

April 14, 1992.

DEDICATION

Dedicated to the faint stars of the night sky.

ABSTRACT

Lens regeneration in the newt *Notophthalmus viridescens* represents a unique case of cell-type conversion in which the pigmented epithelial cells of the dorsal iris dedifferentiate and transform into lens cells. I studied the cytoskeleton and its changes during lens regeneration in flat mount preparations and serial sections of iris rings, using labeled phalloidin and a number of monoclonal antibodies specific for actin and cytokeratin isoforms. The actin-associated cell surface molecule A-CAM or N-cadherin was also studied. Flat mount iris preparations stained with labelled-phalloidin display three main regions: the pupillary (P), the middle (M) and the more external junctional (J) ring. On the basis of the organization of the cytoskeleton and their reactivity with antibodies that react with specific actin and cytokeratin isoforms, the pigmented epithelial cells of the P-ring have now been defined as pigmented myoepithelial cells. Since these cells are the ones that regenerate a lens, the above mentioned finding suggests a possible relationship between the expression of the myoepithelial phenotype and the ability of cells to undergo cell type conversion.

In all iris epithelial cells, F-actin,vinculin and A-CAM colocalize in areas of cell to cell and cell to extracellular matrix contacts suggesting that, in this system, A-CAM in addition to mediating cell to cell adhesion may mediate cell adhesion to the extracellular matrix. During dedifferentiation, actin staining increases considerably as the actin filament bundles (AFBs) thicken, branch, shorten and become preferentially condensed in the basal and apical regions of the cells. These are sites where cells emit and shed cytoplasmic projections for depigmentation. A-CAM is preferentially reduced or eliminated from these sites while colocalization of actin, vinculin and A-CAM is maintained at the mid-lateral region of the cells. During redifferentiation AFBs are reorganized and are preferentially enriched in the basal and apical regions of the elongating lens fibers. A-CAM and vinculin

disappear in the redifferentiating lens fiber. Cytokeratin II is also organized as longitudinal fibers along the longitudinal axis of the cells of the P-ring, and increases during dedifferentiation when it is present as a thick band surrounding the nuclei. Its expression is repressed during lens fiber formation, but is retained in the mitotic cells of the lens stalk and lens epithelium. Results suggest that the expression of these cytoskeletal proteins is differentially regulated during cell type conversion.

ACKNOWLEDGMENTS

I would like to thank my supervisor, Dr. Sara E. Zalik for her concern, encouragement and counsel during these years of study. Her serious, methodical and meticulous approach to science and her honest personality were greatly appreciated.

I am also grateful to Mrs. Irene Ledsham and Mrs. Eva Dimitrov, for their friendly technical advice and assistance.

I wish to acknowledge Dr. E. J. Sanders and Dr. W. Gallin for their critical advice and kind support.

This research was funded by grants from the National Science and Engineering Research Council of Canada to Dr. S. E. Zalik.

TABLE OF CONTENTS

LIST OF FIGURES

LIST OF TABLES

CHAPTER 1. GENERAL INTRODUCTION

1.1. ANATOMY OF THE NEWT EYE

1.1. A. Historical review of studies of lens regeneration

Lens regeneration is an important phenomenon to developmental biologists since it represents a unique, well regulated process of transdifferentiation or cell-type conversion of the adult somatic cell *in situ*. This phenomenon was first noticed early in the 18th century (Bonnet 1781, Blumenbach 1787 as cited by Yamada 1977), and its histology was investigated during the late 19th and early 20th centuries (Colucci 1891, Wolff 1895, 1901, 1903 as cited by Yamada 1977). Through these histological studies, it was found that the regenerated lens was derived from the iris epithelium at the inner border of the dorsal iris, and that this regenerative process involved cell proliferation and depigmentation of the pigmented epithelial cells. In recognition of these fundamental histological studies, this phenomena has been traditionally named "Wolffian lens regeneration". During the middle of the 20th century, cytochemical and autoradiographic studies were conducted revealing an increase in the activity of several tissue enzymes, in the synthesis of DNA, RNA and proteins, and in the synthesis of lens specific proteins in the regenerating iris tissues (reviewed by Yamada 1967b, 1977). Meanwhile, the methodology for *in vitro* culture of the iris was developed and was applied extensively in a variety of studies (reviewed by Yamada 1977). Subsequently, electron microscope studies elucidated ultrastructural changes of the iris cells during lens regeneration, these studies indicated that microfilaments increased during the dedifferentiation phase of lens regeneration (Karasaki 1964, Dumont and Yamada 1972, Reyer 1990a).

Eighteen species of urodeles had been demonstrated to possess the capacity for lens regeneration from the dorsal iris (Stone 1967). Among those species, *Notophthalmus viridescens* has been studied extensively, as a result of these studies a well established staging system was developed, and information on the anatomy of the eye during lens regeneration has been documented in this species (Reyer 1977, Yamada 1977).

1.1. B. Anatomy of the newt eye

A schematic representation of the newt eye is shown in Figure 1-1. This organ is composed, from the anterior to posterior regions, of the cornea (C), the iris-ciliary ring (IC), the lens (L), the zonular fibers (zf), the retina (R), the choroid (ch) and the sclera (sc). The lens, the zonular fibers, and the iris and the associated ciliary body divide the eye chamber into three distinct regions, the anterior chamber, the posterior chamber and the vitreous body (AC, PC and VB respectively). The anterior and posterior chambers are filled with aqueous humour. The vitreous body is occupied by an acellular matrix of glycosaminoglycans and type II collagen which are secreted by the neural retina, the ciliary and iris epithelial cells. In newts, the lens is large in proportion to the size of the eye. This nearly spherical lens is composed of a quantity of lens fibers and of a single layer of lens epithelium which covers the anterior and equatorial region of the lens. The slender and elongated lens fibers are tightly packed concentrically around a central core or nucleus of lens. The primary lens fibers in the central core develop from the lens vesicle during embryogenesis, while the secondary lens fibers in the more peripheral regions of the lens are derived from the lens epithelium which gradually differentiates into lens fibers. The entire surface of the lens is covered by an amorphous basement membrane, the lens capsule (Reyer 1977).

Other structures that constitute the wall of eye are developed from three layers of different tissues, the tunica fibrosa, tunica vasculosa and tunica interna (Reyer 1977).

Figure 1. 1. Schematic illustration of the eye of the newt, Notophthalmus viridescens, as seen in a medial sagittal section (Adopted from Reyer, 1977).

Abbreviations:

AC	anterior chamber
C	cornea
IC	iris-ciliary ring
IEC	iris epithelial cell (also called iris pigmented epithelial cell, iris PEC)
IS	iris stroma
R	retina
L	lens
P	pupil
PC	posterior chamber
VB	vitreous body
ce	corneal epithelium
cs	corneal stroma
ch	choroid
cie	ciliary epithelium
cis	stroma of ciliary body
el	eyelid
gc	ganglion cell layer of neural retina
in	inner nuclear layer of neural retina
ip	inner plexiform layer of neural retina
lc	lens capsule
le	lens epithelium
lf	lens fibers
on	outer layer of neural retina
ont	optic nerve tract
op	outer plexiform layer of neural retina
pr	pigmented retina
rc	layer of rods and cones of the neural retina
sc	sclera
vf	ventral fold of ciliary body
zf	zonular fibers

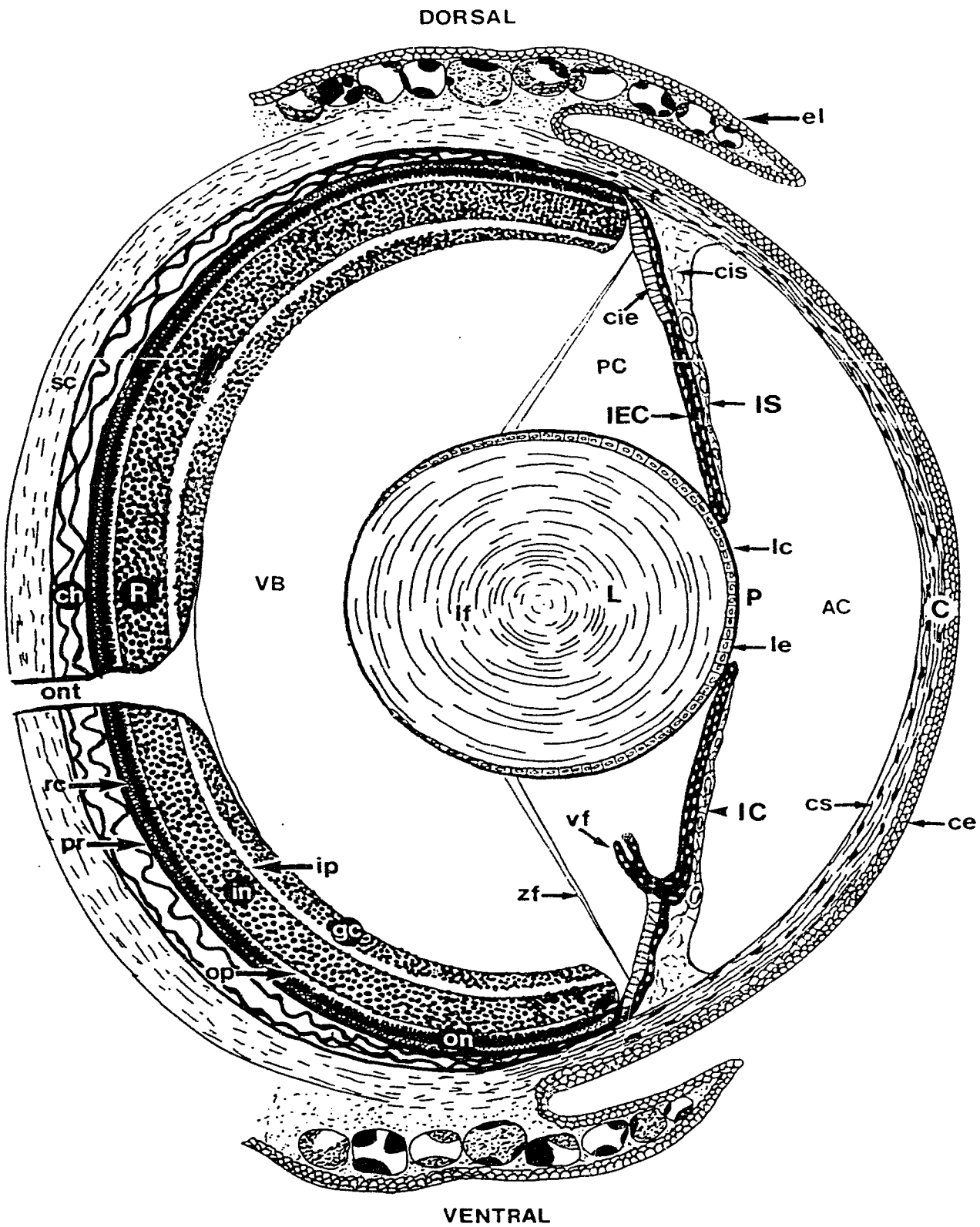
DORSAL
el
cis
cie
PC
IEC
IS
sc
lc
VB
L
lf
P
AC
C
ch
R
le
ont
rc
IC
cs
ce
vf
pr
ip
in
zf
gc
op
on
VENTRAL

The tunica fibrosa, the most external layer of eye, is a layer of fibrous connective tissue which forms the sclera in the posterior region, and the substantia propria of cornea in the anterior region of eye. In the cornea, the substantia propria is covered by a multi-layered epithelium. The tunica vasculosa is a layer of loose connective tissue located in between the external fibrous tunica and the internal tunica of eye. It constitutes the vascularized choroid in the posterior, and the vascularized stroma of the ciliary body and the iris (IS) in the anterior region of eye. The tunica interna, the most internal layer of eyeball, is a double layered epithelial tissue. Posteriorly, the double layered epithelium forms the external pigmented retina and the internal neural retina. This double layered epithelium is continuous anteriorly with the ring shaped ciliary epithelium which, in turn, joins the ring-shaped iris epithelium (figure 1.1, IC). The epithelium of the pigmented retina, the external ciliary epithelial cells and the two layers of the iris epithelium have a cytoplasm which is rich in melanosomes (Achazi and Yamada 1972).

The double layered tunica interna arises from the neural ectoderm of the embryonic optic vesicle, an expansion of the diencephalon. With the infolding of the optic vesicle to form optic cup, the optic cup becomes a double layered structure. The rim of the optic cup gives rise to the iris which encloses the opening of the cup at the anterior region of eye, this opening is called the pupil. Therefore, the two layers of the iris epithelium are continuous at the edge of the pupil while they face each other at their apical surfaces and are covered by a thin extracellular matrix (ECM) membrane at their basal surfaces (figure 1-2).

The epithelial cells of the iris are continuous with the epithelial cells of the ciliary body. Both of these are covered by a vascularized stroma and together they form the iris-ciliary ring (IC in figure 1-1). The stroma of the iris and of the ciliary body adheres to the basal surface of the external layer of the iridal and the ciliary epithelium; this stromal surface faces the anterior chamber (figure 1-1, 1-2). The ciliary epithelium and the lens are connected by the zonular fibers, the latter adhere to the lens capsule and suspend the lens.

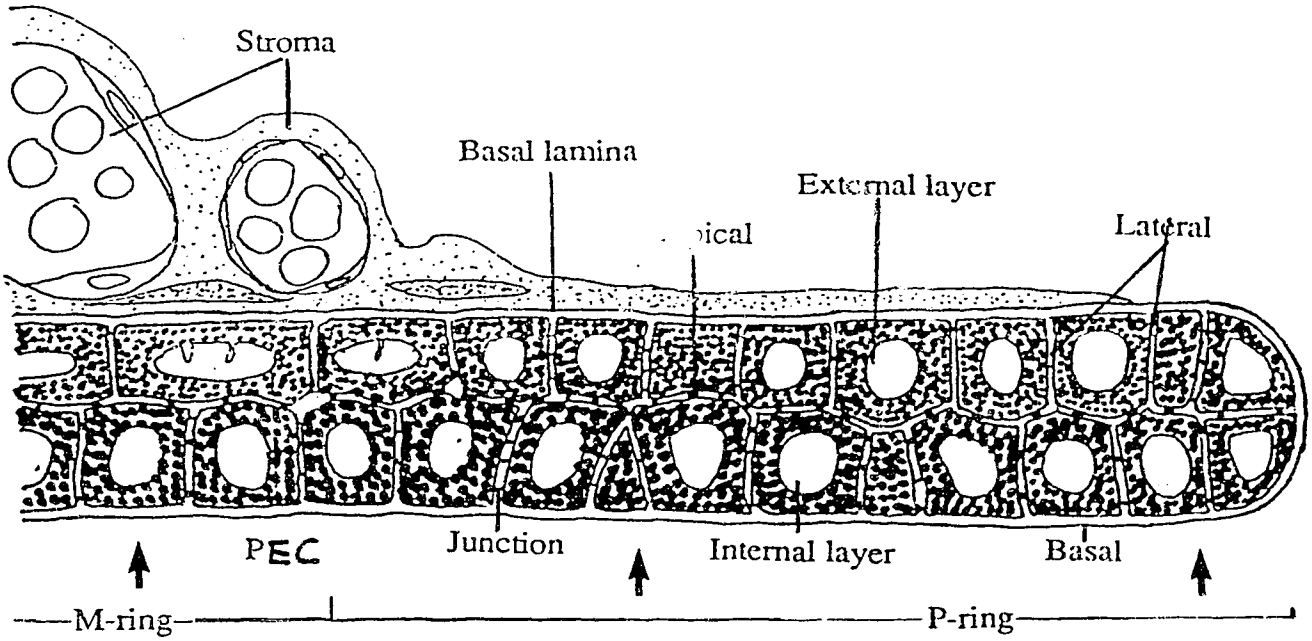

Figure 1. 2. Schematic illustration of a medial sagittal section of the dorsal iris ring showing the basal, lateral and apical compartments of the two layers of the iris epithelium. At the basal compartment the cells contact the basal lamina.

Located within the stroma of the iris are the iridal blood vessels, green iridophores, yellow or red xanthophores and melanophores, these cells give the characteristic pattern of pigmentation to the iris stroma. According to Reyer (1977), the newt iris like that of mammals, has smooth muscle fibers that form the circumferentially oriented sphincter and radial oriented dilator muscles of the pupil, muscles that contract and dilate the pupil respectively.

1. 2. SEQUENCE OF EVENTS DURING LENS REGENERATION

Triggered by lentectomy, newt lens regeneration involves sequential processes of cell dedifferentiation and redifferentiation. Although these processes are continuous during regeneration, for convenience and comparison purposes between different urodele species that regenerate a lens, lens regeneration has been divided into 11 stages in *N. viridescens;* cell dedifferentiation occurs during stages 1-4, while cell redifferentiation takes place during stages 5-10 (Yamada 1967b, Yamada 1977, adopted from Sato 1940). The morphological changes of the dorsal iris epithelial cells during the different stages of lens regeneration are shown in figure 1-3.

Normal iris

The structure of the normal iris has been described above. This structure is composed of a bilayered epithelium covered by an iris stroma at its external surface. In the iris epithelium, the internal and external layers are tightly apposed at their apical surfaces and, within each layer, adjacent cells are tightly apposed at their lateral surfaces. In sagittal sections the epithelial cells in the pupillary margin appear cuboidal in shape, while those peripheral to this area are rectangular (see chapter-2). At the apical and lateral regions, the epithelial cells are joined to each other by zonulae adherentia, desmosomes and gap

Figure 1. 3. Diagram of lens regeneration in adult newt, *N. viridescens*.

The process is divided into 11 stages according to Yamada (1977). Each figure represents a medial sagittal section of the dorsal iris. The pigmented, partially depigmented and completely depigmented iris cells in the figure are shown in black, black dots and white respectively.

Normal

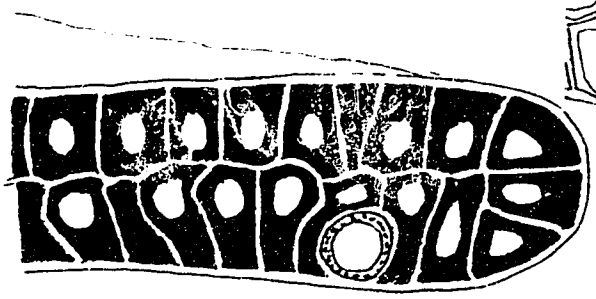

Stage 1-2

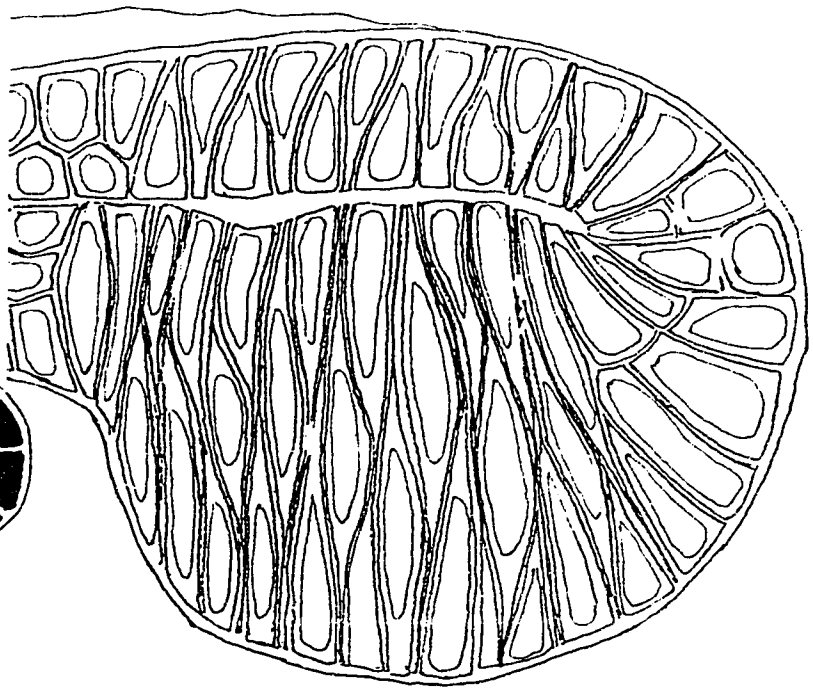

Stage 7-8

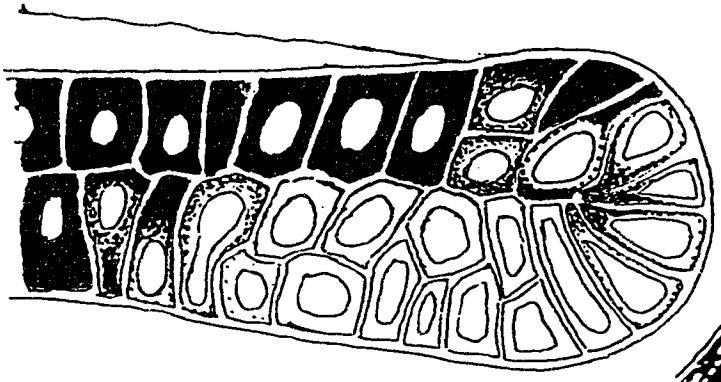

Stage 3

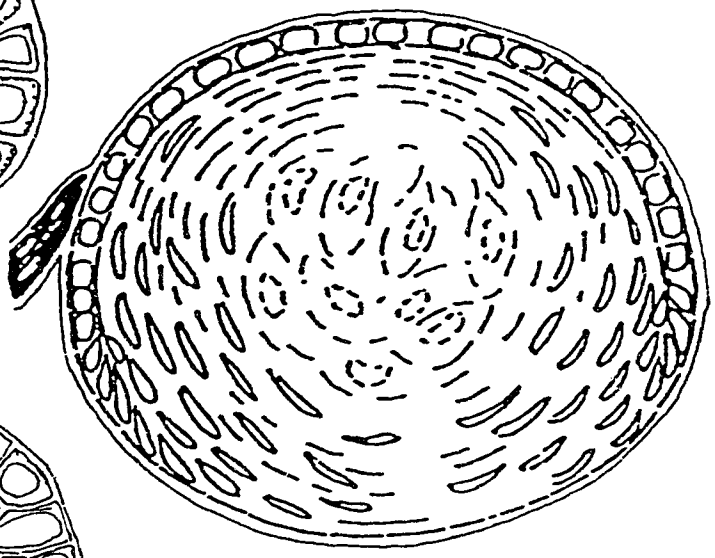

Stage 11

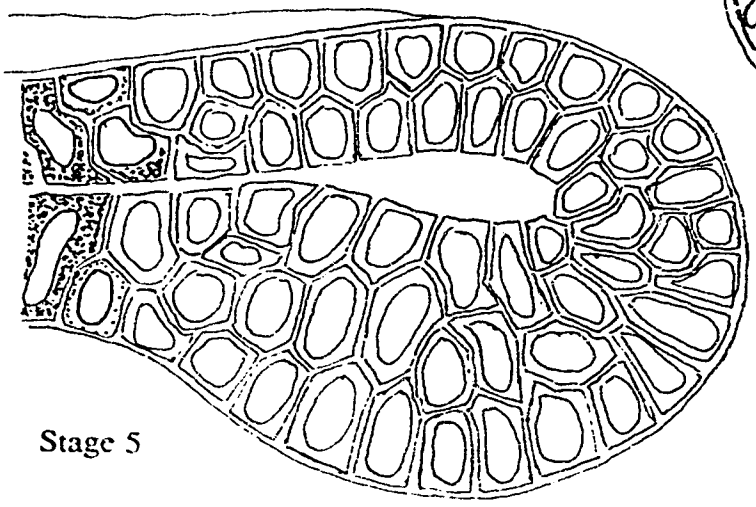

Stage 5

junctions (Karasaki 1964, Dumont and Yamada 1972), while at the basal surfaces these cells rest on a basal lamina, that contains fibronectin (Elgert and Zalik 1989). The cytoplasm of the iris epithelial cells contains numerous melanosomes. The melanosomes in the internal iris epithelium are spherical in shape, those of the external iris epithelium are ellipsoidal and smaller than those of the internal layer (Eguchi 1963, Karasaki 1964). Cells contain irregular contoured nuclei with one or more nucleoli and numerous clumps of heterochromatin (Dumont et al. 1970, Reyer 1990a). In these cells, the population of cytoplasmic organelles is sparse; however, microtubules and microfilaments are clearly distinguishable. Studies using autoradiography have shown that these cells have low levels of protein synthesis and are mitotically quiescent. Because of this, the cells of the iris epithelium are thought to be fully differentiated stable somatic cells (Yamada 1977).

Stage 1. Cell activation

This stage occurs at 1 to 4 days after lentectomy. Cells elongate along their apico-basal axis; this is probably induced by the relaxation of the iris around the pupil caused by lentectomy and by cell growth. During cell growth at this stage, the cell structures involved in cell to cell contact remain intact in most regions of the cells (Karasaki 1964, Dumont & Yamada 1972, Reyer 1990a). Intracellularly, the nucleus and the nucleoli enlarge, the latter increase their granular component, which is accompanied by an increase in cytoplasmic ribosomes (Eguchi 1963, Karasaki 1964, Dumont et al. 1970). Associated with the above changes, there is an increase in the synthesis of ribosomal and heterogeneous nuclear RNA indicating an activation of synthetic activities (Yamada and Karasaki 1963, Reese et al. 1969, Reese 1977). These changes are followed by DNA replication and initiation of cell proliferation at the end of stage 1 (Eisenberg and Yamada 1966, Yamada and Roesel 1969, 1971, Eguchi and Shingai 1971).

Stage 2. Cell proliferation and depigmentation

This stage occurs in regenerates at 6 to 10 days after lens removal. Cell growth continues and there is a 3 to 5 fold increase in the cytoplasmic and nuclear volume, which takes place along with cell depigmentation and proliferation. The nucleus continues to enlarge and the nucleoli also increase in size and numbers, cytoplasmic organelles such as mitochondria, endoplasmic reticulum, Golgi complex and mitochondria become more abundant (Eguchi 1963, Karasaki 1964, Dumont and Yamada 1972, Reyer 1990a). The synthesis of DNA, RNA and protein increase considerably, and the first wave of cell proliferation occurs at this stage.

Also during this stage, the dedifferentiating cells extend pseudopodia-like cytoplasmic processes at their basal surfaces, the intercellular space increases at the lateral and basal regions of the cells and the intercellular junctions decrease (Dumont and Yamada 1972). This occurs parallel to an invasion by macrophages that migrate from the stroma; this migration is also associated with a focal disruption of the basal lamina (Dumont & Yamada 1972, Reyer 1990 a,b). Associated with these changes is the occurrence of depigmentation via cytoplasmic shedding. This comes about via the emission of cytoplasmic protrusions at the peripheral regions of the epithelial cells. Here, the melanosomes become sequestered into these pseudopodial projections that also contain microtubules, microfilaments and mitochondria. The melanosome-containing cytoplasmic protrusions are either engulfed directly by macrophages or become disconnected from the cell body to be phagocytosed later by the macrophages. Subsequently, macrophages migrate back to the iris stroma carrying the engulfed material. Cytoplasmic shedding results in loss of cytoplasm from the depigmenting cells and also brings about pronounced changes in cell shape (figure 1-4) (Dumont and Yamada 1972, Reyer 1990a,b).

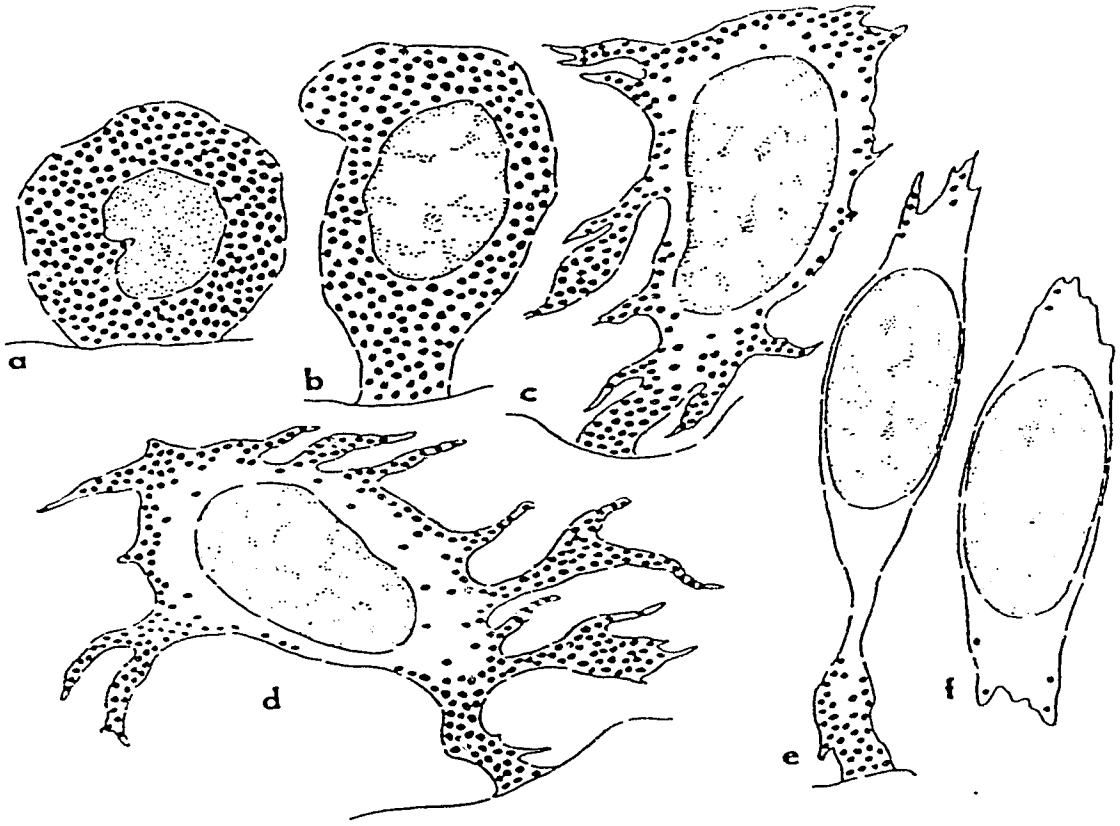

Figure 1. 4. Schematic illustration of changes in cell morphology of marginal dorsal iris epithelial cells during depigmentation.

a, normal; b, 4 days after lentectomy (stage 1-2); c and d, 8 days (stage 2) showing the depigmenting cells with cytoplasmic projections; e, 13 days (stage 3) showing the barely depigmented cell; f, 15 days (stage 4) showing the depigmented cell. The basement membrane is indicated by a curved line and marks the basal end of the cells (Adopted from Dumont & Yamada 1972).

Stage 3. Appearance of completely depigmented cells

This stage occurs in regenerates at 8 to 11 days after lentectomy. As a result of metabolic events, proliferation and depigmentation, completely depigmented cells appear in the mid-dorsal pupillary margin of the internal iris epithelium. Flanking these cells is a population of partially depigmented cells which, in turn, is surrounded by cells at the initial stages of activation. At this stage the external iris epithelium is composed of partially depigmented as well as recently activated cells. Because the cells in different regions of the pupillary iris proceed through the dedifferentiation process at different speeds, regenerates are composed of different cell populations at different phases of dedifferentiation in which one population predominates.

The partially and completely depigmented cells, although reduced in cytoplasmic volume, have a cytoplasm rich in organelles (Reyer 1990a). The nucleus remains enlarged and the nucleoli are increased in volume with an enlarged fibro-granular component indicating active synthetic activity (Karasaki 1964). The iris epithelium at this stage has an increased number of macrophages which penetrate the basement membrane through which the cytoplasmic projections of the iris epithelial cells continue to penetrate (Reyer 1990a).

Stage 4. Formation of lens vesicle

This stage occurs in regenerates at 9 to 15 days after lens removal. At this stage the lens vesicle is evident. This structure is made up of depigmented and dedifferentiated cells contributed by the internal and external iris epithelium at the mid-dorsal central region of the iris. Immediately lateral and dorsal to this vesicle, are cells that are partially depigmented and that are continuous with the main body of the iris, this region is called the lens stalk and connects the lens vesicle with the iris. After the cells of the lens stalk accomplish depigmentation, they are incorporated into the lens vesicle. Also at the later phase of this

stage a second wave of DNA synthesis and mitosis occurs in the dedifferentiating cells (Eguchi and Shingai 1971, Yamada and Roesel 1971)

Stage 5. Active cell proliferation. Synthesis of lens specific proteins

This stage occurs in regenerates at 12 to 15 days after lentectomy. The lens vesicle enlarges through proliferation of dedifferentiated cells and through incorporation of dedifferentiated cells from the lens stalk. As a consequence, the cell population of the lens vesicle increases resulting in a temporal pseudostratification of the cells of the lens vesicle which is particularly prominent in the internal layer (see chapter-3). These events cause the enlargement of the lens vesicle within the pupillary space. The most central cells of the inner layer of the lens vesicle, cease cell division and start to synthesize the lens-specific proteins, the γ and β crystallins (Takata et al. 1964 a,b, 1966, Yamada and McDevitt 1974). The synthesis of these proteins starts first in the central cells of the lens vesicle and subsequently, spreads peripherally to neighboring cells. In other regions of the lens vesicle, cell proliferation and macrophage activity remain high.

Stage 6. Onset of lens fiber differentiation

This stage occurs in regenerates harvested at 12 to 16 days after lentectomy. Lens fiber differentiation occurs in cells of the internal layer of the lens vesicle. After withdrawing from the cell cycle, these cells elongate along their apico-basal axis, continue synthesis of γ and β crystallins and start to differentiate into primary lens fibers. As cells elongate, the nuclei become ellipsoidal in shape and mitochondria and microtubules organize along the long axes of the cells (Eguchi 1964, Hornsby and Zalik 1977). Compared to the normal iris, the level of protein synthesis is increased ten fold at this stage (Yamada and Takata 1963, Takata et al. 1964 a,b). As more cells of the internal lens epithelium elongate into lens fibers, the pseudostratification of the internal layer of the lens epithelium gradually disappears. Cells of the lens stalk continue to proliferate and are

gradually incorporated into the lens vesicle. This results in continuous growth of the lens vesicle.

Stage 7. Formation of the primary lens fiber complex

The progressive differentiation into lens fibers of the internal cells of the lens vesicle results in the formation of the primary lens fiber complex which will become the nucleus of the lens. These cells are in close apposition to each other and their intracellular organelles undergo degeneration (Yamada 1967b). The cells in the external layer of the lens vesicle and in the lens stalk retain a cuboidal cell shape and continue to undergo mitosis. Those cells located in the peripheral region of the dorsal iris epithelium, i.e, surrounding the nascent lens and the lens stalk enter the retrieval pathway in which they will repigment and reconstruct the original iris architecture.

Stage 8. Appearance of the secondary lens fibers

This stage occurs in regenerates harvested 15 to 19 days after lentectomy. Cells at the periphery of the primary lens fiber complex, cease cell division, elongate, synthesize γ and β crystallins and form secondary lens fibers. The lens vesicle of stage 8 regenerates is formed mainly by non-dividing elongated primary lens fibers, surrounded by a population of elongating secondary lens fibers. The latter cell group is surrounded by a group of cuboidal cells that are still undergoing mitosis. At this stage cells of the external layer of the lens vesicle start to produce β crystallins.

Stage 9. Differentiation of the lens epithelium

This stage occurs in regenerates harvested 18 to 20 days after lentectomy. The lens fiber complex continues to increase in size through the addition of newly differentiating secondary lens fibers (Yamada 1967b). In the primary lens fibers nuclear and organelle degeneration continues and α crystallin appears in the lens fiber complex in addition to β

and γ crystallins. The cells located in the external layer and at the periphery of the internal layer of the lens vesicle, flatten to become the lens epithelium. The lens epithelium synthesizes α and β crystallins but not γ crystallins and its cells cover the apical region of the cells forming the lens fiber complex (Takata et al. 1964b, 1966, McDevitt et al. 1969). The cells of the lens stalk continue to be incorporated into the lens vesicle and, as a consequence, this structure narrows down.

Stage 10. Formation of the new lens

This stage occurs in regenerates at 18 to 25 days after lens removal. Lens fiber differentiation proceeds gradually from the most central core of primary lens fibers to the outer region of secondary lens fibers resulting in a concentric arrangement of a series of fiber-like cells, an organization that resembles the mature lens. Within these fibers the nucleus and the cytoplasmic organelles are progressively degraded (Eguchi 1964). At the anterior region of this lens fiber complex, the flattening lens epithelial cells adhere to the lens fibers. The lens epithelium is still mitotically active and contributes cells to the secondary lens fibers and to the growth of the regenerated lens.

Stage 11. Maturation of the new lens

This stage is found in regenerates at 21 days after lentectomy and onwards. The newly regenerated lens has acquired the general appearance of the original lens (Fig 1-3 stage 11). The lens continues to grow through the addition of new cells at the equatorial region as a result of proliferation and differentiation of the equatorial cells of the lens epithelium. The lens stalk disappears and the lens becomes an autonomously growing organ. Within two or more months the new lens will attain the size of the original lens Yamada 1967b).

Retrieval pathway

The events described above occur in the iris epithelial cells at the dorsal pupillary margin. Most of the cells in other regions of the iris epithelium, also become activated by the process of lentectomy (Eguchi and Shingai 1971). These cells dedifferentiate and depigment partially, but they never accomplish complete depigmentation and dedifferentiation. Starting at approximately stage 7 of regeneration, these partially dedifferentiated cells enter the retrieval pathway. Cells gradually decrease proliferation and depigmentation and begin to resynthesize melanosomes to restore the original pigmented cell phenotype (Fig 1-5). While the new lens is being formed, the cells undergoing the pathway of retrieval reconstruct the original iris epithelium (Yamada 1977).

1.3. CELL BIOLOGY OF CELL-TYPE CONVERSION

1.3. A. Initiation of cell-type conversion.

Newt lens regeneration is initiated by lens removal. Experimental evidence indicates that the lens itself maintains the iris epithelium in a quiescent, non dividing state and inhibits cell type conversion. In order to exert this inhibitory influence the lens needs to be in close apposition to the iris epithelium (Eguchi 1961, Williams and Higginbotham 1975). Some experimental evidence indicates that if the lens is separated from the iris by insertion of a membrane, a new lens can form from the iris (Eguchi 1961, Stone 1966). The inhibitory influence exhibited by the lens is not mechanical in nature since, replacement of the original lens by a paraffin embedded lens or by inert objects of a similar shape and size fails to inhibit lens regeneration (Kesselyak 1936, Ikeda and Amatatu 1941, Uno 1943, Stone 1945, 1952). Some investigators have reported that fractions of lens tissue extracts, when injected into a lentectomized eye, retard lens regeneration (Smith 1965, Williams and

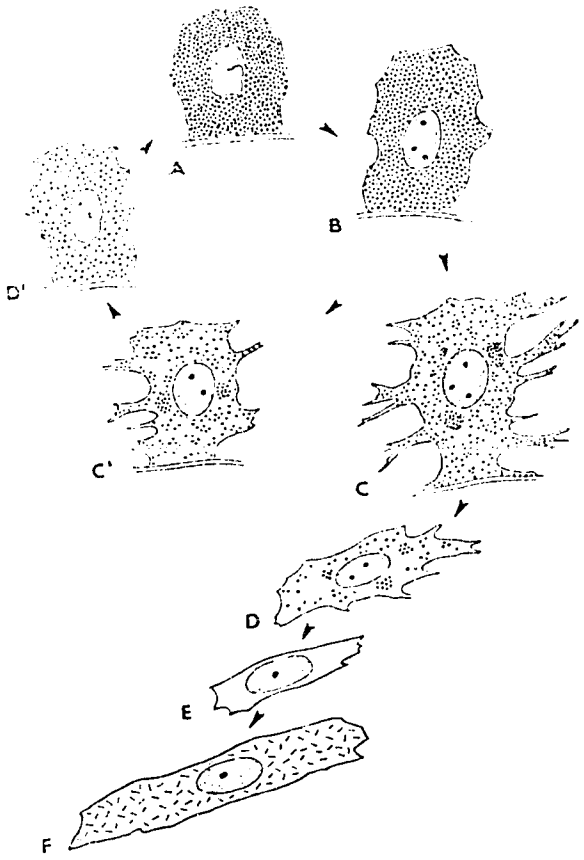

Figure 1. 5. Schematic illustration of the two pathways followed by the proliferating iris epithelial cells during cell-type conversion *in situ*.

A-B-C-D-E-F: the pathway of conversion. A-B-C'-D'-A: the pathway of retrieval. Black dots: melanosomes; short lines: crystallins (Adopted from Yamada 1977).

Reynolds 1977, Moore and Williams 1977). Other investigators have suggested that the inhibitory factors produced by the lens may be discharged into the aqueous humour (Stone and Vultee 1949, Stone 1963). Up to the present time, little is known as to the nature of these substances.

1. 3. B. Regulation of lens regeneration by hormones and growth factors.

It is believed that, in species that regenerate a lens, the capacity to undergo cell type conversion is an inherent characteristic of the iris epithelium. However, this genetically determined capacity needs an environmental stimulus to be expressed. Work from earlier investigators indicates that a factor emanating from the retina could be the stimulus for lens regeneration (Reyer 1954, 1966, Stone 1958 a, b). In a few cases it has been reported that the dorsal iris cultured in the presence of serum can produce a lens in the absence of the retina (Connelly et al. 1973). However most of the evidence indicates that a soluble factor, probably derived from the retina is required for cell type conversion *in vivo*. This factor is thought to promote regeneration by accelerating the proliferation of the iris epithelial cells since, it has been suggested that a certain number of cell divisions are required in order for cells to enter into the cell type conversion pathway (Yamada and McDevitt 1984, Yamada 1977). Several retinal factors such as eye derived growth factor II and acidic fibroblast growth factor have been shown to stimulate lens regeneration *in vitro* (Cuny et al. 1986); it is also probable that the stimulating factors are produced by other tissues since amphibian and mammalian pituitaries, spinal ganglia as well as some hormone preparations stimulate lens regeneration from the iris *in vitro* (Connely et al. 1973, Cuny and Zalik 1981, 1985, Cuny et al. 1984).

1. 3. C. Changes at the cytoskeleton, cell surface and extracellular matrix.

Previous work using cell electrophoresis indicated that during lens regeneration cell surface components, presumably negatively charged glycoproteins, disappear and reappear sequentially during dedifferentiation and redifferentiation (Zalik and Scott 1972, 1973, Zalik et al. 1976). Associated with these changes at the cell surface, are changes in the extracellular matrix which reveal that fibronectin is increased and changed in distribution from a predominant location at the basal lamina, to an homogeneous distribution around the surface of the dedifferentiated cell followed by its disappearance from the surface of the lens fiber (Elgert and Zalik 1989). As these events are occurring, the synthesis of other components of the extracellular matrix such as hyaluronic acid, chondroitin sulfate proteoglycans and heparan sulfate proteoglycans is also stimulated, reaching peak values during dedifferentiation (Kulyk and Zalik 1982, Kulyk et al. 1987). Observations on cell ultrastructure also indicate that during cell type conversion, changes in the cytoskeletal elements and the extracellular matrix take place (Dumont and Yamada 1972). Furthermore, compounds that affect microtubule polymerization also affect lens fiber formation and retard the appearance of cell surface components during redifferentiation (Hornsby and Zalik 1977). All of the above evidence indicates that profound changes at the cytoskeleton, the cell surface and the extracellular matrix occur during lens regeneration.

1.4. STATEMENT OF PURPOSE

As described above, lens regeneration represents a unique system in developmental biology in which to study the mechanisms involved in the regulated conversion in cell type in the adult organism. In this system, the dedifferentiative and redifferentiative changes of the pigmented epithelial cells coincide with changes in the cytoskeleton, the cell surface and

the associated extracellular matrix. In many differentiating and regenerative systems, the cytoskeleton plays an important role in the coordination or the biochemical and structural differentiative events that occur between the nucleus, the cytoplasm, and the cell membrane with its associated extracellular matrix (Wessells et al. 1971, Nagata and Ichikawa 1984, Amsterdam et al. 1989, Lazarides and Woods 1989, Geiger 1989, Bacallao and Fine 1989, Edelman 1988). Actin filaments are increased and reorganized in many type of regenerative cells both *in vivo* and *in vitro* (Mizobuchi et al. 1990, Tashiro and Komiya 1991, Koo et al. 1988, Sobczak et al. 1989, Cowley 1989). During embryonic differentiation, the associated cell surface macromolecules, such as cadherins and other cell adhesion molecules, play a fundamental role on regulating morphogenesis through mediating the cell-cell contacts and cellular communication within tissues (Hatta and Takeichi 1986, Hatta et al. 1987, Takeichi 1988, Duband et al.1988, Detrick et al.1990, Lagunowich and Grunwald, 1989). The regulatory role of these molecules is conveyed to the cytoplasm via their association with the cytoskeleton which in turn affects the assembly of other cytoskeletal proteins influencing cell shape and motility (Geiger and Volk 1986b, Volberg et al. 1986, Matsuzaki et al. 1990, Geiger 1989). Since the cytoskeleton and its associated cell surface glycoproteins play a fundamental role in cell differentiation and regeneration, it is of interest to study the nature of the cytoskeletal elements and of the cytoskeleton-associated cell surface macromolecules of the iris epithelial cells, and to trace the changes in these structures during cell type conversion. These studies could facilitate our understanding on the roles of these cytoskeletal proteins on cell-type conversion.

In this thesis I have studied the expression of actins, some cytokeratin isoforms, vinculin (Geiger 1979, Geiger et al. 1980) and A-CAM (adherens-junction-specific cell adhesion molecule) (Volk and Geiger 1984, 1986a) in the pigmented epithelial cells of the newt iris. Studies were carried out using labelled phalloidin which binds to F-actin and a series of antibodies to the above-mentioned cytoskeletal proteins. Immunohistochemical

studies were conducted in both flat mounts of iris rings and in sectioned irises. Results show that the pigmented epithelial cells that are able to reprogram into lens formation are myoepithelial in nature. I also traced the changes of cytokeratin II, F-actin, vinculin and A-CAM during the processes of lens regeneration. Cytokeratins belong to a family of intermediate filament proteins that is specifically expressed in epithelial cells (Mull et al. 1982, Quinlan et al. 1985, O'Guin et al. 1990). Staining of cytokeratin-II is progressively increased during dedifferentiation, and gradually disappears during lens fiber formation. A-CAM is a cell adhesion molecule whose linkage to the actin cytoskeleton is mediated indirectly by vinculin (Geiger 1989, Otto 1990, Geiger 1991). Results indicate that in the pigmented epithelial cells of the iris, F-actin, vinculin and A-CAM colocalize in areas of both cell to cell and cell to extracellular matrix contacts. During cell-type conversion, actin staining increases considerably showing that the actin filaments increase and reorganize as cells undergo depigmentation and lens fiber elongation. Vinculin is also reorganized during dedifferentiation and disappears from the elongating lens fibers during redifferentiation. During dedifferentiation, A-CAM is preferentially reduced or eliminated from the regions of the cell involved in cytoplasmic shedding and subsequently, its expression is repressed in the redifferentiating lens fibers.

1. 5. LITERATURE CITED

Achazi R, Yamada T. 1972. Tyrosinase activity in the Wolffian lens regenerating system. Dev. Biol. 27:295-306.

Amsterdam A, Rotmensch S, Ben-Ze'ev A. 1989. Coordinated regulation of morphological and biochemical differentiation in steroidogenic cell: the granulosa cell model. TIBS-14:377-382.

Bacallao R, Fine L G. 1989. Molecular events in the organization of renal tubular epithelium: from nephrogenesis to regeneration. Am. J. Physiol. 257:913-924.

Blumenbach W. 1787. Specimen physiologiae comparatae inter animantia calidi et frigidi sanguinis. Comment. Soc. Reg. Sci. Gottingen. 8:95.

Bonnet C. 1781. Sur les reproductions des salamandres. Evures d'Histoire Naturelle et de Philosophie. 2:175-179. (Neuchatel).

Colucci V. 1891. Sulla rigenerazione parziale dell'occhio nei tritoni. Istogenesi e svilluppo. Studio sperimentale. Memorie R. Acad. Sci. Ist. Bologna, Ser. 51:593-629.

Connelly T G, Ortiz J R, Yamada T. 1973. Influence of the pituitary on Wolffian lens regeneration. Dev. Biol. 13:301-315.

Cowley B D Jr, Chadwick L J, Grantham J J, Calvet J P. 1989. Sequential protooncogene expression in regenerating kidney following acute renal injury. J. Biol. Chem. 264:8389-8393.

Cuny R, Jeanny J C and Courtois Y. 1986. Lens regeneration from cultured newt irises stimulated by retina-derived growth factors (EDGFs). Differentiation. 32:221-229.

Cuny R, Zalik S E. 1981. Effect of bovine pituitary hormone preparations on newt lens regeneration in *vitro*: stimulation by thyrotropin. Dev. Biol. 81:23-35.

Cuny R, Zalik S E, Dimitrov E. 1984. Trophic stimulation of conversion of cultured newt iris cells into lens cells by a bovine thyrotropin preparation. Can. J. Zool. 62:862-869.

Cuny R, Zalik S E. 1985. Comparison of newt lens regeneration stimulating activity in preparations of mammalian thyrotropin and fibroblast growth factor purified by various methods. Exp. Eye Res. 41:629-637.

Detrick R J, Dickey D, Kintner C R. 1990. The effects of N-cadherin misexpression on morphogenesis in *Xenopus* embryos. Neuron. 4:493-506.

Duband J L, Volberg T, Sabanay I, Thiery J P, Geiger B. 1988. Spatial and temporal distribution of the adherens-junction-associated adhesion molecule A-CAM during avian embryogenesis. Development. 103:325-344.

Dumont J N, Yamada T. 1972. Dedifferentiation of iris epithelial cells. Dev. Biol. 29:385-401.

Dumont J N, Yamada T, Cones M V. 1970. Alteration of nucleolar ultrastructure in iris epithelial cells during initiation of Wolffian lens regeneration. J. Exp. Zool. 174:184-204.

Edelman G M. 1988. Morphoregulatory molecules. Biochemistry. 27:3533-3543.

Eguchi G. 1961. The inhibitory effect of the injured and the displaced lens on the lens-formation in *Triturus* larvae. Embryologia. 6:13-35.

Eguchi G. 1963. Electron microscopic studies on lens regeneration. I. mechanism of depigmentation of the iris. Embryologia. 8:47-64.

Eguchi G. 1964. Electron microscopic studies on lens regeneration. II. formation and growth of lens vesicle and differentiation of lens fibers. Embryologia. 8:247-287.

Eguchi G, Shingai R. 1971. Cellular analysis on localization of lens forming potency in the newt iris epithelium. Devel. Growth Differ. 13:337-349.

Eisenberg S, Yamada T. 1966. A study of DNA synthesis during the transformation of the iris into lens in the lentectomized newt. J. Exp. Zool. 162:353-368.

Elgert K, Zalik S E. 1989. Fibronectin distribution during cell-type conversion in newt lens regeneration. Anat. Embryol. 180:131-142.

Geiger B. 1979. A 130K protein from chicken gizzard: its localization at the termini of microfilament bundles in culture chicken cells. Cell. 18:193-205.

Geiger B. 1989. Cytoskeleton-associated cell contacts. Current Opinion in Cell Biology. 1:103-109.

Geiger B. 1991. Adherin' with cadherin. Current Biol. 1:237-238.

Geiger B, Tokuyasu K T, Dutton A H, Singer S J. 1980. Vinculin, an intracellular protein localized at specialized sites where microfilament bundles terminate at the cell membrane. Proc. Natl. Acad. Sci. USA. 77:4127-4131.

Hatta K, Takeichi M. 1986. Expression of N-cadherin adhesion molecule associated with early morphogenetic events in chick development. Nature, Lond. 320:447-449.

Hatta K, Takagi S, Fujisawa H, Takeichi M. 1987. Spatial and temporal expression pattern of N-cadherin cell adhesion molecule correlated with morphogenetic processes of chicken embryos. Dev. Biol. 120:215-227.

Hornsby S, Zalik S E. 1977. Redifferentiation, cellular elongation and cell surface during lens regeneration. J. Embryol. Exp. Morph. 39:23-43.

Ikeda Y, Amatatu H. 1941. Uber den Unterschied der Erhaltungsmoglichkeit der linse bei zwei Urodelenarten (*Triturus pyrrhogaster* und *Hynobius nebulosus*), die sich

bezuglich der Fahigkeit zur Wolffschen linsenregeneration voneinander wesentlich verschieden verhalten. Jpn. J. Med. Sci. 1 Anat. 8:205-226.

Karasaki S. 1964. An electron microscopic study of Wolffian lens regeneration in the adult newt. J. Ultrastruct. Res. 11:246-273

Kesselyak A. 1936. Beitrage zur kenntnis der Auslosungsfaktoren der Wolffschen linsenregeneration. Arch. Entwicklungsmech Org. 134:331-347.

Koo E H, Hoffman P N, Price D L. 1988. Levels of neurotransmitter and cytoskeletal protein mRNAs during nerve regeneration in sympathetic ganglia. Brain Res. 449:361-363.

Kulyk W M, Zalik S E. 1982. Synthesis of sulfated glycosaminoglycans in the newt iris during lens regeneration. Differentiation. 23:29-35.

Kulyk W M, Zalik S E, Dimitrov E. 1987. Hyaluronic acid production and hyaluronidase activity in the newt iris during lens regeneration. Exp. Cell Res. 172:180-191

Lagunowich L A, Grunwald G B. 1989. Expression of calcium-dependent cell adhesion during ocular development: a biochemical, histochemical and functional analysis. Dev. Biol. 135:158-171.

Lazarides E, Woods C. 1989. Biogenesis of the red blood cell membrane-skeleton and the control of erythroid morphogenesis. Annu. Rev. Cell Biol. 5:427-452.

Matsuzaki F, Mege R M, Jaffe S H, Friedlander D R, Gallin W J, Goldberg J I, Cunningham B A, Edelman G M. 1990. cDNA of cell adhesion molecules of different specificity induce changes in cell shape and border formation in cultured S180 cells. J. Cell Biol. 110:1239-1252.

McDevitt D S, Meza I, Yamada T. 1969. An immunofluorescence study of the location of gamma-crystallins during embryonic lens development. Dev. Biol. 19:581-607.

Mizobuchi T, Yagi Y, Mizuno A. 1990. Changes in α-tubulin and actin gene expression during optic nerve regeneration in frog retina. J. Neurochem. 55:54-59.

Moore M D, Williams L A. 1977. The effect of lens components on Wolffian lens regeneration in *Notophthalmus*. Am. Zool. 17:95.

Mull R, Franke W W, Schiller D L. 1982. The catalog of human cytokeratins: patterns of expression in normal epithelia, tumors and cultured cells. Cell. 31:11-24.

Nagata K, Ichikawa Y. 1984. Changes in actin during cell differentiation. *In*: Cell and muscle motility, vol 5. The cytoskeleton. Shay J W, ed. Plenum Press, New Yolk and London.

O'Guin W M, Schermer A, Lynch M, Sun T T. 1990. Differentiation-specific expression of keratin pairs. In Cellular and Molecular Biology of Intermediate Filaments. R D Goldman, P M Steinert (ed.), Plenum Publishing Corporation. pp 301-334.

Otto J J. 1990. Vinculin. Cell Motil. Cytoskeleton 16: 1-6.

Quinlan R A, Schiller D L, Hatzfeld M, Achtstatter T, Moll R, Jorcano J L, Magin T M, Franke W W. 1985. Patterns of expression and organization of cytokeratin intermediate filaments. Ann. N. Y. Acad. Sci. 455:282-306.

Reese D H, Puccia E, Yamada T. 1969. Activation of ribosomal RNA synthesis in initiation of Wolffian lens regeneration. J. Exp. Zool. 170:259-268.

Reese D H. 1977. Ribosomal RNA synthesis in the Eastern North-American newt, *Notophthalmus viridenscens* . Differentiation. 7:99-106.

Reyer R W. 1954. Regeneration of the lens in the amphibian eye. Q. Rev. Biol. 29:1-46.

Reyer R W. 1966. The influence of neural retina and lens on lens regeneration from dorsal iris implants in *Triturus viridescens*. larvae. Dev. Biol. 14:214-245.

Reyer RW. 1977. The Amphibian Eye: Development and Regeneration. *In*:: Handbook of Sensory Physiology. Vol. VII/5. F.Crescitelli, ed. Springer-Verlag, Berlin. pp 309-390.

Reyer R W. 1990a. Macrophage invasion and phagocytic activity during lens regeneration form the iris epithelium in newts. Am. J. Anat. 188:239-344.

Reyer R W. 1990b. Macrophage mobilization and morphology during lens regeneration form the iris epithelium in newts: studies with correlated scanning and transmission electron microscopy. Am. J. Anat. 188:345-365.

Sato T. 1940. Vergleichende studien uber die geschwindigkeit der Wolffschen linsenregeneration bei *Triton taeniatus* and bei *Diemyctylus pyrrhogaster*. Arch. EntwMech. Org. 140:573-613.

Smith S D. 1965. The effects of electrophoretically separated lens proteins on lens regeneration in *Diemyctylus viridescens*. J. Exp. Zool. 159:149-166.

Sobczak J, Tournier M F, Lotti A M, Duguet M. 1989. Gene expression in regenerating liver in relation to cell proliferation and stress. Eur. J. Biochem. 180:49-53.

Stone L S. 1945. Heteroplastic lens grafts related to factors inhibiting lens regeneration in *Triturus*. Proc. Soc. Exp. Biol. Med. 60:10.

Stone L S, Vultee J H. 1949. Inhibition and release of lens regeneration in the dorsal iris of *Triturus v.viridescens*. Anat. Rec. 103:144-145.

Stone L S. 1952. An experimental study of the inhibition and release of lens regeneration in adult eyes of *Triturus viridescens*. J. Exp. Zool. 121:181-223.

Stone L S. 1958a. Inhibition of lens regeneration in newt eyes by isolating the dorsal iris from the neural retina. Anat. Rec. 131:151-172.

Stone L S. 1958b. Lens regeneration in adult newt eyes related to retina pigment cells and the neural retina factor. J. Exp. Zool. 139:69-84.

Stone L S. 1963. Experiments dealing with the role played by the aqueous humor and retina in lens regeneration of adult newts. J. Exp. Zool. 153:197-210.

Stone L S. 1966. Experiments dealing with the inhibition and release of lens regeneration in eyes of adult newts. J. Exp. Zool. 161:83-94.

Stone L S. 1967. An investigation recording all salamanders which can and cannot regenerate a lens from the dorsal iris. J. Exp. Zool. 164: 87-104.

Takata C, Albright J F, Yamada T. 1964a. Study of lens antigens in the developing newt lens with immunofluorescence. Exp. Cell Res. 34:207-210.

Takata C, Albright J F, Yamada T. 1964b. Lens antigens in a lens-regenerating system studied by the immunofluorescent technique. Dev. Biol. 9:385-397.

Takata C, Albright J F, Yamada T. 1966. γ-crystallins in Wolffian lens regeneration demonstrated by immunofluorescence. Dev. Biol. 14:382-400.

Takeichi M. 1988. The cadherins: cell-cell adhesion molecules controlling animal morphogenesis. Development. 102:639-655.

Tashiro T, Komiya Y. 1991. Changes in organization and axonal transport of cytoskeletal proteins during regeneration. J. Neurochem. 56:1559-1563.

Uno M. 1943. Zur Frage des mechanismus der Wolffschen linsenregeneration. Jap. J. Med. Sci. (I. Anat.) 11:75-100.

Volberg T, Geiger B, Kartenbeck J, Franke W W. 1986. Changes in membrane microfilament interaction in intercellular adherens junction upon removal of extracellular Ca^{2+} ions. J. Cell Biol. 102:1832-42.

Volk T, Geiger B. 1984. A 135-kd membrane protein of intercellular adherens junctions. The EMBO J. 3:2249-2260.

Volk T, Geiger B. 1986a. A-CAM: a 135-kd receptor of intercellular adherens junctions. I. immunoelectron microscopic localization and biochemical studies. J. Cell Biol. 103:1441-1450.

Volk T, Geiger B. 1986b. A-CAM: a 135-kd receptor of intercellular adherens junctions. II. antibody-mediated modulation of junction formation. J. Cell Biol. 103:1451-1464.

Wessells N K, Spooner B S, Ash J F. Bradley M O, Luduena M A, Taylor E L, Wrenn J T, Yamada KM. 1971. Microfilaments in cellular and developmental processes. Science. 171:135-143.

Williams L A, Higginbotham L. 1975. The role of a normal lens in Wolffian lens regeneration. J. Exp. Zool. 191:233-251.

Williams L A, Reynolds H T. 1977. Electrophoretically separated lens components and their effects on lens regeneration. Am. Zool. 17:905.

Wolff G. 1895. Entw cklungsphysiologische studien. I. die regeneration der urodelenlinse. Arch. EntwMech. Org. 1:380-390.

Wolff G. 1901. Entwicklungsphysiologische studien. II. weitere mitteilungen zur regeneration der urodelenlinse. Arch. EntwMech. Org. 12:307-351.

Wolff G.1903. Entwicklungsphysiologische studien. III. zur analyse der entwicklungspotenzen des irisepithels bei *Triton*. Arch. Mikrosk. Anat. 63:1-9.

Yamada T, Karasaki S. 1963. Nuclear RNA synthesis in newt iris cells engaged in regenerative transformation into lens cells. Dev. Biol. 7:595-604.

Yamada T, McDevitt D S. 1984. Conversion of iris epithelial cells as a model of differentiation control. Differentiation. 27:1-12.

Yamada T, Roesel M E. 1969. Activation of DNA replication in the iris epithelium by lens removal. J. Exp. Zool. 171:425-431.

Yamada T, Roesel M E. 1971. Control of mitotic activity in Wolffian lens regeneration. J. Exp. Zool. 177:119-128.

Yamada T, Takata C. 1963. An autoradiographic study of protein synthesis in regenerative tissue transformation of iris into lens in the newt. Dev. Biol. 8:358-369.

Yamada T. 1967b. Cellular and subcellular events in Wolffian lens regeneration. Curr. Top. Dev. Biol. 2:247-283.

Yamada T. 1977. Control mechanisms in cell-type conversion in newt lens regeneration. *In*: Monographs in Developmental Biology. Vol.13. A Wolsky, ed. S Karger, New York. pp 1-126.

Zalik S E, Scott V. 1972. Cell surface changes during dedifferentiation in the metaplastic transformation of iris into lens. J. Cell Biol. 55:134-146.

Zalik S E, Scott V. 1973. Sequential disappearance of cell surface components during dedifferentiation in lens regeneration. Nature (New Biology). 244:212-214.

Zalik S E, Scott V, Dimitrov E 1976. Changes at the cell surface during *in vivo* and *in vitro* dedifferentiation in cellular metaplasia. *In*: Progress in Differentiation Research. N Muller-Berat et al. eds. North-Holland, Amsterdam. pp 361-367.

CHAPTER 2. CHARACTERIZATION OF THE IRIS CELLS THAT UNDERGO CELL-TYPE CONVERSION AS A MYOEPITHELIUM

2.1 INTRODUCTION

In the adult newt *Notophthalmus viridescens* and several other species of urodeles, the pigmented epithelial cell (PEC) of the iris of the eye is unique because it can undergo cell-type conversion to produce a new lens *in situ* after the old one has been removed (Stone 1967). During this process, the PEC in the dorsal pupillary margin of the iris first dedifferentiates with its melanosomes being discharged through cytoplasmic shedding, and redifferentiates to synthesize lens specific α, β and γ crystallins to form a transparent lens cell (Yamada 1977). This unique property of cell-type conversion suggests an inherent special capacity of the iris PEC of the newt. Morphologically and histologically, the PEC at the pupillary margin does not show any distinctive features that differentiates it from the PECs of other regions of iris or from the PECs of the eyes of other vertebrates. During embryogenesis, the iris PECs of the newt develop from the rim of the optic cup as a consequence of the invagination of the optic vesicle to form the optic cup. The PECs, also called iris epithelial cells (IECs), are subsequently arranged as a double layered iris epithelium (IE) that borders the pupillary margin. These two layers of PECs or IECs are continuous at the margin of the pupil; they adhere to each other at their apical surfaces and contact the extracellular matrix (ECM) via their basal surfaces. Apposed to the basal lamina, the external IE has, in addition, a layer of connective tissue, called iris stroma (Reyer 1977).

The majority of the morphological and histological studies of the iris PECs of the

newt have been carried out in sagittal sections. In these studies, the PEC at the dorsal margin of the pupil was shown to be cuboidal in shape, and to have the cellular and ultrastructural features of an epithelial cell (Karasaki 1964, Dumont and Yamada 1972, Reyer 1990a, Yamada 1977, Reyer 1977). Because of its ectodermal origin and its resemblance to epithelial cells, investigators have considered the PEC as an epithelial cell.

In many differentiating systems, the cytoskeleton plays an important role in the coordination of the biochemical and structural differentiative events that occur between the nucleus, the cytoplasm and the cell membrane with its associated extracellular matrix (Amsterdam et al. 1989, Lazarides and Woods 1989, Geiger 1989, Nagata and Ichikawa 1984, Gotlieb 1990). In several of these, morphogenesis is affected by compounds that interact with the cytoskeleton (Wessels et al. 1971). During newt lens regeneration, changes at the cell surface and in the extracellular matrix macromolecules occur during dedifferentiation and redifferentiation (Zalik and Scott 1972, 1973, Kulyk and Zalik 1982, Kulyk et al.1987, Elgert and Zalik 1989). Previous studies from this laboratory, indicated that drugs that interact with the microtubular cytoskeleton affected lens fiber differentiation but compounds that interacted with the actin cytoskeleton had no effect on this process (Hornsby and Zalik 1977). These results were surprising since investigations with the electron microscope indicated that changes in the microfilament system occur during the different phases of lens regeneration (Dumont and Yamada 1972, Hornsby and Zalik 1977, Reyer 1990a). We therefore decided to further examine the actin cytoskeleton using specific actin ligands and antibodies. These studies were also conducted using flat iris tissue mounts which enabled us to obtain a global view of the organization of the actin cytoskeleton within the epithelial cells themselves and among the epithelial cells of the iris.

Preliminary experiments in which the actin cytoskeleton was visualized using fluorescein-labelled phalloidin, which binds mainly to filamentous actin (Wieland 1977, Wieland and Faultstch 1978, Estes et al. 1981, Cooper 1987), revealed that the cells of the

iris epithelium had an elongated shape and displayed an elaborate actin cytoskeleton. This cytoskeleton consisted of actin filament bundles (AFB), organized along the long axis of the cell and interconnected by a meshwork fine filaments. The shape of these cells as well as the organization of the actin cytoskeleton resembled that of smooth muscle or myoepithelial cells, suggesting the possibility that the PEC may belong to these cell types. To test this hypothesis, it was decided to determine whether the PEC expressed some of the proteins that are expressed by mammalian myoepithelial cells. For this purpose, I used as probes several antibodies to smooth muscle actins and to cytokeratins. Results indicate that the PECs of the pupillary iris that have the capacity to undergo cell type conversion express several cytoskeletal proteins typical of myoepithelial cells.

2. 2. MATERIALS AND METHODS

Antibodies, ligands and stains

Mouse monoclonal antibodies to α-smooth muscle actin (1A4) and to cytokeratin peptide-14 (CKB1), mouse ascites fluid (NS1), and DAPI (4'-6-Diamino-2-Phenylindole) were purchased from Sigma. Fluorescein-labelled sheep anti mouse IgG was from Amersham. Rhodamine- or fluorescein-labelled phalloidin was from Molecular Probes Inc. Hybridoma supernatants containing anti-cytokeratin II (1h5) and anti-vimentin (14h7) antibodies, and non-immune serum (NS1) were obtained from the Developmental Studies Hybridoma bank (U of Iowa, IA). Mouse monoclonal antibodies to A-CAM (adherens junction specific cell adhesion molecule, ID: 7.2.3) were kindly provided by Drs. T. Volk and B. Geiger (Weizmann Inst of Science, Israel), and mouse monoclonal anti-muscle actin (HHF-35) was a gift from Dr. A. M. Gown , Department of Pathology, University of Washington.

Fixation and manipulation of newt tissues

Adult newts, *Notophthalmus viridescens*, were purchased from Lee's Newt Farm, Oak Ridge, Tennessee. The animals were sacrificed by prolonged anesthesia (40-50 min) in 0.1 % Tricaine (3-aminobenzoic acid ethyl ester, MS-222; Sigma) in distilled water. The head was immersed in the fixative and fixed for 30 min. During the first 5 minutes in fixative, the front one third of eyeball consisting of the cornea and the iris-ciliary rings was dissected and used for histochemical staining. Tissues used as positive controls were cornea, newt abdominal skin and intestine; the latter two were also fixed for 30 min immediately after dissection. Two fixatives were used in these experiments: a) 3% paraformaldehyde in A-PBS (amphibian phosphate-buffered saline: 6.5g NaCl, 0.2g KCl, 0.2g KH_2PO_4,and l.15g of Na_2HPO_4 in one liter of water, adjusted to PH 7.3 with 0.5 N NaOH), and b) Methacarn, consisting of 60 % methanol, 30 % chloroform and 10 % glacial acetic acid (Mitchell et al. 1985).

After fixation, the dissected iris was transferred and rinsed in three changes of APBS 10 min each, with gentle shaking. During the rinsing periods, the cornea was separated from the iris-ciliary ring complex by microdissection; at this stage amorphous viscous material that adhered to the iris tissue was carefully removed with the aid of forceps. In some experiments, in order to visualize the external PECs in flat mount preparations, the iris stroma was removed by microdissection. For this purpose, the iris stroma was grasped with two fine forceps and pulled in opposite directions, this helps to separate the stroma from the epithelium. Then, while holding the ciliary ring on to the bottom of dish, the stroma was grasped at its broken end with forceps and gently peeled away from the underlying epithelium.

Labelled-ligand and immunofluorescence staining of flat iris tissue mounts

For phalloidin staining of F-actin, after rinsing in APBS, the paraformaldehyde fixed iris tissue was permeabilized in acetone at -20 °C for 5 minutes, rehydrated in APBS at room temperature for 20 minutes, and incubated for 30 minutes in rhodamine or fluorescein-labelled phalloidin at a concentration of 1.65 X 10^{-6}M in APBS (Emerman and Vogl 1986, Moore et al.1987). Tissues were washed in three changes of APBS, 5 to 10 minutes each and mounted between two 24 X 50 mm cover slips in Mowiol mounting medium (Osborn and Weber 1982), modified by the addition of 0.5 g of DABCO (2,4-diazabicyclo (2,2,2) octane, Sigma) per 24 ml of Mowiol solution. Aliquots of this medium were kept in the dark at - 20 °C until required.

To mount an iris ring, the iris was transferred onto one cover slip with its internal face adhering to the glass. The surrounding solution was adsorbed with filter paper, and the iris was flattened on the glass with forceps while the tissue still had some moisture. The tissue was further dried at room temperature for about 2-5 minutes. The flattening and drying procedures help to maintain the flattened state of the iris on the cover slip; this is important to maintain the tissue stretched. A drop of Mowiol was added to the stretched iris; the tissue was covered with another cover slip and gently pressed between the two glass surface. The maintenance of the tissue in a stretched condition is essential for the optimal observation of cellular detail with immunofluorescence.

For immunohistochemical detection of actin isoforms, cytokeratin-II, vimentin and A-CAM, paraformaldehyde fixed iris tissue was used. The tissue was permeabilized in acetone and rehydrated as described above. Subsequently, the iris was incubated for 2 hours in primary antibody solutions with approximately 300-500 µl solution per iris. This was followed by three washes in APBS, 10 minutes each, with gentle shaking. Then, the

tissue was incubated for 1 hour with fluorescein-labelled sheep anti-mouse IgG. Following washing as above, the tissue was mounted in Mowiol mounting medium between cover slips as described above.

The antibodies were diluted in antibody buffer (1% BSA, 0.1% Triton X-100 in APBS). The primary antibodies, i.e mouse monoclonal antibodies to α-smooth muscle actin (1A4), α and γ muscle actin (HHF-35) and A-CAM (ID: 7.2.3.), were diluted 1:400, 1:500 and 1:50 respectively in antibody buffer. Controls consisted of hybridoma supernatant containing anti-vimentin antibodies, non-immune mouse hybridoma supernatant (NS1) and non-immune mouse ascites fluid (NS1). The mouse hybridoma supernatants containing anti-cytokeratin II (1h5) and anti-vimentin (14h7) antibodies, or non-antibodies (NS1) were applied undiluted. Fluorescein-labelled sheep anti-mouse IgG was diluted 1:30 in antibody buffer.

For detection of cytokeratin-14, methacarn fixation was required (Mitchell et al. 1985). The anti-cytokeratin-14 antibody (CKB1) was used at a 1:200 dilution. In some experiments, instead of using acetone, the tissue was permeabilized with 0.1 % Triton X-100 in APBS for 5-10 minutes.

Labelled-ligand and immunofluorescence staining of tissue sections

Cryostat sections were prepared using paraformaldehyde fixed tissues. Immediately after fixation, the newt tissues were washed three times in 2% sucrose in APBS on ice (0-4 °C), 10 minutes each with gentle shaking. Tissues were infiltrated overnight at 4 °C with O.C.T. Tissue Tek compound (Canlab), transferred to a plastic mold and embedded in O.C.T. by immediate freezing at -20 °C. Sagittal sections, 6 µm in thickness, were cut on model 855 (American Optical) or Tissue-TEK II (Miles) cryomicrotomes at -20 to -23 °C, and were melted onto microscope slides which had been previously cleaned with 70 % alcohol and coated with a thin film of rubber cement

(Lepage's). For incubation with antibodies, slides were washed in APBS to remove the O.C.T. medium. Before each antibody incubation, sections were rinsed briefly in distilled water, and the remaining fluid was absorbed with filter paper. Antibody solutions were added to sections with a pipette (about 20-50 µl per section), and incubations were carried out in a moist chamber in the dark. Incubation periods for the primary and secondary antibodies were 2 and 1 hour respectively. Following each incubation, sections were washed in APBS three times with gentle shaking for 10 minutes. The concentrations of the primary and secondary antibodies were the same as those described in the previous section for flat mounts. The stained sections were mounted with Mowiol and kept in the dark.

Detection of cytokeratin-14 required methacarn fixation and paraffin sections (Mitchell et al. 1985). The staining procedure was the same as that described for the immunofluorescence staining of cryostat sections. The anti-cytokeratin 14 antibodies were also diluted 1:200 in the same antibody buffer as that mentioned above. Paraffin sections of methacarn and paraformaldehyde fixed tissues were also used for the immunohistochemical detection of α-smooth muscle actin, α and γ muscle actin and cytokeratin II.

Electron microscopy

For electron microscopy, the normal iris tissue was dissected and fixed for 30 min in freshly prepared 3% paraformaldehyde in APBS, processed and cleaned as described for flat mounts of iris tissue. Immediately after washing, the dorsal iris was post-fixed for 1 hour in cold 1 % osmium tetroxide in APBS, dehydrated in an ascending alcohol series, infiltrated with, and embedded in Epon (Dumont and Yamada 1972). Ultrathin sections (600 to 900 nm) were cut using a glass knife with a Reichert Om U2 ultramicrotome. Sections were placed on formvar and carbon coated grids, stained with uranyl acetate and lead citrate, and examined with a Phillips 201 electron microscope.

For viewing by scanning electron microscopy (SEM), the iris ring was mounted on aluminum stubs using silver paint with the stroma side down and the internal basal surface of the iris facing upward. Other irises were fractured and mounted with the fractured surface facing upward. The tissues were sputter-coated with gold using a Nanotech Semprep II coating unit, and observed with a Cambridge stereoscan 250 SEM.

2. 3. RESULTS

2. 3. A. CELL MORPHOLOGY

Morphology of epithelial cells in the flat mounted iris

The iris ring is mainly composed of a double layered pigmented epithelium that, during embryogenesis, develops from the rim of the optic cup after invagination of the optic vesicle. In flat mount preparations, the internal PECs can be observed directly from their basal surfaces, while it is necessary to remove the stroma to expose the basal surfaces of the external layer of the iris epithelium. Observations of flat mounts of iris tissues give a global view of the morphology of the PECs.

The morphology of PECs in flat mount preparations is best visualized by immunofluorescent staining of the tissue with anti-A-CAM (Volk and Geiger 198 , 1986a) antibodies because the antibodies recognize a cell surface molecule that delineates cell boundaries (figure 2-1). In flat mount preparations, the choroid fissure is always distinguishable and it serves as a reference point since it marks the ventral central axis of iris (figure 2-1 A). At the central region of iris epithelial ring, the cells enclosing the pupil are spindle-shaped and are oriented with their long axis parallel to the pupillary margin (figure 2-1 A). In this pupillary margin, as one moves from the lateral to the dorsal or to the ventral regions, the number of rows of cells increases from 4 to 5 to about 8 to 12; and

Figure 2-1. Cell morphology of the PECs of the newt iris observed in flat mount preparations by immunofluorescent staining with anti-A-CAM antibody.

A, is a photograph of the internal face of an entire iris ring showing the differences in cell morphology of the iris PECs in the following three regions, the pupillary marginal (P) ring, the middle (M) ring and the junctional (J) ring. The PECs are observed from their basal surfaces. CE, ciliary epithelium; c, the remaining amorphous viscous material probably arising from the vitreous body or from the zonular fibers that adhere to the iris.

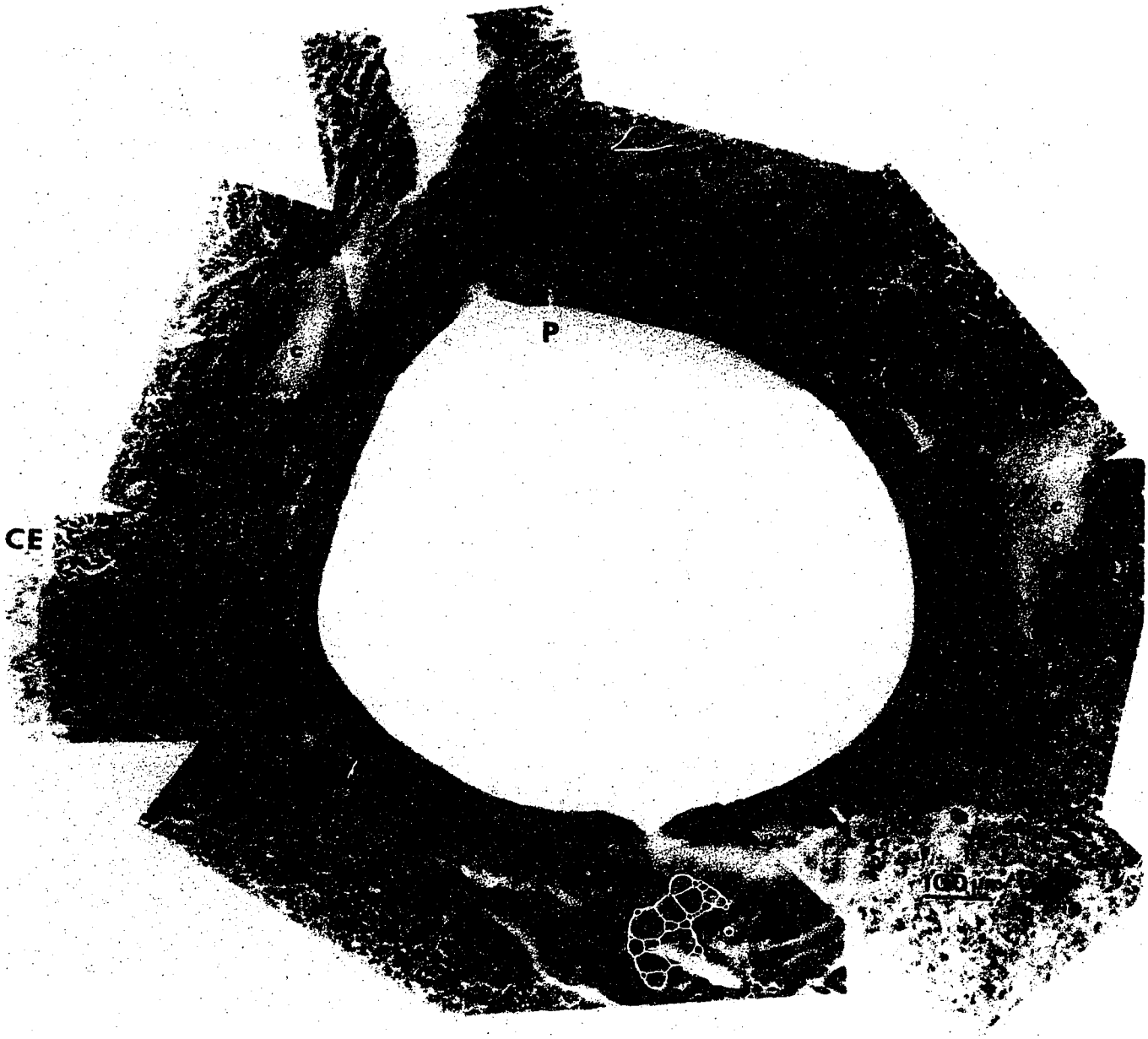
P
CE

Figure 2-1. Cell morphology of the PECs of the newt iris observed in flat mount preparations by immunofluorescent staining with anti-A-CAM antibody.

B, shows the internal PECs; C, and D, show the external surface of the external iris epithelial ring from which the stroma has been removed. All PECs are observed from their basal surfaces. B, an enlargement of the dorsal P-ring showing the elongated spindle shaped cells. C, the external M-ring in the dorsal region of the iris showing the roughly rectangular shaped cells oriented with their long axis perpendicular to the pupillary margin. The cells at the transitional zone (tM) between the P-ring and M-ring change in shape. D, external M- and J-rings in the lateral regions of the iris epithelial ring showing the more longitudinal rectangular shaped cells oriented with their long axes perpendicular to the pupillary margin. Notice that the width of the cells in the dorsal area (C) is larger than that of the cells in the lateral region. P, pupillary ring; tM, transitional zone of the middle ring; J, junctional ring of iris epithelium; s, the undetached piece of stroma tissue that has strong autofluorescence; each unlabeled bar = 10 μm.

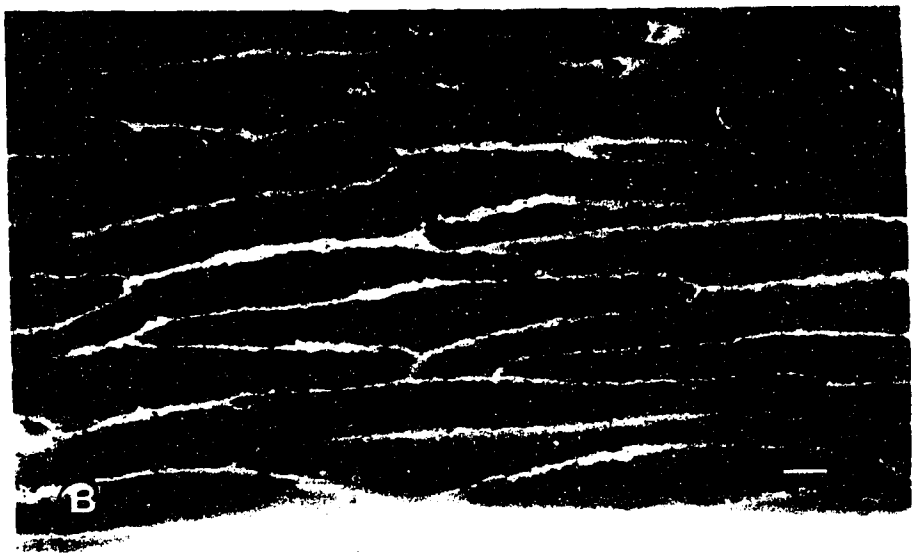
B


C
tM

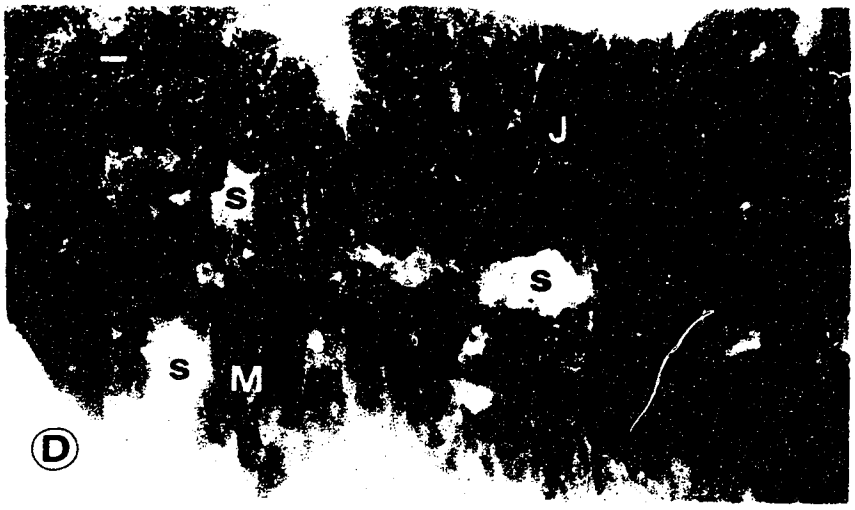
J
S
S
S
M
D

the long axis of the spindle-shaped cells also increases in length (figure 2-1 A, B). The cells adjacent and external to the spindle-shaped cells, form abundant projections which intermingle with those of neighboring cells giving the appearance of zigzag-like cell outlines. The cell shape changes from irregular spindle-like shape in the region close to the pupillary margin to irregular and cuboidal in the more peripheral region (figure 2-1 A, 2-5 B). At the most peripheral region of the IE ring, the outlines of cells are not distinguishable, this could possibly be due to the abundance of cell projections (fig 2-1 A).

In order to better describe the different regions of flat mount preparations of iris rings, based on cell morphology and organization of actin cytoskeleton, the internal IE ring has been arbitrarily divided into three main regions (see figure 2-1 A, 2-2, 2-5). A). the pupillary ring (P-ring) consists of 5-12 rows of spindle-shaped cells with smooth cell outlines; b) the middle ring (M-ring), next to the P-ring is composed of irregular spindle and cuboidal-like shaped cells with zigzag cell outlines; c). the junctional ring (J-ring) is the most peripheral region of the iris that is adjacent to and connected with the ciliary epithelium; the morphology of the cells in this ring is barely distinguishable (figure 2-1 A, 2-5 B). There is no distinct boundary line between the J-ring and the M-ring. This division of the internal IE ring is also illustrated schematically in figure 2-2. The dorsal and ventral regions of the P-ring are expanded since these regions contain more rows of cells than those of the lateral P-ring. The expansion of the P-ring iris is most prominent in the dorsal region, where up to 12-14 rows of spindle shaped cells are detectable (figure 2-1 A, B). The spindle shaped cells are 15-20 μm wide and 100-180 μm long. A new lens is directly regenerated from these cells of the dorsal P-ring iris during cell-type conversion.

To observe the external IE, the stroma has to be removed since, with exception of the 3-6 rows of cells closest to the free border of the pupil, the stroma covers most of the external surface of the IE. The external P-ring IE is also composed 4 to 12 rows of spindle shaped cells. In regards to cell shape and organization, the cells of the external P-ring

Figure 2-1. Cell morphology of the PECs of the newt iris observed in flat mount preparations by immunofluorescent staining with anti-A-CAM antibody.

E, and F, show the external basal surface of the external iris epithelial ring from which the stroma has been removed. E, the external P-ring cells in the dorsal region of iris are elongated spindle shaped similar to the internal P-ring cells (B) and cells in the transitional zone of M-ring (tM) change in shape. F, a high magnification of the external M-ring cells of the dorsal iris showing that the cells are oriented with their long axes perpendicular to the pupillary margin (direction is pointed by the arrow). P, pupillary marginal ring; M, middle ring; s, the undetached piece of stroma tissue with strong yellowish autofluorescence; each unlabeled bar = 10 μm.

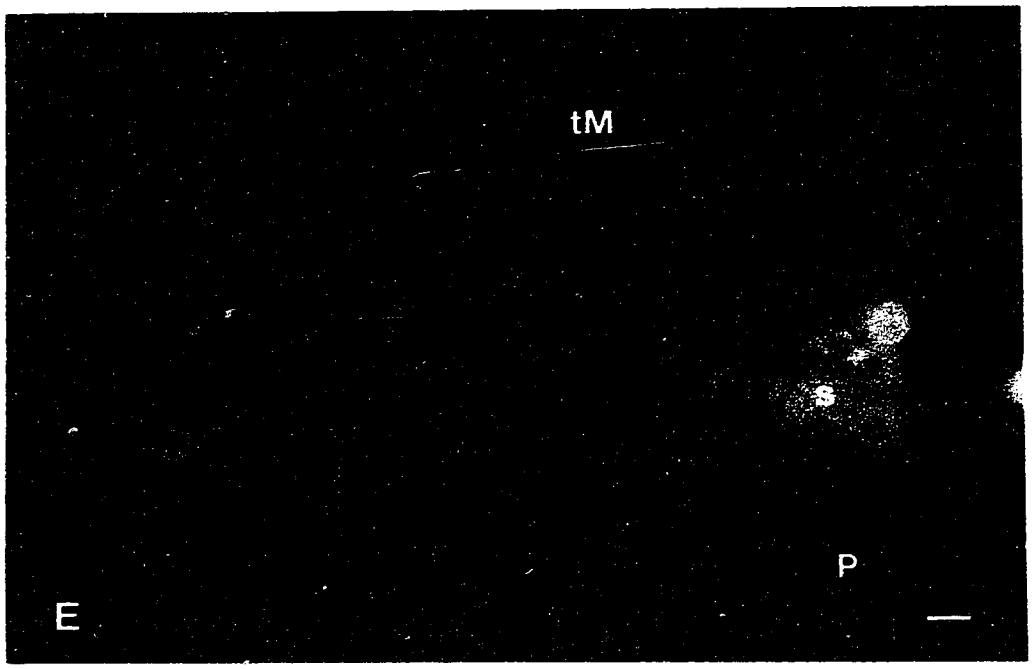
tM
S
P
E


S
S
F

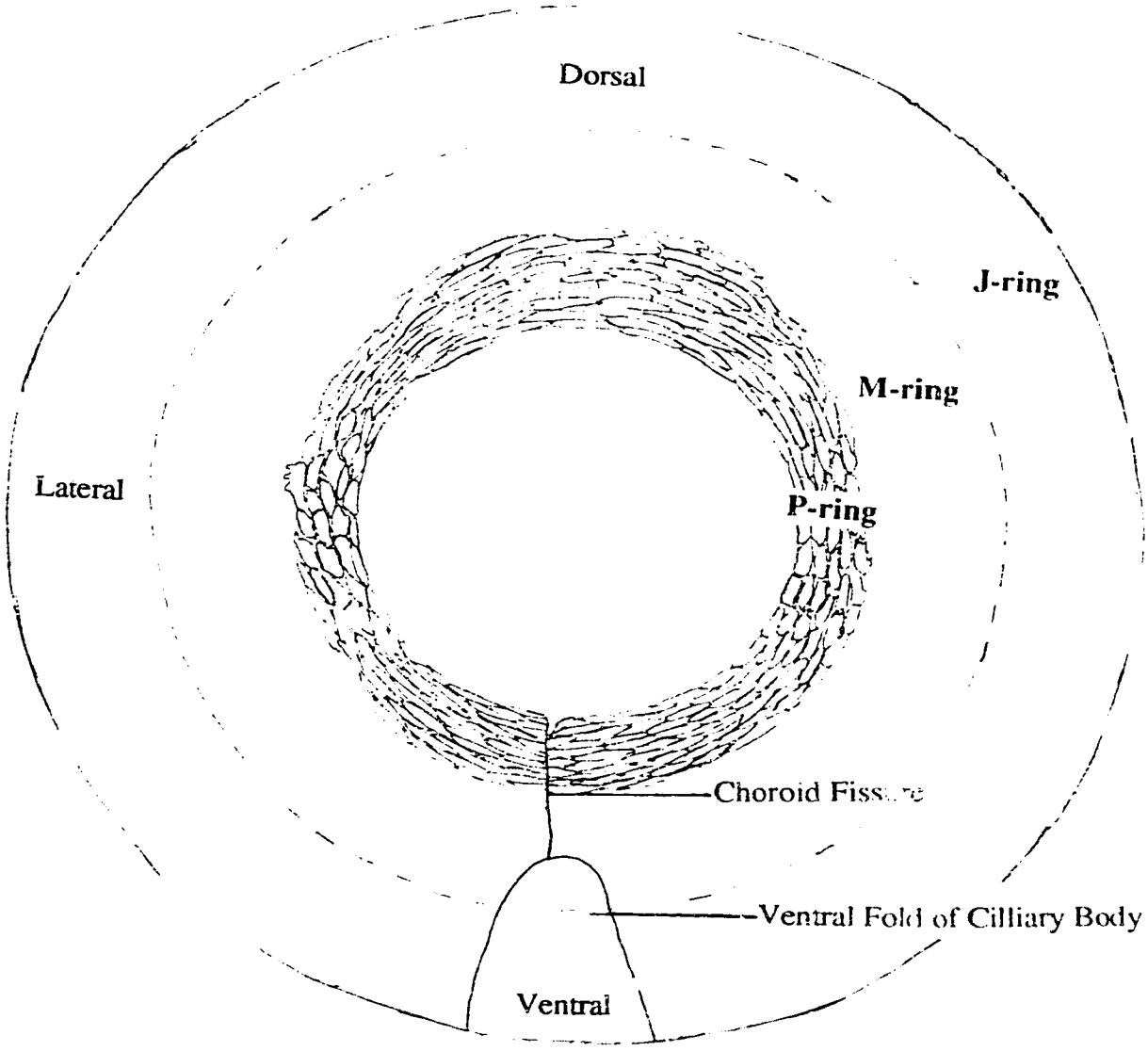

Figure 2-2. Schematic illustrations of the three divisions of iris epithelial ring.

Internal view of a flat mount of an iris epithelial ring showing the three divisions of the internal iris epithelium ring and the cell morphology of the cells of the pupillary ring (P-ring) iris. The P-ring is defined as the central annular zone formed by both layers of IECs. These cells have spindle or elongated morphology with their long axes parallel to the pupillary margin. The cell morphology of the cells of the M- and J-ring iris is not shown in this figure. P-ring, pupillary marginal ring; M-ring, middle ring; J-ring, junctional ring of the IE.

resemble those of the internal layer (figure 2-1 E). Next to the P-ring, the cells in M- and J-ring regions are thin and almost rectangular in shape. Unlike the P-ring cells that are oriented with their long axes parallel to the pupillary margin, the cells of the external M and J ring iris are positioned with their long axes perpendicular to the pupillary margin (figure 2-1 C, D, F). The orientation of the long axes of cells from parallel to perpendicular to the pupillary margin is changed fairly sharply in a narrow transitional zone between the M-ring and the P-ring (figure 2-1 C, E: tM). As one moves from this transitional zone to the periphery of the J-ring, and from the dorsal or ventral to the lateral regions of IE ring, the width of the cells decreases (figure 2-1 C, D).

Electron microscopic obs[illegible]ations of iris epithelial cells

The normal IE was observed in both cross and sagittal sections. In sagittal sections, the P-ring cells appear cuboidal or short rectangular in shape, while the M- and J-ring cells, especially those at the external layer, are rectangular or even long rectangular in cell shape (figure 2-3 A). In all PECs, the cytoplasm is full of electron dense melanosomes (figure 2-3 A, B; 2-4 C, D) (Achazi and Yamada 1972). In the internal PECs, the melanosomes are round and larger than those present in the external PECs; in the latter cells the melanosomes are also oval in shape. In general, small and ovoid melanosomes are present in the external iris epithelial cells that are covered by stroma (figure 2-3 A, B) (Eguchi 1963, Karasaki 1964, Reyer 1990a). The nuclei of the P-ring cells have a scalloped contour containing clumps of heterochromatin (figure 2-3 A, B) (Reyer 1990a), and one or more small dense nucleoli (Dumont et al. 1970). Aside from the melanosomes, mitochondria, endoplasmic reticulum and free ribosomes are observed in the cytoplasm (figure 2-3) (Karasaki 1964, Dumont and Yamada 1972, Reyer 1990a). The Golgi complex that is seldom observed in the normal iris, is shown situated close to the nucleus (figure 2-3 G). Glycogen are also observed (figure 2-3 E, H, I).

The cells of the P-ring as well as other PECs adhere to each other at their lateral and apical surfaces, via three types of junctional membrane complexes. Desmosomal junctions have been described to be frequently present at the lateral surfaces (Karasaki 1964, Dumont and Yamada 1972); these junctions are also shown to be abundant at the apical surfaces between the internal and external iris epithelium (figure 2-3 B). Structures that resemble gap junctions, are also observed at the apical and lateral regions of cells (figure 2-3 B ,C). At the junctional site, the distance between the membrane domain of adjacent cells is in the range of 6.5-7.5 nm. Membrane structures resembling adherens junctions are found scattered along the apical and lateral surfaces of cells of IE (figure 2-3 B, D, E). These are organized as a cytoplasmic dense plaque joined to a similar plaque in the adjacent cell by a series of thin filamentous structures across a distance of approximately 13-20 nm, similar intermembrane structures have also been reported in avian retinal PECs (Kodama et al. 1991). The membrane domain associated with the dense plaque probably contains A-CAM which are receptors for the adherens junctions. The PECs of the iris also adhere to a basement membrane at their basal surfaces, but in these studies no obvious junctional structures in the area of cell to ECM contact could be identified (figure 2-3 F, G, H, J).

The cells of the P-ring have some cellular projections that protrude into the intercellular space. In some cases, the thin cell processes adhere to the main body of a neighboring cell forming adherens-like junctions (figure 2-3 D). The external cells of the P-ring also send some thin cellular projections at their basal surface towards the basement membrane (figure 2-3 J). The stroma tissue adheres to the external IECs, and can protrude into the iris epithelium in between cells without breaking through the basement membrane (not shown). A few pinocytotic vesicles are found in scant amount at the basal area of the internal cells of the P-ring where cells are exposed to the fluids of the eye chamber (figure 2-3 F, G). The cells of M- and J-ring differ from those of the P-ring in that they exhibit abundant groups of cellular projections at the apical, lateral and basal regions of the cells.

Figure 2-3. Transmission electron micrographs of the dorsal iris epithelium

All figures are sagittal sections of the dorsal iris. A, shows the PECs at the transitional zone between the P-ring (p-arrow) and M-ring (m-arrow); the rest of the illustrations show the dorsal P-ring cells. A, is a low magnification of the double layered PECs; part of the nucleus of the stroma cell (sn) is shown above the iris epithelium (e). The region of the stroma was deliberately underdeveloped in order to highlight the organization of the pigment granules in the epithelium. B, an apical area of a region of cell-cell contact showing desmosomes (arrows-d), gap like (arrows-g) and adherens-like (arrows-a) junctional membrane structures. In this figure, the internal layer of IEC is at the left hand side. The internal IECs have pigment granules that are larger then those present in the external IEC on the right hand side. C, a high magnification of another apical region showing the gap-like junctional membrane structures (arrow); D, and E, high magnifications of the lateral and apical regions of IE showing the adherens-like junctional membrane structures; notice the fibers in between the apposed membranes of the junctional structures (white arrows). F, and G, the basal region of the internal P-ring cells showing a pinocytotic vesicle and an open caveola. In some cells one can observe mitochondria (m in B), Golgi complex (Go in G), cellular projections (arrow-p in B) and microtubules (arrow** in B). Microfilaments can be seen in the cortical regions of cells (arrows* in B, D, G). Each unlabeled bar = 100 nm.

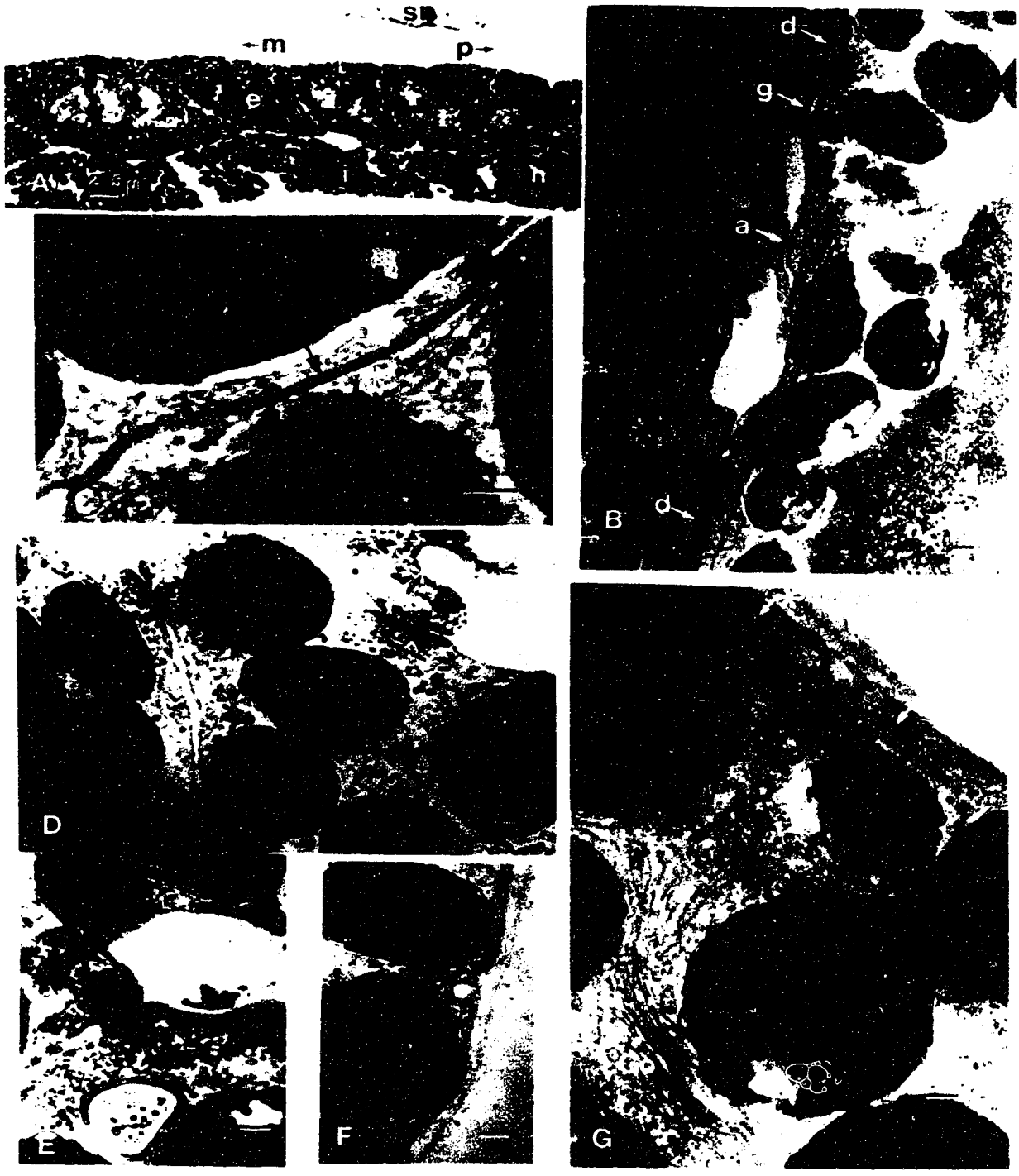
s
m
p
e
h
d
g
a
d
B
D
E
F
G

Microfilaments (approximately 3.5-6.5 nm in diameter) are present and restricted to the cell cortex at the basal, lateral and apical regions of cells (figure 2-3 arrow* in B, G, H, I). Being most abundant in the basal region, these microfilaments traverse the cells just beneath the cell membrane along their long axes; this can be observed in cross sections of the dorsal P-ring iris (figure 2-3 H, I). Also, in sagittal sections, the microfilaments can be observed as interspersed aggregates in the cell cortex which are prominent at the basal region (Dumont and Yamada 1972, Reyer 1990a). In addition, microtubules (approximately 25 nm in thickness) have been observed in the cytoplasm next to the microfilament bundles (figure 2-3 arrow** in B, H).

Using the scanning electron microscope, the basal surfaces of cells of the internal IE were also observed. Here, the profiles of the cells are consistent with those observed using immunofluorescence since the cells of the dorsal P-ring also show the contours of an elongated spindle (figure 2-4 A, B). Fractured cells of the P-ring iris, show that cells have abundant melanosomes suspended in the cytoplasmic meshwork, probably containing membranes and cytoskeletal proteins (figure 2-4 C, D).

Figure 2-3. Transmission electron micrographs of the dorsal iris epithelium.

H, and I, are cross sections, and J, is a sagittal section of the dorsal iris. H, and I, the basal and apical regions of PECs showing the longitudinal microfilaments in the cortical regions (arrows*). J, the basal regions of the external P-ring cells showing the protrusion of a thin cellular projection from PEC into the stroma (s) with the intact basement membranes (b). m, mitochondria; arrow**, microtubule; each unlabeled bar = 100 nm.

H
b
I
m
J

Figure 2-4. Scanning electron micrographs of the dorsal iris epithelium.

A, and B, shows the internal IE viewed from its basal surface through a thin layer of basement membrane; C, and D, are fractures of the dorsal P-ring iris. A, shows the three divisions of the dorsal IE. B, is a high magnification of the P-ring iris showing the elongated spindle profile of the P-ring cells (arrow). C, shows the double layered IE. D, a high magnification of the internal PEC showing the pigment granules surrounded by cytoplasm. P, pupillary ring; M, middle ring; J, junctional ring; CE, ciliary epithelium; R, retina; e, external; i, internal layer of the IE; s, stroma.

2. 3. B. EXPRESSION OF ACTINS

2. 3. B-1. Organization of F-actin in epithelial cells of iris flat mounts

Phalloidin a compound isolated from a mushroom of the genus *Amanita* is a cyclic polypeptide of seven amino acids. This polypeptide binds to and stabilizes polymerized actin filaments (Wieland 1977, Wieland and Faulstch 1978, Estes et al. 1981, Cooper 1987); rhodamine or fluorescein-labelled phalloidin was, therefore, used to stain filamentous actin (F-actin). In cells of both internal and external epithelium of the P-ring, the longitudinal actin filament bundles (AFBs) stained by labelled phalloidin traverse the long axes of the spindle shaped cells and are oriented parallel to each other and to the pupillary margin (figure 2-5 A, B, C). In cells of the internal epithelium of the M- and J-rings, actin staining is prominent at the peripheral region where the cells are rich in cellular projections (figure 2-5 A , B). Especially in the cells of the epithelium of the M-ring, this prominent actin staining confers a zigzag outline to the short spindle-like to cuboidal like cells. The cells of the J-ring have a much more prominent actin cytoskeleton than those of the M-ring (figure 2-5 A, B). In these two groups of cells, the actin filaments are organized as irregular networks. In cells of the external M-and J-rings, the longitudinal actin filaments also traverse the roughly rectangular shaped cells. These filaments are oriented parallel to each other, along the long axes of the cells, which are in turn positioned perpendicularly to the pupillary margin. The actin filaments observed in the external M- and J-ring iris appear thinner than those in the epithelial cells of the P-ring and have regular varicosities (not shown). The staining of F-actin in these cells is weaker compared to that observed in cells in other areas. The latter could be due to poor penetration of the labeled phalloidin because of the presence of the iris stroma or to a lower abundance of actin. In sagittal sections of IE, the staining of actin filaments is located at the cortical area of PECs in the basal, lateral and apical regions (figure 2-5 E).

Figure 2-5. Organization of F-actin in PECs stained by labelled phalloidin.

A, and B, the internal face of an iris flat mounts showing the basal surfaces of cells. A, a photograph of an entire iris ring showing differential actin staining in the three regions of iris epithelium (IE). B, an enlargement of the dorsal iris ring showing that in the cells of P-ring iris, actin staining appears as longitudinal actin filament bundles (AFBs) (large arrow); in the cells of the dorsal M-ring iris, actin staining is prominent in the boundaries of the cells where the cells are rich in cellular projections delineating the cell shapes of irregular spindle and roughly cuboidal profiles (small arrow); in the cells of J-ring, actin staining is very intense and appears as irregular networks (arrowhead). Notice that from the region close to the P-ring to the more distal region of M-ring, the shape of the cell changes from an irregular spindle to a roughly cuboidal shape. P, P-ring; M, M-ring; J, J-ring; NL, naso-lateral; TL, temporo-lateral.


CE
Ⓐ
Ⓑ

Figure 2-5. Organization of F-actin in PECs stained by labelled phalloidin.

C, and D, the internal surface of a flat mount of an iris epithelial ring which is shown at its basal surface, E, is a sagittal section of the dorsal IE. C, an enlargement of the dorsal P-ring showing the longitudinal AFBs transversing the cells (large arrow) and the fine network of actin filaments in between the AFBs (small arrow). D, when the iris is fixed after dissection from the eye, the AFBs are thinner and display regular varicosities (large arrow). The peripheral outlines of the spindle shaped cells are also shown (small arrow). E, shows the punctate staining of the AFBs (arrow) in the cortical area of the cells in the basal, lateral and apical regions. s, stroma of the iris; e, external IE; i, internal IE.


C

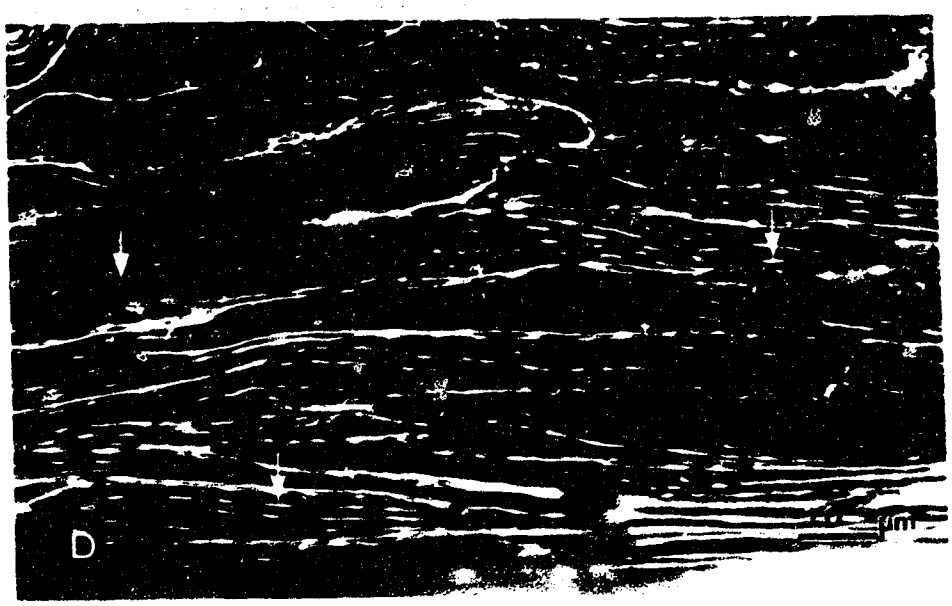
D


s
e
i
E

The elaborate actin cytoskeleton in PECs of the P-ring is reminiscent of that of smooth muscle or of myoepithelial cells. As observed at higher magnification, the longitudinal AFBs are connected to each other by a fine filamentous network of very thin actin filaments (figure 2-5 C). In sagittal sections, the AFBs appear as minute dots located at the cell cortex of cells (figure 2-5 E). The organization of actin filaments appears to be consistent with the ultrastructural observations of microfilaments at the cortical regions of the cells (see figure 2-3 arrow* in B, G, H, I).

The time elapsed between dissection and fixation of tissue also appears to influence the organization and thickness of AFBs. In irises fixed and dissected *in situ*, the AFB are thick and homogeneous as described above. When fixation takes place after dissection of the iris rings, the actin filaments are thinner and appear to have regular varicosities along their length (figure 2-5 D). The cell outlines are also stained by labelled phalloidin; in this case the cell morphology is similar to that observed after immunofluorescent staining with antibodies against A-CAM (see figure 2-1 A, B, 2-5 B, D).

2. 3. B-2. Organization of actin isoforms in the epithelial cells of the iris

Phalloidin staining shows all actin isoforms expressed by cells. To further characterize the PECs of the newt iris, expression of specific actin isoforms was studied since the expression of actin isoforms can yield information about the cell phenotype . In vertebrates there are at least six actin isoforms including α skeletal muscle, α cardiac muscle, α smooth muscle, γ smooth muscle, β cytoplasmic and γ cytoplasmic actins (Vandekerckhove and Weber 1978a, b, 1979, 1981). By comparison of the amino acid sequences among different species, these different isoforms of actin are found to be expressed in a cell-type specific manner which are tissue specific dependent and species independent (Vandekerckhove and Weber 1978b, 1979, 1981). Therefore, these actin

isoforms can be reliable markers for different cell phenotypes across species.

In mammals, the six actin isoforms have similar lengths and amino acid sequences. These proteins have a 90% homology and differ in length by maximally one amino acid residue. A NH_2-terminal segment of this molecule 17 to 18 amino acids in length has only a 60% homology and is responsible for most of the variation found among different actin isoforms. Post translational modification such as acetylation also contributes to the variability of these molecules within this multiple gene family of actins (Vandekerckhove and Weber 1978 b, 1979, 1981). Because of the specificity of actin isoforms, antibodies have been produced against sequences characteristic of particular actin isoforms.

The anti-muscle actin antibody HHF-35,was raised against α and γ actins from human tissue (Tsukada et al. 1987a). This antibody recognizes all muscle cells including cardiac, skeletal, smooth muscle cells, as well as myoepithelial cells (Tsukada et al. 1987a, Tsukada et al. 1987b). Another monoclonal anti-α smooth muscle actin antibody was raised against an acetylated NH_2-terminal decapetide of α smooth muscle actin (Skalli et al. 1986, Vandekerckhove and Weber 1981). This antibody decorates smooth muscle cells and myoepithelial cells of exocrine glands of mammals (Skalli al. 1986, Gugliotta et al. 1988). These antibodies were used in this studies to detect the possible smooth muscle nature of the pigmented iris epithelial cells.

Reactivity of anti-α and γ muscle actin antibodies with newt tissues and with the iris epithelium

The specificity of these antibodies was first assessed by determining their reactivity with other newt tissues. The anti-α and γ muscle actin antibody HHF-35 reacts with skeletal muscle, with smooth muscle of the intestinal mucosa, and with some cells present at the periphery of cutaneous glands which are presumed to be smooth muscle fibers or myoepithelial cells (figure 2-6 A, B). Mouse ascites fluid (NS1) from non-immunized

animals, which was used as a control, did not result in any staining (figure 2-6 C). Anti-vimentin antibody was used as a negative control for all of the antibodies used and it showed no reactivity with the PECs of iris (not shown). Also omission of the primary antibody did not cause any staining (not shown). These controls suggest that the anti-α and γ muscle actin antibody reacts with the proper tissues.

When the iris tissue is reacted with HHF-35 antibody, the P-ring cells are predominantly stained. The cells in M- and J-ring iris, however, show almost non-staining (figure 2-6 D). The staining reveals that the α and γ muscle actin filaments are also organized as longitudinal filamentous bundles traversing along the long axes of the elongated spindle-shaped cells of the P-ring. This organization of the α and γ muscle actin filaments is similar to that of F-actin seen after staining with phalloidin but varies in intensity along its margins (refer to figure 2-5 B, C). In the internal P-ring iris, the staining is more pronounced in the dorsal and ventral regions with weaker staining at its lateral margin; staining intensity also varies among individual cells (figure 2-6 D). This variation in intensity of staining is also observed in cells of the P-ring of the iris in sagittal sections (not shown).

Reactivity of anti-α smooth muscle actin antibodies with newt tissues and with the iris epithelium

The anti-α smooth muscle actin antibody (1A4) has been used as a more specific probe for the detection of the smooth muscle characteristics. The specificity of this antibody was first assessed by examining its reactivity with several newt tissues. The anti-α smooth muscle actin antibody reacts only with the smooth muscle cells of the intestinal mucosa and with presumably myoepithelial cells or smooth muscle cells of the skin gland, this antibody showed no reactivity against skeletal muscle cells (figure 2-7 A, B), which are stained by the anti-α and γ muscle actin antibody HHF-3 (figure 2-6 B). As described

Figure 2-6. Immunofluorescent detection of α and γ muscle actin in newt tissue.

Tissues were stained with anti-α and γ muscle actin antibodies (HHF-35). A, an intestinal villus in cross section. B, sections of skin with attached skeletal muscle: C, and D, the internal surface of iris flat mounts showing the actin staining from the basal surfaces of the dorsal P- and M-rings. A, and B, show positive controls in which the staining of α and γ muscle actin is limited to the smooth muscle cells beneath the mucosa of intestine (arrow in A); in the skeletal muscle (long arrow in B) and in the presumably smooth muscle or myoepithelial cells at the periphery of the skin gland (short arrow in B). C, shows a control in which the ascites fluid of non-immunized mouse does not stain the tissue. D, shows filamentous staining of α and γ muscle actin in the dorsal P-ring cells (arrow). The M-ring cells appear very weekly stained. M, M-ring; P, P-ring; e, epithelium; g, skin gland; m, skeletal muscle; each bar =10 μm.

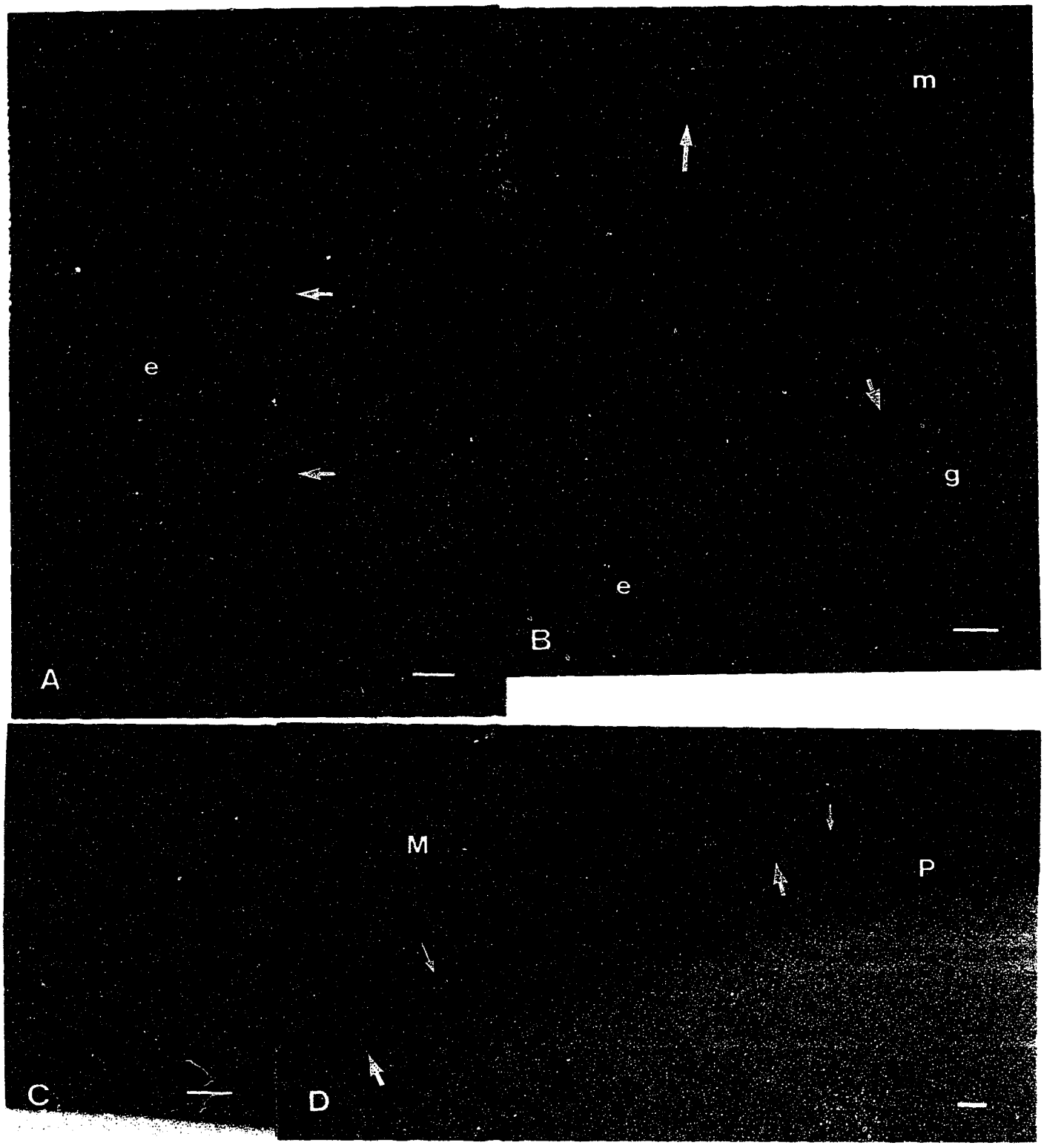
m
e
g
e
B
A
M
P
C
D

Figure 2-7. Immunofluorescent detection of α smooth muscle actin in newt tissue.

Tissues were stained with anti-α smooth muscle actin antibodies (1A4). A, cross section of the intestine; B, cross section of skin with the attached skeletal muscle; C, and D, are sagittal sections of the dorsal and latero-ventral P-ring of the iris; E, is a flat mount of the dorsal P-ring iris. A, shows the selective staining of α smooth muscle actin in the smooth muscle cells beneath the mucosa and muscularis mucosa of the intestine (arrows). B, shows staining in the smooth muscle or myoepithelial cells of the skin gland (small arrow); and lack of staining in the skeletal muscle cells (large arrow), in contrast to the positive staining exhibited by the anti-α and γ muscle actin antibodies (refer to figure 2-4 B). C, shows a negative control in which the ascites fluid of non-immunized mouse does not stain the P-ring iris tissue. D, and E, show that a smooth muscle actin is restricted to the P-ring cells. Notice that the density of the staining varies among the cells (large and small arrows). M-, M-ring; P-, P-ring; e, epithelium; g, skin gland; m, skeletal muscle; each bar = 10 μm.

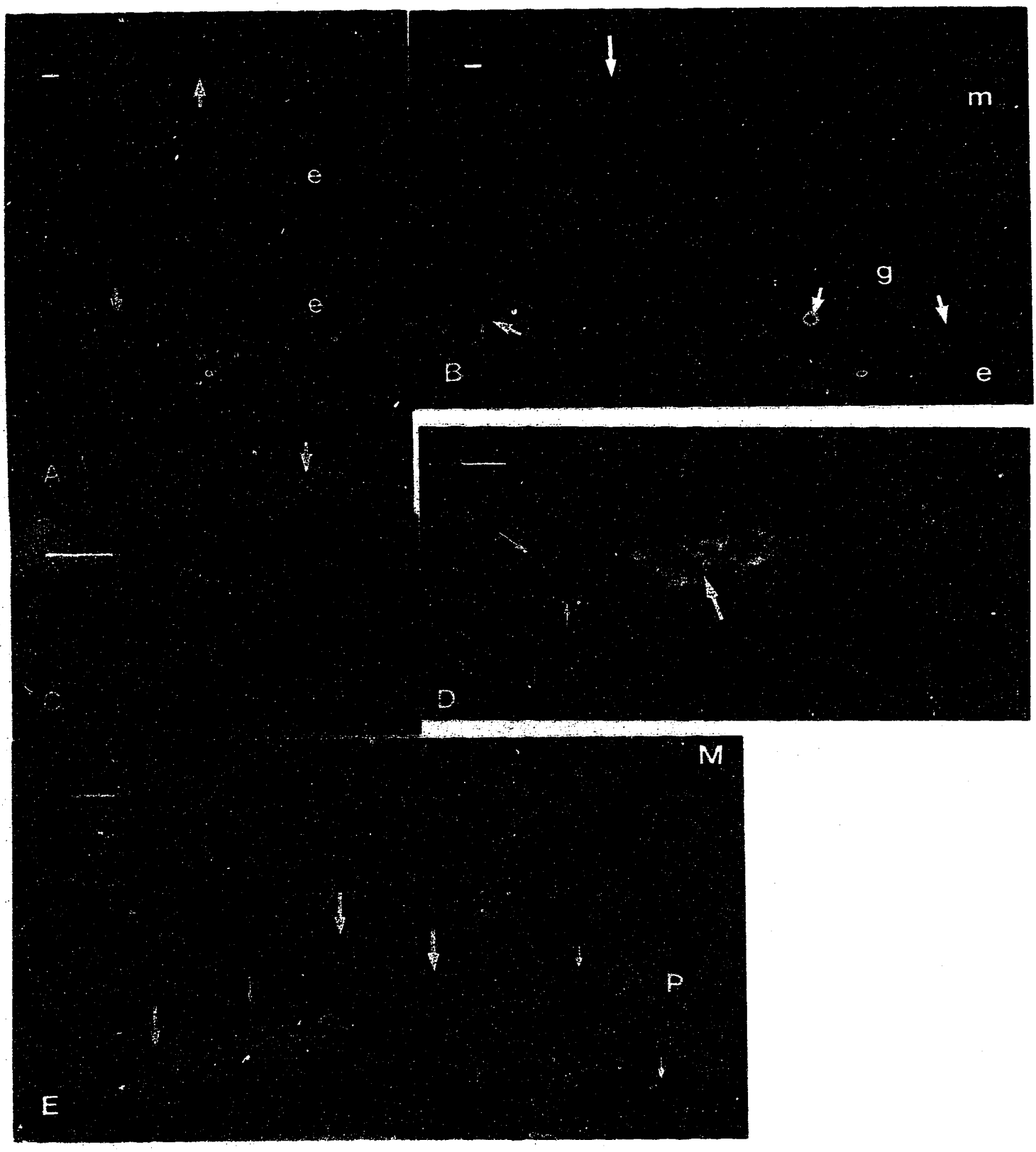
e
e
A
m
g
B
e
D
M
P
E

above, the negative controls show no staining (NS1 is shown in figure 2-7 C). These experiments indicate that, in the newt, this antibody is also specific for smooth muscle actin.

When the iris tissue was reacted with this antibody only some of the cells of the P-ring were stained while those of the M and J-rings did not express this protein (figure 2-7 E). The actin filaments had the same orientation as described previously. The intensity of staining also varies in different areas the P-ring. The cells in the dorsal and ventral P-ring have moderate to intense staining; the cells in the lateral region of the internal P-ring exhibit the weakest staining, while the lateral cells of the external P-ring showed the highest reactivity (not shown). This variation in staining intensity is also observed in sagittal sections which show that, while some cells are strongly stained, some other cells showed little reactivity (figure 2-7 D). The expression of both skeletal muscle and smooth muscle actins, as well as the variation in staining intensity among the epithelial cells of the P-ring, suggests that the expression of these actins differs quantitatively among these cells. This is in contrast with the uniform staining of F-actin observed when labelled phalloidin was used as a probe.

2. 3. C. EXPRESSION OF CYTOKERATINS IN IRIS EPITHELIAL CELLS

Cytokeratin is a protein of the intermediate filament family that is expressed specifically in epithelial cells (Franke et al. 1980). Cytokeratins are heteropolymers of acidic (type I), and neutral/basic (type II) cytokeratins. These proteins belong to a gene family that include at least 25 members (Mull et al.1982, Quinlan et al.1985, O'Guin et al. 1990). Besides the 10 members characteristic of hair and nail-forming cells (Heid et al. 1988), the different cytokeratins are expressed in a cell-type specific manner in different

subtypes of epithelial cells and in some carcinoma cells (Steinert and Roop 1988, O'Guin et al. 1990). Cytokeratins have been used as valuable markers in pathological diagnosis for identification of subtypes of epithelial cells (Cooper et al.1985, Osborn et al. 1986), such as myoepithelium (Franke et al. 1980, Hori et al. 1985, Asch et al. 1981, Dairkee et al. 1985), which can not be distinguished by morphological criteria alone (Pinkstaff 1980, Garrett and Harrison 1971, Puchtler et al.1974, Seifert and Donath 1976).

The cells of the iris epithelium are derived from the diencephalon, a neural structure. Nevertheless, these cells have been considered to be epithelial in nature. In these studies, cytokeratin-II was used as a general marker to confirm the epithelial character of newt iris epithelium. The monoclonal antibody (1h5) was raised against a 56 kD neutral/basic cytokeratin derived from the kidney epithelial cell line A6 from *Xenopus laevis*. Since studies mentioned in the previous section indicated that the PEC of the iris express actin isoforms specific for myoepithelial cells, the epithelial cells of the iris were screened for the presence of cytokeratin-14 which is the cytokeratin specifically expressed by myoepithelial cells (Caslitz et al. 1986a). For this purpose the anti-cytokeratin 14 antibody CKBI was used. This antibody recognizes myoepithelial cell in various human exocrine glands as well as some basal and supra-basal cells in certain hyperplastic conditions. This antibody has been used to screen for normal and neoplastic tissues of myoepithelial origin (Caselitz et al. 1986b, Osborn et al. 1986, Dardick et al. 1988).

Reactivity of anti-cytokeratin II antibodies with newt tissues and with the iris epithelium

The specificity of the anti-cytokeratin II antibody was determined by testing its reactivity with several newt tissues. This antibody stains mostly the epithelial cells of the skin and the epithelial cells of the intestine (figure 2-8 A, B). In the PECs of the iris, this antibody detected cytokeratin-II only in the internal cells of the iris epithelium and only in a

few external epithelial cells of the P-ring iris that are not covered by the iris stroma (table 2-1, figure 2-8 E). In the cells of the P-ring, cytokeratin-II is organized as longitudinal filament bundles oriented along the axes of cells (figure 2-8 D), an orientation similar to that of tonofilaments in mammalian myoepithelial cells (Franke et al.1980), and similar to that of AFBs. In the internal cells of the epithelium of the M- and J-ring this protein is organized as irregular networks (figure 2-8 D). The intermediate filaments are also observed under electron microscope in both internal and external PECs of the dorsal P-ring iris (not shown). It appears that these cytokeratin filaments are aligned together with the AFBs at the basal cortical region of the cells. The special orientation of the cytokeratin-II in the cells of the P-ring may be associated with the contractile property of this group of cells. Expression of cytokeratin-II confirms the epithelial nature mainly of the internal IECs. The external IECs that are covered by the stroma do not express this protein.

Reactivity of anti-cytokeratin 14 antibodies with newt tissues and with the iris epithelium

The anti-cytokeratin-14 antibody reacts only with the cells of the P ring of the iris and does not stain other newt tissues, such as intestine and skin (Table 2-2). Staining is more pronounced in cells of the dorsal P-ring where it is present in only a small group of cells. Staining is not as intense as with other antibodies (figure 2-8 F, G). Control antibodies from non-immunized animals do not stain the iris tissue (figure 2-8 C).

Figure 2-8. Immunofluorescent detection of cytokeratin-II and cytokeratin-14 in newt tissue

A, B, D, and E, were stained with anti-cytokeratin II antibodies (1h5), C, was reacted with control hybridoma supernatant from non-immunized mouse (NS1), and F, and G, were stained with anti cytokeratin peptide-14 antibodies (CKB1). A, a section showing corneal epithelium; B, a section showing the intestinal epithelium; C, D, and F, show the internal surface of iris flat mounts showing the basal surfaces of cells of the dorsal P-ring; E, and G, are sagittal sections of the dorsal iris. A, and B, show the positive staining of cytokeratin-II in epithelial cells of the cornea (arrow in A) and of the intestine (arrow in B). C, shows a negative control. D, shows that cytokeratin-II is organized as longitudinal filament fibers traversing the P-ring cells (large arrow), while in the M-ring cells, it appears as irregular networks (small arrow). E, shows that cytokeratin-II is present in the internal PECs (large arrow) and in the external P-ring cells that are not covered by the stroma (small arrow). Here the staining is present mainly in the peripheral region of the cells in the iris tissue. The tissue was fixed in methacarn and embedded in paraffin. In the cryostat section of the paraformaldehyde fixed tissue, cytokeratin-II is present throughout the cytoplasm of cells (see chapter-3, figure 3-6 A). F, and G, show that cytokeratin peptide 14, a mammalian myoepithelial specific protein, is restricted to the P-ring cells (arrows). M, M-ring; P, P-ring; e, external layer of the IE; i, internal layer of the IE; s, stroma: each bar = 10 μm.

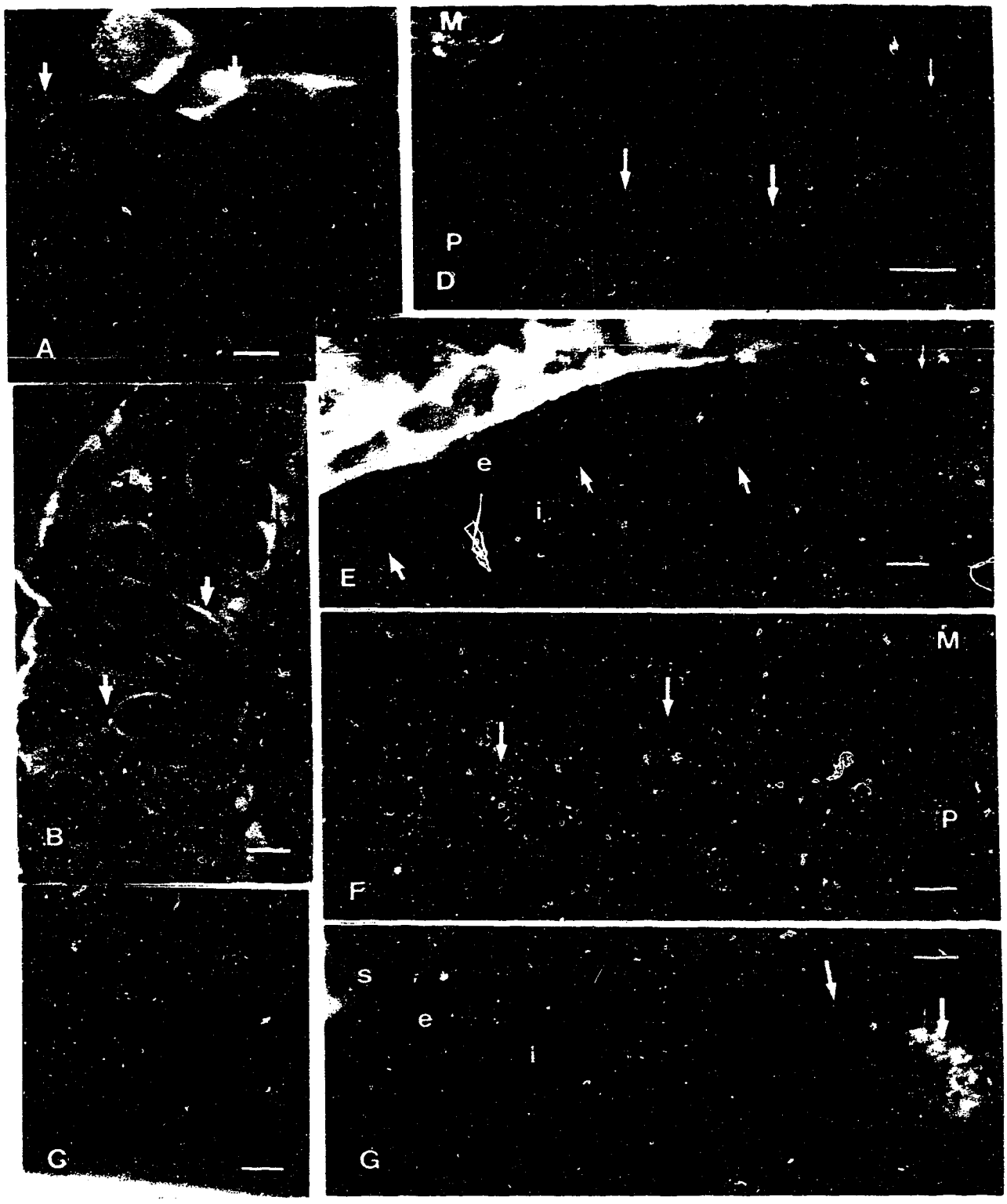
A
M
P
D
e
i
E
B
M
P
F
G
s
e
i
G

Table 2-1. Characterization of the P-ring iris as a myoepithelium

	Pupillary ring of both layers of IE	Middle and Ciliary ring of the Internal IE	Middle and Ciliary ring of External IE
Ability for lens regeneration	Dorsal half of P-ring gives rise to a new lens Ventral & lateral P-ring can regenerate *in vitro*	Dedifferentiate and depigment partially, enter the retrieval pathway	Not involved
Cell morphology	Elongated spindle-shaped with long axis parallel to pupillary margin	Irregular shape, form many projections intermingled with those of neighbouring cells	Thin rectangular shape, long axis perpendicular to pupillary margin
Relationship with stroma tissue	Part of external P-ring covered by a thin layer of stroma, the rest faces the lens	Not covered by stroma, basal surface faces the lens	Covered by stroma, exposed to anterior of eye chamber
F-actin	Longitudinal AFB parallel to long axis of cell and to pupillary margin, located in cortical area of cell	Irregular networks, in cortical area of cell *	Thin AFB parallel to long axis of cell perpendicular to pupillary margin, and in cortical area of cell
α & γ muscle actin (HHF-35)	Longitudinal AFB	Not detected	Not detected
α smooth muscle actin (1A4)	Longitudinal AFB	Not detected	Not detected
Cytokeratin II (1h5)	Long fibers parallel to the pupil margin, in cytoplasm among pigment granules	Irregular networks, *in cytoplasm among pigment granules	Not detected
Cytokeratin-14 (CKB1)	Mainly in internal layer of P-ring	Not detected	Not detected
Vimentin (14h7)	Not detected	Not detected	Not detected

Explanation: IE- Iris epithelium, P-ring- Pupillary ring of IE, M-ring- Middle ring of IE, C-ring- Ciliary ring of IE, PEC- Pigmented epithelial cell of iris, ECM-Extracellular matrix, AFB-Actin filament bundles, F-actin - filamentous actin that includes all isoforms of actin expressed by cells, *-The staining is observed to be increased gradually as one moves from P- to M- and toward C-ring of IE.

Table 2-2. Specificity of the marker antibodies for actin and cytokeratin isoforms

Tissue origins		Iris Epithelium (IE)			Intestine	Skin	Intestine			
Cell types		MyoE	Epithelium				Smooth Muscle			Skeletal muscle
Markers	Tissues Antibodies	P-ring	External	Internal	Epithelium (of mucosa)	Epidermis	*Skin gland	*Muscularis	*Submucosa *Lamina Propria	
Smooth muscle markers	α and γ muscle actin (HHF-35)	+	--	--	-	-	+	++	+	++
	α smooth muscle actin	+	-	-	-	-	+	++	+	--
Epithelial marker	Cytokeratin-II (1h5)	+	-*	++	++	++	0	*--	*--	0
Myoepithelial marker	Cytokeratin-14 (CKB1)	+	-	-	0	-	-	0	0	0

Abbreviations: +, positive; -, negative; ++, strong staining; MyoE, myoepithelium; IE, iris epithelium; P-ring, pupillary ring of IE; External, external layer of IE; Internal, internal layer of IE; 0, not done yet.

-*: the cells covered by the stroma are not stained, but a few cells in the external P-ring at the central region of the iris are positive to cytokeratin II (see figure 2-8)

*--: staining restricted to a few undefined cells.

*Skin gland: refer to possible smooth muscle cells in the periphery of the gland (Figure 2-6, 2-7).

*Muscularis: refer to both muscularis mucosa and muscularis externa that are composed of smooth muscle cells.

*Submucosa and *Lamina propria: contain connective tissue with associated capillaries and smooth muscle cells. The submucosa also contains Brunner's glands that are mainly epithelium.

2. 4. DISCUSSION

To obtain a better characterization of the PECs of the newt iris, I studied, using immunohistochemistry, the expression of several proteins, the cell surface protein A-CAM, and molecular variants of the cytoskeletal proteins, actins and cytokeratins. These studies were complemented with electron microscopic observations on cell ultrastructure. The most important finding in this studies is that the PEC of the P-ring of the iris share many features in common with myoepithelial cells; because of this it is proposed that these cells should be regarded as pigmented myoepithelial cells (PMC). The findings that support this view are the spindle shape of the cells, the organization pattern of the actin and cytokeratin cytoskeleton, and the expression of smooth muscle and myoepithelial markers, such as, α and γ muscle actin, α smooth muscle actin and cytokeratin 14 respectively (table 2-1 and 2-2). The dorsal PMCs of the iris are the ones that are able to complete cell-type conversion to form a new lens *in situ*, while the PECs of the M- and J-rings do not change in cell type during lens regeneration. In addition, the latter cells do not express the protein markers of smooth muscle or myoepithelial cells (table 2-2). These findings suggest a possible relationship between the expression of the myoepithelial phenotype and the ability of certain cells to undergo cell type conversion in this system.

In vertebrates, the myoepithelial cells that have been studied so far are those present in exocrine glands of mammals (Hamperl 1970, Batsakis 1983). With the exception of the pancreas, these mammalian myoepithelial cells are present in all exocrine glands. These cells exhibit either a basket-like configuration or a spindle shape and are situated between the luminal epithelial cells and the basal lamina, with their basal side facing the stroma. As a consequence of their ability to contract like muscle fibers, these cells have a major function in the extrusion of the secretions of the exocrine glands. The cytoplasmic organelles that are common to these myoepithelial cells include Golgi complexes situated close to the nucleus, a few cisterna of rough endoplasmic reticulum, unattached ribosomes,

lysosome-like bodies, a few mitochondria in the perikaryon, a few neutral fat globules and glycogen (Hamperl 1970, Batsakis 1983). These cells also form desmosomes with each other and with the luminal epithelial cells, and display pinocytic vesicles at their basal cell surfaces. Although the presence of these structures can not be considered good criteria for the classification of cells types, the cellular structures that are common to mammalian myoepithelial cells are also present in the PMC of the newt iris (figure 2-3). In addition, the iris epithelial cells of the P-ring also express actins and cytokeratin variants specific for myoepithelial cells and exhibit a similar pattern of organization of microfilaments and intermediate filaments (Hamperl 1970, Batsakis 1983, Franke et al. 1980). While mammalian myoepithelial cells have the potential to store relatively large numbers of glycogen particles, the cytoplasm of the newt PMCs is laden with melanosomes (Achazi and Yamada 1972). These findings strongly support the idea that the cells of the P-ring of the iris are of a myoepithelial type. To my knowledge this is the first report of a group of myoepithelial cells that are also pigmented.

The myoepithelial characteristics of the cells of the P-ring suggest a strong contractile capacity and a possible function of these cells in the contraction of the pupil. In the eyes of mammals, two groups of smooth muscle cells, called sphincter and dilator cells, control the contraction of the pupil (Rodriguez et al. 1982, Davson 1990). The sphincter and dilator smooth muscle cells are derived from the anterior layer of iris PECs of the neuroectoderm during embryogenesis (Fine and Yanoff 1972, Rodriguez et al. 1982, Snell and Lemp 1989). These cells migrate from the iris epithelium into the iris stroma and are separated from the iris epithelium by a basement membrane, collagen fibrils, and some connective tissue of the stroma. Because of this origin, the apical portion of the dilator muscle cells sometimes remains heavily pigmented and their melanin granules are characteristic in size and shape of neuroepithelium (Tousimis and Fine 1959). These pigmented smooth muscle cells are, therefore, also called myoepithelial cells. Although it

has been assumed that the sphincter and dilator smooth muscle cells are also present in the newt eye (Reyer 1977), these cells have never been observed. It is possible that in the newt the smooth muscle cells and epithelial cells have not been evolutionarily separated and consist of a group of cells with characteristics of both smooth muscle and epithelium, the myoepithelial cells. Results from the present research strongly suggest that, in the newt, the dilation and contraction of the pupil are a function of the myoepithelial cells of the P-ring. The development of sphincter cells in the mammalian eye, may have resulted from a divergent evolution of a pigmented iris myoepithelial cell. It remains to be determined whether other amphibians display the same characteristics in the iris epithelium.

The actin as well as the cytokeratin cytoskeleton are organized differently among different groups of iris epithelial cells. While in the PMC of the P-ring of the iris the longitudinal AFBs are organized parallel to pupillary margin, in the external cells of the M-ring and in the J-ring the actin filaments are oriented perpendicular to the pupillary margin; the internal cells of M- and J-rings also have irregular actin filament networks. Correspondingly, in the PECs of the M- and J-rings, the intermediate filaments are arranged as irregular networks and, in the PMC of the P-ring, cytokeratin-II is organized, at least at the basal region of cells, as longitudinal fibers aligned along the long axes of cells. This differential organization of actin and cytokeratin filaments may be necessary for maintaining the integrity of the ring shaped architecture of iris epithelium.

While in the PMC, the staining of F-actin is uniformly distributed among the cells, staining of α and γ muscle actin and α smooth muscle actin is noticeably different among the PMCs in different regions of the P-ring and between the cells of the same region. These results suggest that in the PMC, actin isoforms are differentially expressed possibly in regards to quantity or state of polymerization of a particular isoform. It is also possible that PMC express multiple isoforms of actin. The co-expression of muscle or smooth muscle α actins and the non-muscle actins has also been reported in cultures of skeletal

and smooth muscle cells from chick and mouse (Rubenstein and Spudich 1977, Rubenstein et al. 1982, Otey et al. 1988, Shires and Rubenstein 1989). The functional role of the expression of multiple actin isotypes in the cell is not yet understood.

As discussed above, the differential expression of actin and cytokeratins among different groups of IECs within the iris may be related to cell shape, cell location and tissue interactions. The cells that are covered by stroma have small pigment granules that differ in shape from those of other cells not covered by stroma. While the former do not express cytokeratin-II, the latter cells express this protein of the intermediate filament cytoskeleton. Especially in the M- and J-ring iris, the external PECs are different from the internal ones. It is not known whether these differences are due to the presence of the stroma. Taking these differences into consideration, the IECs can be classified into three groups: the PMC of the P-ring, the internal PECs of the M- and J-rings, and the external PECs of the M- and J-ring. The different characteristics of these cells are summarized in Table 2-1. During lens regeneration, it has been reported that, with the exception of the cells of the pupillary margin of the dorsal iris that produce a new lens, other PECs of of the iris also undergo proliferation, depigmentation and dedifferentiation, [illegible] in contrast [illegible] the retrieval pathway to reconstruct the iris epithelium (Eguchi and Shingai 1971, Yamada 1977). The difference in ultrastructure as well as in the expression of components of the actin and cytokeratin cytoskeleton may be related to the lack of ability of these cells to undergo cell type conversion *in vivo*.

The association between the expression of a myoepithelial smooth muscle-like phenotype and the ability to undergo cell type conversion, may not be restricted to the newt lens regeneration system. In the anthomedusa *Podocoryne carnea* , cell type conversion can be induced in the striated muscle of the medusa by collagenase treatment. During this process, in the absence of DNA synthesis, the striated mononucleated muscle cell first transforms into a cell with a smooth muscle-like phenotype which subsequently undergoes

DNA synthesis and gives rise first to nerve cells, and subsequently to other cell types (Schmid et al.1982, Schmid and Alder 1984, Alder and Schmid 1987). These striated and smooth muscle cells belong to the myoepithelial category (Chapman et al. 1962). It appears that myoepithelial phenotype of cells is associated with the capability of the cells for transdifferentiation or cell-type conversion in either vertebrates or invertebrates. It would be interesting to determine if other systems of transdifferentiation such as the transdifferentiation of imaginal disc (Szabad et al. 1979), or the transdifferentiation of the embryonic cultured retina into lens (Eguchi, 1988), require a cell with a smooth muscle-like phenotype prior to cell type conversion.

These studies were restricted to the study of the organization of several actin isoforms as well as two variants of intermediate filament proteins of the cytokeratin family. Although, under the present experimental conditions I could not detect the presence of vimentin in the iris cells, it would be of interest to determine the expression of other cytoskeletal proteins in this system. In mammary glands, myoepithelial cells also express a particular membrane antigen (LeBien and McCormack 1989); but in the present studies, this antigen is not detected in the iris epithelium. It will be important to determine whether other cell surface antigens and cytoskeletal proteins are expressed differentially in the newt iris. These proteins may change during dedifferentiation and redifferentiation and could serve as markers for particular differentiative states.

2.5. LITERATURE CITED

Achazi R, Yamada T. 1972. Tyrosinase activity in the Wolffian lens regenerating system. Dev. Biol. 27:295-306.

Alder H, Schmid V. 1987. Cell cycles and *in vitro* transdifferentiation and regeneratic isolated, striated muscle of jellyfish. Dev. Biol. 124:358-369.

Amsterdam A, Rotmensch S, Ben-Ze'ev A. 1989. Coordinated regulation of morphologic and biochemical differ ..tiation in steroidogenic cell: the granulosa cell model. TIBS-14:377-382.

Asch B B, Burstein N A, Vidrich A, Sun T. 1981. Identification of mouse mammary epithelial cells by immunofluorescence with rabbit and guinea pig anti-keratin antisera. Proc. Natl. Acad. Sci. USA. 78:5643-5647.

Batsakis J G, Kraemer B and Sciubba J. 1983. The pathology of head and neck tumors: the myoepithelial cell and its participation in salivary gland neoplasia, part 17. Head Neck Surg. 5:222-233.

Caselitz J, Walther B, Wustrow J, Seifert G, Weber K. 1986a. A monoclonal antibody that detects myoepithelial cells in exocrine gland, basal cells in other epithelia and basal and super basal cells in certain hyperplastic tissues. Virchows Arch [pathol Anat] 409:725-738.

Caselitz J, Osborn M, Wustrow J, Seifert G, Weber K. 1986b. Immunohistochemical investigations on the epimyoepithelial islands in lymphoepithelial lesions - use of monoclonal keratin antibodies. Lab. Invest. 55:427-438.

Chapman D M, Pantin C F A, Robson E A. 1962. Muscle in Coelenterates. Rev. Can. Biol. 21:267-278.

Cooper D, Schermer A, Sun T. 1985. Classification of human epithelia and their neoplasms using monoclonal antibodies to keratins: strategies, applications, and limitations. Lab. Invest. 52:243-256.

Cooper J A. 1987. Effects of cytochalasin and phalloidin on actin. J. Cell Biol. 105:1473-1478.

Dairkee S H, Blayney C, Smith H S, Hackett A J. 1985. Monoclonal antibody that defines human myoepithelium. Proc. Natl. Acad. Sci. USA. 82:7409-7413.

Dardick I, Claude A, Parks W R, Hoppe D, Stinson J, Burns B F. 1988. Warthin's tumor: an ultrastructural and immunohistochemical study of basilar epithelium. Ultrastructural Pathology. 12:419-432.

Davson H. 1990. The pupil. *In*: Physiology of The Eye. 5th ed. H Davson, ed. Pergamon Press, Inc. New York. pp 754-766.

Dumont J N, Yamada T, Cones M V. 1970. Alteration of nucleolar ultrastructure in iris epithelial cells during initiation of Wolffian lens regeneration. J. Exp. Zool. 174:184-204.

Dumont J N, Yamada T. 1972. Dedifferentiation of iris epithelial cells. Dev. Biol. 29:385-401.

Eguchi G, Shingai R. 1971. Cellular analysis on localization of lens forming potency in the newt iris epithelium. Devel. Grow. Differ. 13:337-349.

Eguchi G. 1963. Electron microscopic studies on lens regeneration. I. Mechanism of depigmentation of the iris. Embryologia. 8:47-64.

Eguchi G. 1988. Cellular and molecular background of Wolffian lens regeneration. *In*: Regulatory Mechanisms in Developmental Processes. G Eguchi, T S Okada, L Saxen, eds. Elsevier Scientific Publishers Ireland Ltd. pp 147-158.

Elgert K, Zalik S E. 1989. Fibronectin distribution during cell-type conversion in newt lens regeneration. Anat. Embryol. 180:131-142.

Emerman J T, Vogl A W. 1986. Cell size and shape changes in the myoepithelium of the mammary gland during differentiation. Anat. Rec. 216:405-415.

Estes J E, Selden L A, Gershman L C. 1981. Mechanism of action of phalloidin on the polymerization of muscle actin. Biochemistry. 20:708-712.

Fine B S, Yanoff M. 1972. The uveal tract. In: Ocular Histology - A Text and Atlas. Medical Department, Harper & Row, Publishers, Inc. New York. pp 167-212.

Franke WW, Schmid E, Freudenstein C, Appelhans B, Osborn M, Weber K, Keenan T W. 1980. Intermediate-sized filaments of the prekeratin type in myoepithelial cells. J. Cell Biol. 84:633-654.

Franke WW, Jahn L, Knapp A C. 1989. Cytokeratins and desmosomal proteins in certain epithelioid and nonepithelial cells. *In*:: Cytoskeletal Proteins in Tumor Diagnosis. M Osborn and K Weber, ed. Cold Spring Harbor Laboratory Press, Cold Spring Harbor, NY. pp 151-172.

Garrett J R, Harrison J D. 1971. Alkaline phosphatase and adenosine triphosphatase histochemical reactions in the salivary glands of cat, dog and man, with particular reference to the myoepithelial cells. Histochemie. 24:214-229.

Geiger B. 1989. Cytoskeleton-associated cell contacts. Current Opinion in Cell Biology. 1:103-109.

Gotlieb A. 1990. The endothelial cytoskeleton: organization in normal and regenerating endothelium. Toxicol. Pathol. 18:603-617.

Gugliotta P, Sapino A, Macri L, Skalli O, Gabbiani G, Bussolati G. 1988. Specific demonstration of myoepithelial cells by anti-alpha smooth muscle actin antibody. J.

Histochem. Cytochem. 36:659-663.

Hamperl H. 1970. The myothelia (myoepithelial cells): normal state, regressive changes, hyperplasia, tumors. Curr. Top. Pathol. 53:161-220.

Heid H W, Moll I, Franke W W. 1988. Patterns of expression of trichocytic and epithelial cytokeratins in mammalian tissues. I. human and bovine hair follicles. Differentiation. 37:137-157.

Hori K, Hashimoto K, Eto H, Dekio S. 1985. Keratin type intermediate filaments in sweat gland myoepithelial cells. J Invest. Dermat. 85:453-459.

Hornsby S, Zalik S E. 1977. Redifferentiation, cellular elongation and cell surface during lens regeneration. J. Embryol. Exp. Morph. 39: 23-43.

Karasaki S. 1964. An electron microscopic study of Wolffian lens regeneration in the adult newt. J. Ultrastruct. Res. 11:246-273.

Kodama R, Eguchi G and Kelley R.O. (1991): Ultrastructural and immunocytochemical analysis of the circumferential microfilament bundle in avian retinal pigmented epithelial cells in vitro. Cell Tissue Res. 263: 29-40.

Kulyk [illegible] ulik S E, Dimitrov E. 1987. Hyaluronic acid production and hyaluronidase activity in the newt iris during lens regeneration. Exp. Cell Res. 172:180-191

Kulyk W M, Zalik S E. 1982. Synthesis of sulfated glycosaminoglycans in the newt iris during lens regeneration. Differentiation 23:29-35.

Lazarides E, Woods C. 1989. Biogenesis of the red blood cell membrane-skeleton and the control of erythroid morphogenesis. Annu. Rev. Cell Biol. 5:427-452.

LeBien T W, McCormack R T. 1989. The common acute lymphoblastic leukemia antigen (CD10) - Emancipation from a functional enigma. Blood. 73:625-635.

Mitchell D, Ibrahim S, Gusterson B A. 1985. Improved immunohistochemical localization of tissue antigens using modified methacarn fixation. J. Histochem. Cytochem. 33:491-495.

Moore D M, Vogl A W, Baimbridge K, Emerman J T. 1987. Effect of calcium on oxytocin-induced contraction of mammary gland myoepithelium as visualized by NBD-phalloidin. J. Cell Sci. 88:563-569.

Mull R, Franke W W, Schiller D L. 1982. The catalog of human cytokeratins: patterns of expression in normal epithelia, tumors and cultured cells. Cell. 31:11-24.

Nagata K, Ichikawa Y. 1984. Changes in actin during cell differentiation. *In*: Cell and muscle motility, vol 5. The cytoskeleton. Shay J W, ed. Plenum Press, New York and London.

O'Guin W M, Schermer A, Lynch M, Sun T T. 1990. Differentiation-specific expression of keratin pairs. In Cellular and Molecular Biology of Intermediate Filaments. R D

Goldman, P M Steinert , ed. Plenum Publishing Corporation. pp 301-334.

Osborn M, Weber K. 1982. Immumofluorescence and immunocytochemical procedures with affinity purified antibodies: Tubulin-containing structures. In Method in Cell Biology. L Wilson, ed. 24: 97-132.

Osborn M, Lessen G V, Weber K, Kloppel G, Altmannsberger M. 1986. Methods in laboratory investigation Differential diagnosis of gastrointestinal carcinomas by using monoclonal antibodies specific for individual keratin polypeptides. Lab. Invest. 55:497-504.

Otey C A, Kalnoski M H, Bulinski J C. 1988. Immunolocalization of muscle and nonmuscle isoforms of actin in myogenic cells and adult skeletal muscle. Cell Motil. Cytoskeleton. 9:337-348.

Otto J.J. (1990): Vinculin. Cell Motility and the cytoskeleton 16: 1-6.

Pinkstaff C A. 1980. The cytology of salivary glands. Int. Rev. Cytol. 63:141-261.

Puchtler H, Waldrop F S, Carter M G, Valentine L S. 1974. Investigation of staining, polarization and fluorescence microscopic properties of myoepithelial cells. Histochemistry. 40:281-289.

Quinlan R A, Schiller D L, Hatzfeld M, Achtstatter T, Moll R, Jorcano J L, Magin T M, Franke W W. 1985. Patterns of expression and organization of cytokeratin intermediate filaments. Ann. N. Y. Acad. Sci. 455:282-306.

Reyer R W. 1990a. Macrophage invasion and phagocytic activity during lens regeneration form the iris epitheliun in newts. Am. J. Anat. 188:239-344.

Reyer R W. 1990b. Macrophage mobilization and morphology during lens regeneration form the iris epitheliun in newts: studies with correlated scanning and transmission electron microscopy. Am. J. Anat. 188:345-365.

Reyer RW. 1977. The Amphibian Eye: Development and Regeneration. *In*:: Handbook of Sensory Physiology. Vol. VII/5. F Crescitelli, ed. Springer-Verlag, Berlin. pp 309-390.

Rodriguez M M, Hackett J, Donohoo P. 1982. Iris. *In*:: Ocular Anatomy Embryology and Teratology. Jakobiec F A, ed. Happer & Row, Publishers, Philadelphia. pp 285-302.

Rubenstein P A, Spudich J A. 1977. Actin microheterogeneity in chick embryo fibroblast cells. Proc. Natl. Acad. Sci. USA. 74:120-123.

Rubenstein P, Ruppert T, Sandra A. 1982. Selective isoactin release from cultured embryonic skeletal muscle cells. J. Cell Biol. 92:164-169.

Schmid V, Wydler M, Alder H. 1982. Transdifferentiation and regeneration *in vitro*. Dev. Biol. 92:476-488.

Schmid V, Alder H. 1984. Isolated, mononucleated, striated muscle can undergo pluripotent transdifferentiation [illegible] form a complex regenerate. Cell. 38:801-809.

Seifert G, Donath K. 1976. Classi[illegible]n of the pathohistology of diseases of the salivary glands - Review of 2600 cas[illegible]e salivary gland register. Beitr. Pathol. 159:1-32.

Shires A K, Rubenstein P A. 19[illegible] [illegible]uniform behavior of multiple isoactins in the same cell is a cell-dependent phe[illegible]enon. Cell Motil. Cytoskeleton. 14:236-270.

Skalli O, Ropraz P, Trzeciak A, Benzonana G, Gillessen D, Gabbiani G. 1986. A monoclonal antibody against α-smooth muscle actin: a new probe for smooth muscle differentiation. J Cell Biol. 103; 2787-2796.

Snell R S, Lemp M A. 1989. Development of the eye and the ocular appendages. *In*: Clinical Anatomy of The Eye. Blackwell Scientific Publications, Inc. pp 1-18.

Steinert P M, Roop D R. 1988. Molecular and cellular biology of intermediate filaments. Annu. Rev. Biochem. 57:593-625.

Stone L S. 1967. An investigation recording all salamanders which can and can not regenerate a lens from the dorsal iris. J. Exp. Zool. 164: 87-104.

Szabad J, Simpson P, Nothiger R. 1979. Regeneration and compartments in *Drosophila*. J. Embryol. Exp. Morphol. 49:229-241.

Tousimis A J, Fine B S. 1959. Ultrastructure of the iris: An electron microscopic study. Amer. J. Ophthal. 48:397.

Tsukada T, Tippens D, Gordon D, Ross R, Gown A M. 1987a. HHF-35, a muscle actin-specific monoclonal antibody - I. immunocytochemical and biochemical characterization. Am. J. Pathol. 127:51-60.

Tsukada T, McNutt M A, Ross R, Gown A M. 1987b. HHF-35, a muscle actin-specific monoclonal antibody - II. reactivity in normal, reactive, and neoplastic human tissues. Am. J. Pathol. 127:389-402.

Vandekerckhove J, Weber K. 1978a. Actin amino-acid sequences. Eur. J. Biochem. 90:451-462.

Vandekerckhove J, Weber K. 1978b. At least six different actins are expressed in higher mammals: an analysis based on the amino acid sequence of the amino-terminal tryptic peptide. J. Mol. Biol. 126:783-802.

Vandekerckhove J, Weber K. 1979. The complete amino acid sequence of actins from bovine aorta, bovine heart, bovine fast skeletal muscle and rabbit slow skeletal muscle. Differentiation. 14:123-133.

Vandekerckhove J, Weber K. 1980. Vegetative *Dictyostelium* cells containing 17 actin genes express a single major actin. Nature. 284:475-477.

Vandekerckhove J, Weber K. 1981. Actin typing on total cellular extracts. Eur. J.

Biochem. 113:595-603.

Volk T, Geiger B. 1984. A 135-kd membrane protein of intercellular adherens junctions. EMBO J. 3:2249-2260.

Volk T, Geiger B. 1986a. A-CAM: a 135-kd receptor of intercellular adherens junctions. I. immunoelectron microscopic localization and biochemical studies. J. Cell Biol. 103: 1441-1450.

Volk T, Geiger B. 1986a. A-CAM: a 135-kd receptor of intercellular adherens junctions. I. immunoelectron microscopic localization and biochemical studies. J. Cell Biol. 103:1441-1450.

Wessells N K, Spooner B S, Ash J F, Bradley M O, Luduena M A, Taylor E L, Wrenn J T, Yamada KM. 1971. Microfilaments in cellular and developmental processes. Science. 171:135-143.

Wieland T, Faulstich H. 1978. Amatoxins, phallotoxins, phallolysin, and antamanide: the biological active components of poisonous *Amanita* mushrooms. CRC Crit. Rev. Biochem. 5:185-260.

Wieland T. 1977. Modification of actins by phallotoxins. Naturwissenschaften. 64:303-309.

Yamada T. 1977. Control mechanisms in cell-type conversion in newt lens regeneration. *In*: Monographs in Developmental Biology. Vol.13. A Wolsky, ed. S.Karger, New York. pp 1-126.

Zalik S E, Scott V. 1972. Cell surface changes during dedifferentiation in the metaplastic transformation of iris into lens. J. Cell Biol. 55:134-146.

Zalik S E, Scott V. 1973. Sequential disappearance of cell surface components during dedifferentiation in lens regeneration. Nature (New Biology). 244:212-214.

CHAPTER 3. CHANGES OF ACTIN, VINCULIN AND CYTOKERATIN DURING NEWT LENS REGENERATION

3. 1. INTRODUCTION

Humans and higher vertebrates can't regenerate lost parts such as the ocular lens when the latter is removed from the eye. Several species of newts, however, are able to regenerate a new lens after lentectomy (Stone 1967). In the newt, *Notophthalmus viridescens*, the pigmented epithelial cells of the dorsal iris change their original commitment and differentiate into a new lens. This instance of lens regeneration represents a unique system in developmental biology in which to study the mechanisms involved in the regulated conversion in cell type in the adult organism (McDevitt 1989). This is important because a cell expressing the differentiated traits of the pigmented epithelium, withdraws from its original commitment and engages in a new differentiative pathway, that of the lens. Based on the expression of several cytoskeletal proteins, the pigmented epithelial cell (PEC) that gives rise to the new lens has been recently characterized as the pigmented myoepithelial cell (PMC) (chapter 2). Located in the pupillary marginal ring (P-ring) of the iris epithelium, the PMC of the dorsal iris has an elongated spindle shape and is oriented with its long axis parallel to the pupillary margin (chapter 2). When observed in sagittal sections, this cell appears cuboidal in shape (Dumont & Yamada 1972). In the iris the PMCs are organized as a double layered epithelium. The external layer of this epithelium is covered partially by a layer of connective tissue, the so-called stroma. The cells forming the double layered epithelium adhere to each other at their apical and lateral surfaces with adherens-like junction and desmosomes scattered along the cell surface (chapter 2). At their basal surfaces these cells adhere to an extracellular matrix (ECM) that contains fibronectin (Elgert & Zalik 1989).

Two main processes occur sequentially during lens regeneration, the dedifferentiation of the pigmented iris epithelial cell (PEC, also called IEC) into a depigmented cell type, followed by the redifferentiation of the latter into a lens cell (Yamada 1977). During the process of dedifferentiation cells progress from the non dividing G0 phase into the G1 phase of cell cycle to become a dividing cell population (around 4 days after lentectomy) with significant increase in synthesis of DNA, RNA and proteins (Yamada & Roesel 1971, Eguchi & Shingai 1971, Yamada & Karasaki 1963, Yamada & Takata 1963). Following activation, cells depigment by shedding their melanosomes and associated cytoplasm as membrane bound complexes (Eguchi 1963, 1964, Dumont & Yamada 1972, Reyer 1990 a, b). This is accompanied by the invasion of macrophages from the stroma. During early differentiation there is also an increase in the extracellular space and IEC undergo pronounced changes in cell shape (Dumont & Yamada 1972). After dedifferentiation (12 to 15 days after lentectomy), cells continue to proliferate (Eguchi & Shingai 1971, Yamada & Roesel 1971) and eventually cease cell division. Cells then elongate and synthesize the lens-specific proteins α, β and γ crystallins and differentiate into lens fibers. Some cells flatten to form the lens epithelium (Takata et al. 1964 a, b, 1966, Eisenberg & Yamada 1966, Eguchi 1964, Yamada 1967 b).

In many differentiating and regenerative systems, the cytoskeleton plays an important role in the coordination of the biochemical and structural differentiative events that occur between the nucleus, the cytoplasm, and the cell membrane with its associated extracellular matrix (Wessells et al. 1971, Amsterdam et al. 1989, Gottlieb 1990, Lazarides & Woods 1989, Geiger 1989, Nagata & Ichikawa 1984, Opas et al. 1985, Ben Ze'ev 1986, Bacallao & Fine 1989). During the processes of newt lens regeneration, the morphological changes of cells coincide with changes in the extracellular matrix (ECM) macromolecules, and with the cell surface macromolecules (Elgert & Zalik 1989, Zalik & Scott 1972, 1973, Kulyk & Zalik 1982, Kulyk et al. 1987). A cell adhesion molecule, A-CAM or N-cadherin

(Volk & Geiger 1984, 1986a, Hatta et al. 1985, Hatta & Takeichi 1986) undergoes changes during depigmentation and is down-regulated during redifferentiation (chapter 4). Ultrastructural evidence also indicates that microtubules and microfilaments are increased at the cell periphery during dedifferentiation (Dumont & Yamada 1972, Reyer 1990a).

Previous studies from this laboratory in this system had indicated that, while compounds that affect microtubules affected lens fiber elongation, compounds such as cytochalasin B that affect the actin cytoskeleton, had no effect on lens regeneration (Hornsby & Zalik 1977). This was surprising since as was mentioned previously, electron microscopic observations indicated that the microfilament cytoskeleton changes during lens regeneration. With the availability of specific actin ligands, such as phalloidin as well as specific antibodies to actin isoforms, new probes became available for the study of the actin cytoskeleton. It was decided to use these molecules as probes to further examine changes in the actin cytoskeleton during lens regeneration. In addition a new kind of iris preparation was developed consisting of flat iris tissue mounts. Using these preparations, a global view of the organization and changes of the cytoskeleton in individual iris cells as well as among the iris epithelium can be obtained.

The pigmented myoepithelial cells of the normal iris, have microfilaments (approximately 4.0 - 6.5 nm in thickness) that are organized as longitudinal actin filament bundles (AFBs) transversing the long axis of cells at the cortical region. These AFBs contain several isoforms of actin including α and γ muscle and α smooth muscle actins, suggesting that these cells exhibit a myoepithelial phenotype (chapter 2). The actin filaments are observed to be colocalized with A-CAM in regions of both cell to cell and cell to extracellular matrix contact (chapters 2, 4), suggesting an association of these two types of proteins at those sites. In many epithelial cells, at sites of adherens junctions, actin filaments are connected with transmembrane glycoproteins through actin binding proteins, such as vinculin. Vinculin is a 130-kd protein that is believed to function to fasten actin

filaments end to end or laterally to the cytoplasmic face of the cell membrane at both cell to cell and cell to substrate contact regions (Geiger 1979, 1989, Geiger et al. 1980, Geiger et al 1981, Geiger et al 1985, Opas et al. 1985, Opas & Kalnins 1985). The pigmented myoepithelial cells of the normal iris also express cytokeratin II, a member of the intermediate filament family of proteins. This protein is organized as longitudinal fibers at the basal surface of cells, which have a similar orientation as the AFB(Chapter 2). Since these cells also display desmosomes in areas of cell to cell contact, it is possible the cytokeratin II in the intermediate filament cytoskeleton may be also linked with these adhesive structures.

To further study these cytoskeletal proteins during lens regeneration, I have traced the changes in organization and distribution of F-actin, vinculin and cytokeratin-II, using immunohistochemistry and the actin-ligand phalloidin. These studies could contribute to our understanding on the roles that these cytoskeletal proteins play in cell-type conversion. The studies were carried out in flat mounts and sagittal sections of the irises which have allowed me to discern the two dimensional and in some cases the three dimensional organization of the cytoskeletal proteins under study. The results show that during depigmentation, the AFBs initially thicken; subsequently, during early stages of redifferentiation, these filaments reorganize reflecting a change in cell shape. As cells elongate to form lens fibers these filaments accumulate preferentially at the basal and apical cytoplasm. It appears that actin expression is up-regulated during the whole process of cell-type conversion. Vinculin colocalizes with AFB and is detected at the apical, lateral and basal regions of PMC and other PECs of the iris epithelium, suggesting its involvement in both cell-cell and cell-ECM contacts *in vivo*. When observed from the basal surface of the cells, this protein can be visualized as discrete stained areas located slightly peripheral to the AFBs. During dedifferentiation, vinculin is reorganized as the AFBs reorient. Subsequently, this protein disappears from the redifferentiating lens cell.

Cytokeratin-II is up regulated during dedifferentiation and is also down regulated during redifferentiation.

3.2. MATERIALS AND METHODS

Animals and Lentectomy

Adult newts, *N. viridescens*, were purchased from Lee' s Newt Farm, Oak Ridge, Tennessee. The animals were anesthetized in 0.1 % Tricaine (4-aminobenzoic acid ethyl ester, MS-222, Sigma) in distilled water. For lentectomy, a horizontal incision was made to the cornea, through this incision the lens was carefully clasped with fine forceps and removed. The lentectomized newts were held in dechlorinated water at room temperature with weekly feedings for different time interval. Regenerates were staged according to Yamada (1977).

Antibodies, ligands and stains

Rhodamine or fluorescein-labelled phalloidin were purchased from Molecular Probes Inc. Rabbit anti-chick muscle actin antibodies and fluorescein labelled goat anti-rabbit IgG antibodies were from Miles, non immune rabbit serum used as control was available in our laboratory. Mouse monoclonal antibodies to vinculin (ID: 11.5) were kindly provided by Drs. Volk and Geiger (Weizmann Inst of Science, Israel). Hybridoma supernatants containing anti-cytokeratin II (1h5), anti-vimentin (14h7) antibodies, and the non-immune hybridoma supernatant (NS1) were obtained from Developmental Studies Hybridoma bank (U of Iowa). Fluorescein-labelled sheep anti mouse IgG antibodies were from Amersham; control mouse ascites fluid (NS1) and DAPI (4'-6-Diamino-2-Phenylindole) were from Sigma. Immunoblot analysis of the reactivity of anti-vinculin antibodies was performed and is described in chapter 4.

Fixation and manipulation of iris tissue

Newts were sacrificed by prolonged anesthesia (40 to 50 min) in 0.1% Tricaine. The head of the newt was immersed in a fixative consisting of 3% freshly prepared paraformaldehyde in amphibian phosphate buffered saline (APBS: 6.5g NaCl, 0.2g KCl, 0.2g KH_2PO_4, 1.15g Na_2HPO_4 in one liter of water pH 7.3), and fixed for 30 min. During the first 5 minute period in the fixative, the front one third of the eyeball consisting of the cornea and the iris-ciliary rings was dissected. After fixation, the dissected tissue was transferred and rinsed in 3 changes of APBS or of APBS containing 0.1 M glycine, 10 min each with gentle shaking. During the rinsing periods the cornea was separated from the iris-ciliary ring complex by microdissection, at this stage amorphous viscous material that adhered to the iris tissue was also carefully removed with the aid of forceps. In some experiments, in order to visualize the external PECs or IECs, the iris stroma was removed by microdissection. The procedure has been described in chapter 2. The removal of the iris stroma from regenerates is much easier than separating the stroma tissue from the normal iris, possibly because these two tissues have separated during the processes of regeneration.

Staining of flat mount preparations of iris tissue

The procedure for staining of F-actin with labelled phalloidin for flat mount preparations has been described in the previous chapter (2). For immunofluorescent detection of actin (Bussolati et al. 1980), vinculin and cytokeratin-II, paraformaldehyde fixed iris tissues were rinsed in A-PBS, permeabilized in acetone at -20 °C for 5 minutes, and rehydrated in A-PBS at room temperature for 20 minutes. The tissues were subsequently incubated for 2 hours with 400-500 µl per iris of rabbit anti-actin or mouse anti-vinculin antibody solutions diluted 1:40 and 1:50 in antibody buffer (1% BSA, 0.1% Triton X-100 in APBS), or with the mouse hybridoma supernatants containing anti-

cytokeratin II antibodies. This was followed by three washes in A-PBS, 10 minutes each with gentle shaking. The irises were subsequently incubated for 1 hour with 300 µl with fluorescein-labelled goat anti-rabbit IgG or sheep anti-mouse IgG antibody solution diluted 1:50 and 1:30 in the antibody buffer. The incubations were followed by the same washing procedure as before. The controls consisted of non immune rabbit serum, non-immune mouse ascites fluid and hybridoma supernatants. The tissue was mounted between two 24 x 50 mm cover slips in Mowiol mounting medium (Osborn and Weber 1982) (Mowiol 4-88, Calbiochem), modified by the addition of 0.5 g of DABCO (2,4-diazabicyclo (2,2,2) octane, Sigma) per 24 ml of Mowiol solution. The mounting procedure was described in chapter-2.

To observe the colocalization of cytokeratin-II and vinculin with F-actin, the tissues were further incubated in 1.65 X 10^{-6}M rhodamine phalloidin in A-PBS for 30 minutes, followed by three washes in APBS for a total of 5 minutes. The double staining can also be achieved by dissolving the rhodamine phalloidin in the buffer containing the secondary antibodies. In some experiments, the nucleus was also stained to serve as a reference for cell arrangement using DAPI, a drug that binds to DNA (Coleman et al. 1981, Russel 1975). For this purpose, the iris tissues were further incubated for 2-5 minutes in 0.2-0.5 µg / ml DAPI in APBS, followed by three brief rinses in saline before mounting.

Staining of sagittal sections of iris tissue

Cryostat sections of iris tissue were prepared immediately after fixation with paraformaldehyde. The iris tissue was washed in 3 changes of ice cold solution of 2% sucrose in A-PBS, 10 minutes each with gentle shaking. The tissue was infiltrated overnight at 4 °C with O.C.T. Tissue Tek compound (Canlab), transferred to a plastic mold, and embedded in O.C.T. by immediate freezing at -20 °C. Sagittal sections 6 µm in thickness were cut on model 855 (American Optical) or Tissue-TEK II (Miles)

cryomicrotomes at -20 to -23 °C. Sections were melted onto microscope slides which had been previously cleaned with 70 % alcohol and coated with a thin film of rubber cement (Lepage's).

For incubation with antibodies, the slides were washed in APBS to remove the O.C.T. medium. The antibody solutions were added to the sections with a pipette at a ratio of about 20-50 µl per section, incubations with antibody solutions were carried out in a moist chamber at room temperature as above. The concentrations of the primary and secondary antibodies were the same as described above. Before antibody incubation, the sections were rinsed briefly in distilled water, and the remaining fluid was absorbed with filter paper. Following each antibody incubation, the sections were washed in A-PBS three times with gentle shaking for 10 minutes. The stained sections were mounted in Mowiol and kept in the dark (Chapter 2). For double staining of vinculin with F-actin and triple staining of vinculin, F-actin and DNA, the sections were further treated with rhodamine phalloidin and DAPI as described in the above section.

Microscopical observations were conducted using a Zeiss fluorescence Photomicroscope-III or a Zeiss Axiophot. Photographs were taken using Tri-X Pan black and white film and Kodachrome 200 color film.

3. 3. RESULTS

As described in chapter 1, the iris is composed of a double layered pigment epithelium and a layer of connective tissue, the iris stroma, apposed to the basal lamina of the external layer of iris epithelium. The cells of the pigmented iris epithelium adhere to each other at their apical and lateral surfaces by desmosomes and by structures that ultrastructurally resemble gap and adherens junctions. These cells adhere to the

extracellular matrix (ECM) at their basal surfaces. Up to the present time no morphologically identifiable junctional structures have been reported at the basal surfaces (chapter 2). In flat mounts of iris rings the iris epithelium was divided into three main regions: the pupillary (P) ring, the middle (M) ring and the junctional (J) ring. This division is based on differences in cell morphology and in the expression of cytoskeletal proteins. The epithelial cells forming the P-ring iris have been defined as pigmented myoepithelial cell (PMC) (chapter 2). A new lens is directly regenerated from the dorsal PMC. Since the main focus of my research was to trace the changes of the cytoskeletal proteins during the cell-type conversion, this report will deal mainly with the PMC of the dorsal iris.

3. 3. A. ACTIN AND VINCULIN IN THE NORMAL IRIS

Actin

Phalloidin is a cyclic polypeptide of 7 amino-acids isolated from the mushroom of the genus *Amanita*. This compound binds to actin and protects actin filaments from depolymerization (Wieland 1977, Wieland & Faulstich 1978, Estes et al. 1981, Cooper 1987). Since this compound binds more tightly to filamentous (F) actin that to globular (G) actin, phalloidin staining reveals mainly the location of F-actin. Using rhodamine or fluorescein -labelled phalloidin, the organization of F-actin in the normal PMC was described in chapter 2. In order to trace the changes of F-actin during regeneration, the organization of F-actin in PMC of the normal iris epithelium is briefly reviewed. When observed from the basal surface of PMC in flat mount preparations, F-actin appears as longitudinal actin filament bundles (AFBs). These AFBs are oriented along the long axes of the spindle shaped cells, that are parallel to each other and to the pupillary margin. The AFBs are also connected to each other by a fine filamentous network of very thin actin

filaments (figure 2-5 in chapter 2). In sagittal sections of the iris, the AFBs appear as minute dots located at the cell cortex of the apical, lateral and basal regions (figure 2-5 chapter 2). When tissue is stained with monoclonal anti-actin antibodies the actin cytoskeleton exhibits the same pattern of organization of AFBs as that shown by phalloidin staining (not shown). Under the electron microscope, cortical microfilaments, 4.0 -6.5 nm in thickness, are found at the apical, lateral and basal regions of cell, being most abundant in the basal area (figure 2-3. chapter 2). The organization of actin filaments observed after staining with rhodamine phalloidin and immunofluorescence is consistent with the ultrastructural observation of microfilaments.

Vinculin

The specificity of the anti-vinculin antibodies used in these studies was determined by immunoblot analysis using newt tissue extract. This is described in chapter 4. The antibodies react with a band of an approximate m.w. of 130 kD that comigrates with a band of similar molecular weight also present in extracts of chick heart. In contrast, the control mouse ascites fluid as well as antibodies to digoxin, a non relevant plant glycoside from *Digitalis*, do not result in any staining of the protein bands. These results suggest that the antibody against chick vinculin recognizes the corresponding protein in the newt.

Vinculin is present in PMC and PECs of the newt iris at the apical, lateral and basal regions of the cells. In flat mount preparations of iris tissue, vinculin staining appears as elongated patches as well as spots oriented along the AFBs (figure 3-1 A, C). At the tips of the spindle shaped cells, vinculin is also present at the termini of AFBs (figure 3-1 A). In sections, this protein is located at the apical, lateral and basal cortical regions of cells (not shown). In these areas, vinculin staining always colocalizes with actin staining (figure 3-1 B, C). This colocalization of vinculin with actin is in agreement with the function of vinculin as an actin binding protein, i.e, to fasten the actin filaments to the plasma

Figure 3. 1. Distribution of vinculin in the normal pigmented myoepithelial cells in iris flat mounts.

A, and C, were stained with anti-vinculin antibodies; B, was stained with rhodamine phalloidin. A, shows that vinculin staining appears as elongated patches or spots aligned in arrays at the basal region of the cells (arrows). At the end of the elongated spindle shaped cells, vinculin is present in the region where actin filament bundles terminate (large arrow). B, and C, correspond to the same iris tissue that was double stained with labelled phalloidin (B) and anti-vinculin antibodies (C) showing that vinculin staining is colocalized with actin staining (arrows in B and C). In C, some of the red fluorescence of rhodamine phalloidin is not entirely blocked by the fluorescein filter, this "leaked" fluorescence can be seen as brown staining in this photograph showing the green fluorescein staining of vinculin. This brown staining of actin fibers is shown by an arrowhead. Each bar =10 μm.

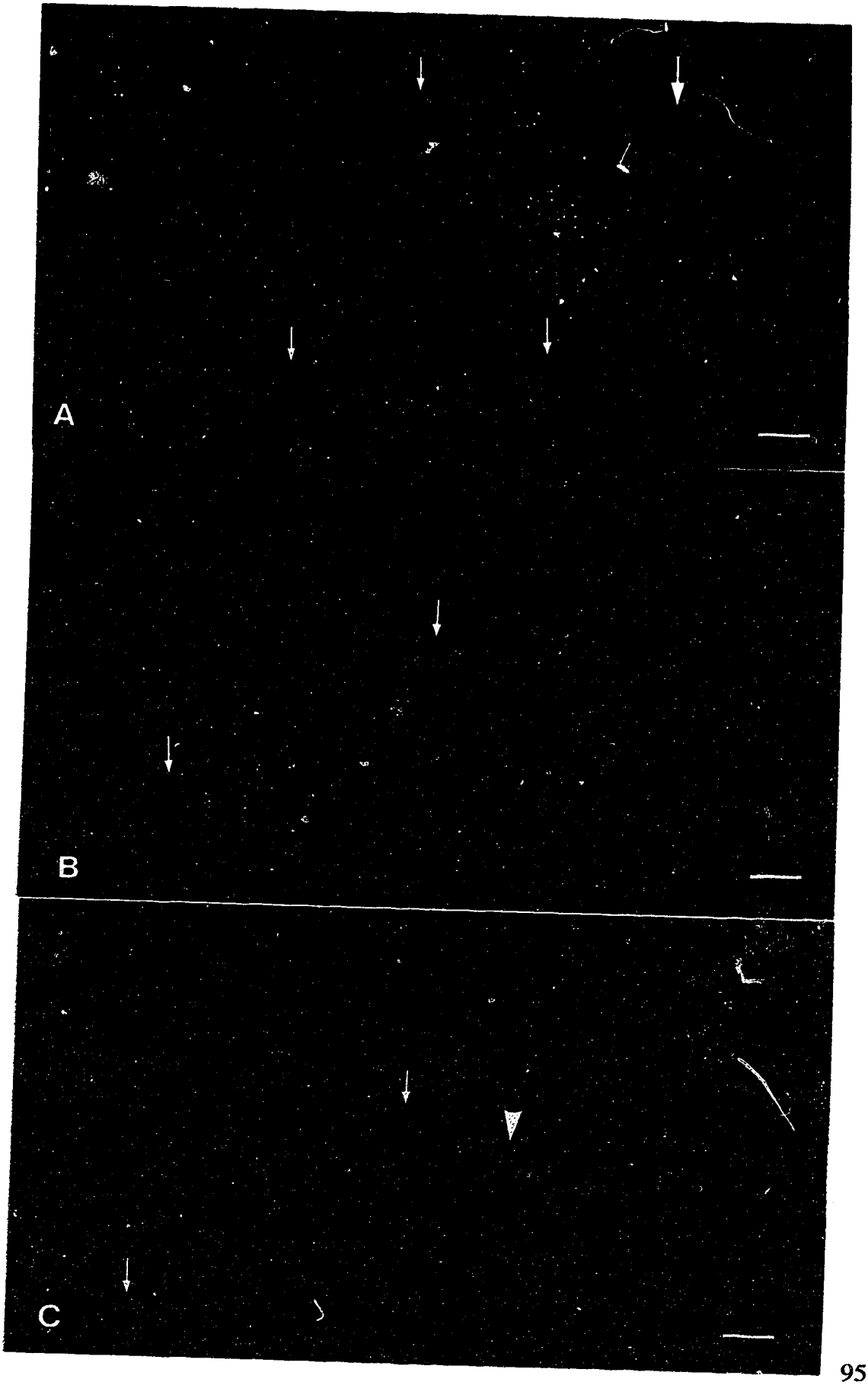
A
B
C

membrane of cells (Geiger 1979, Geiger et al. 1980, Geiger et al. 1981, Opas & Kalnins 1985). The location of vinculin at the basal region of cells also suggest that *in vivo* this protein functions in the areas not only of cell-cell but also cell-ECM contact. Vinculin is also observed in ciliary epithelial cells at all lateral, apical and basal regions of cells where it is colocalized with actin; in the cornea, vinculin is found in the epithelial cells and in the substantia propria (not shown).

3. 3. B. CHANGES IN ACTIN AND VINCULIN DURING LENS REGENERATION

3. 3. B-1. Review of Lens Regeneration

Newt lens regeneration can be divided into eleven stages, which have been reviewed in chapter 1 (see figure 1-4). In the processes of lens regeneration, cells dedifferentiate during stages 1-4. During these stages, the cells first undergo the transition from the G0 to the G1 phase, increase in metabolic synthesis, grow, proliferate and depigment through cytoplasmic shedding. The cytoplasmic projections from which the pigment granules are shed, are mainly present at the basal compartment of cells at late stage 2, and at the apical compartment of cells at stages 2-3 (see below). The resulting depigmented and dedifferentiated cells undergo redifferentiation in the following stages 5-11 of lens regeneration. During these stages, the cells elongate to form the primary and secondary lens fibers with synthesis of γ and β crystallins. This activity starts in a few cells at the central region of the internal layer of lens vesicle at stage 5, and then spreads to most of the cells in the central region of the internal layer of lens vesicle at stages 6-10. The external layer of lens vesicle is flattened to form a lens epithelium. While cells in the central region of the internal layer of lens vesicle are elongating, the cells in the lens stalk area as well as those of the external layer of lens vesicle, proliferate actively to add more

cells to the lens fiber area, these cells subsequently cease division and engage in redifferentiation. Therefore, cells in different areas of the lens vesicle are actually at the different phases of regeneration with the cells at more advanced phases of regeneration towards the center of the internal layer of lens vesicle.

3. 3. B-2. Changes in actin during lens regeneration

Flat mounts of early lens regenerates stained with labelled phalloidin show changes in the appearance and organization of AFBs. First of all, lentectomy does not induce any significant changes in organization of AFBs in PMC at stage 1 within 3-4 days of regeneration. Starting from early stage 2, the AFBs in PMCs become thickened, clustered, branched, some even curved, and shortened in length (figure 3-2 A, 3.3). The AFBs also lose their parallel orientation with those in their neighboring cells and along the pupillary margin. These changes occur at the same time as the spindle-shaped PMC expands along its apico-lateral axes, shortens considerably in length, and the intercellular space increases. Concomitantly, cells also send cytoplasmic processes first towards the basal and later on towards their apical regions. Observed in sagittal sections of regenerates at the mid-stage 2, a more pronounced staining of the cortical actin at the basal and baso-lateral regions is shown to enclose the cytoplasmic projections (figure 3-2 C small arrow). These AFBs correspond to those thickened AFBs observed at the basal region of PMCs in flat mount preparations of regenerates. With ensuing dedifferentiation (stages 2 and 3), the increase in intensity of actin staining also takes place at the apical region of the cells which reflects the thickening or clustering of the AFBs in this region (figure 3-2 C, D: arrowheads). The changes in actin organization occur concomitantly with the cytoplasmic shedding that occurs during depigmentation. In the completely depigmented cells, the staining of the AFB is further intensified as observed in sections (figure 3-2 D). In these cells, the AFBs remain longitudinal with varicosities on them and are oriented roughly parallel to the pupillary margin (figure 3-2 B). These cells have shortened considerably

Figure 3-2 Changes of F-actin during dedifferentiation in cell-type conversion.

A, and B, are flat mount preparations of regenerates of stages 2 and 4. A, shows the internal layer and B, shows the external layer of the dorsal iris epithelium in which the basal surfaces of the cells are observed. A, shows that the actin filament bundles (AFBs) at the basal region of the cells are thickened, clustered (large arrow) and branched (small arrow). B, denotes that in the depigmented and dedifferentiated cells of lens vesicle of stage 4 the longitudinal AFBs have varicosities along them (small arrow), and are still organized roughly parallel to the pupillary margin (large arrow), an orientation similar to that present in the normal pigmented myoepithelial cell.

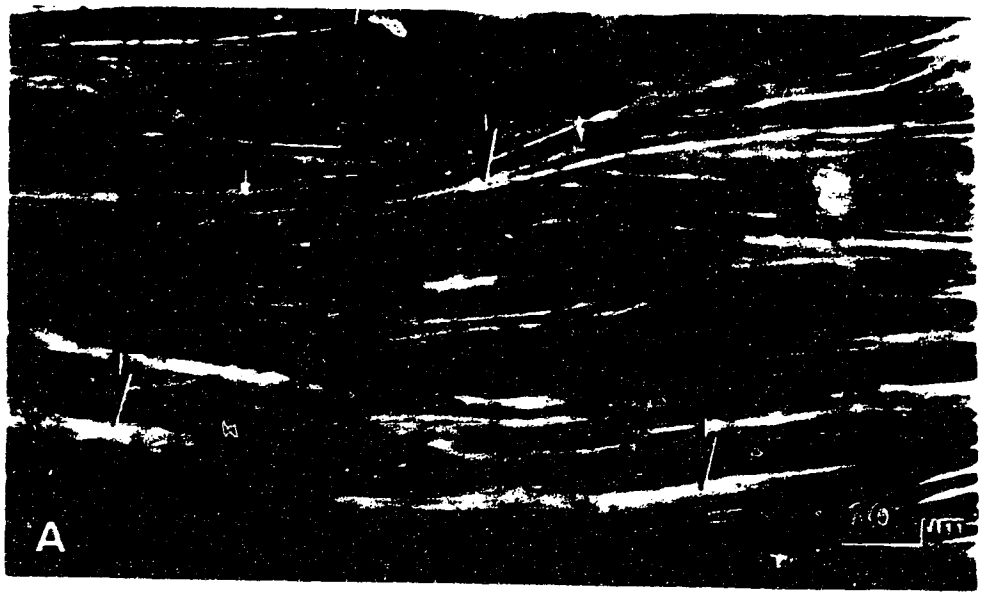
A

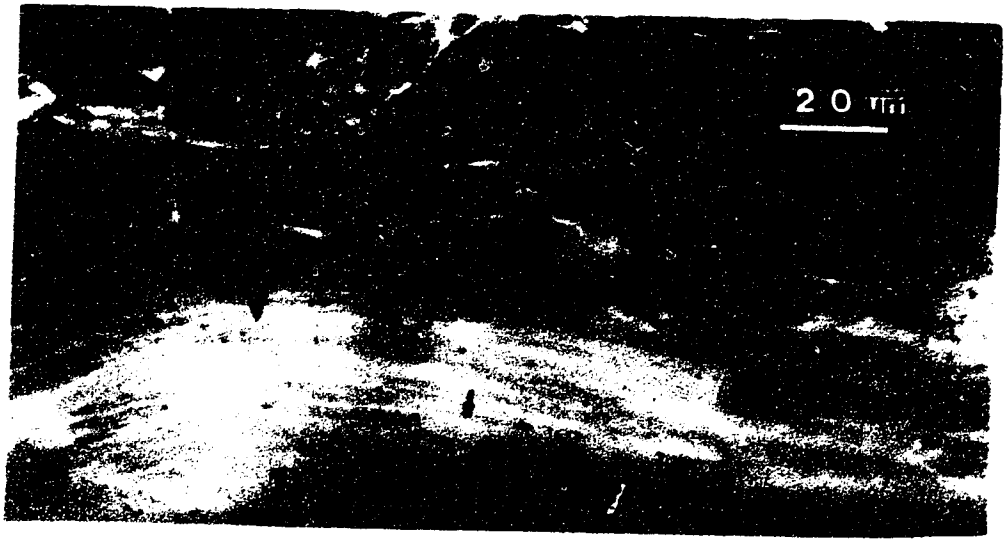
20 μm

Figure 3-2 Changes of F-actin during dedifferentiation in cell-type conversion.

C, and D, are sagittal sections of the dorsal iris from regenerates of stages 2 and 3. C, shows that the thickened AFBs observed in flat mounts are evident in this section as discrete areas of staining of cortical actin that is preferentially located at the basal regions of the cells (large arrow). The prominent staining of AFBs is also present at the lateral (small arrow), as well as the apical region of cells (arrowheads). At the basal and apical region of cells, some of AFBs appear yellow in colour. This is the consequence of the very intense staining of these regions with labelled phalloidin that results in their over exposure in the photograph. D, shows the intense staining of actin at the apical region of depigmenting cell (arrowhead) and in the newly depigmented cells (arrow). In the latter group of cells the AFBs, when observed in flat mounts, are organized longitudinally roughly parallel to the pupillary margin as shown in figure B. S, stroma; E, external layer; I, internal layer of the iris epithelium; each bar = 10 μm.

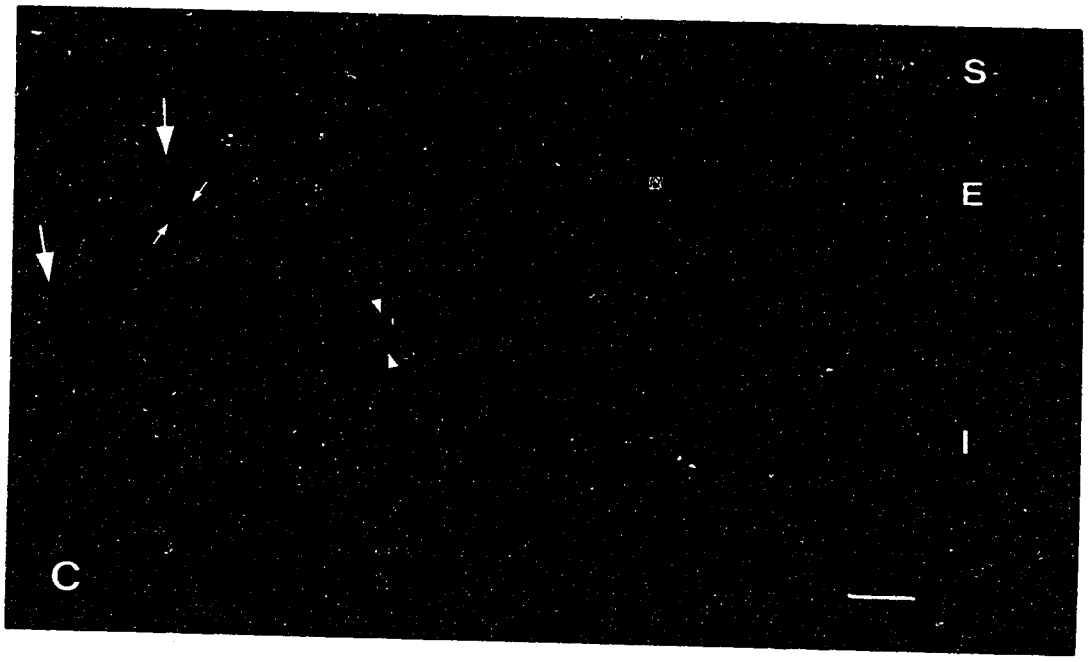
S
E
I
C


S
E
I
D

Figure 3. 3. Changes of F-actin in the iris epithelium of the pupillary ring in a stage 2 regenerate.

The P-ring iris epithelium at the early stage of depigmentation is shown in a flat mount. The AFBs in all internal pigmented myoepithelial cells are thickened, clustered, and branched. The change in the organization of the AFBs is very pronounced when compared to the normal iris (figure 2-5 in chapter 2). NL, naso-lateral; TL, temporo-lateral; F, choroid fissure.

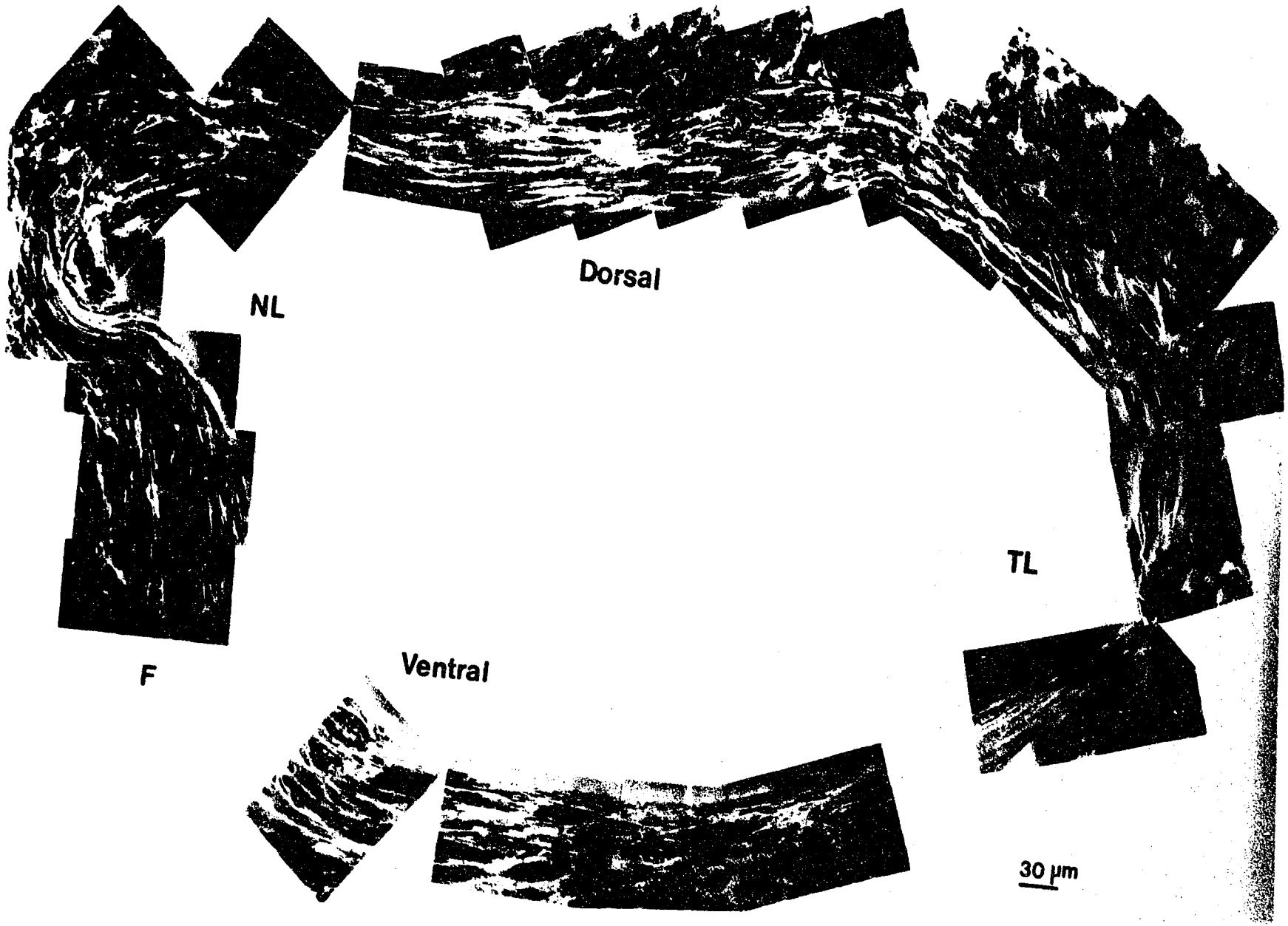
NL
Dorsal
TL
F
Ventral
30 µm

and retain the spindle to roughly rectangular shape (refer to figure 3-4 A).

In conclusion, the actin cytoskeleton loses its original organization, and the amount of actin is consistently increased with preferential condensations of the AFB at the basal and the apical region of the cells at stages 2 and 3. The latter finding is consistent with observations of other investigators in which microfilaments were found to be increased mainly at the basal region of the extensions of cells (Dumont & Yamada 1977, Reyer 1990a). These investigators suggested that the increase of actin is associated with depigmentation. The increase of AFBs is also accompanied by 3-5 fold increase in size of cells resulting from cell growth at early phases of depigmentation (Dumont & Yamada 1972) and active metabolic synthetic activities of the cell (Yamada 1967b, 1977). It is possible that the increase in the amount of actin is achieved through elevation of synthesis of this protein. Thickening of the AFBs could also be due to synthesis or polymerization of new actin filaments, and contraction of the AFBs.

In stages 5 and 6, while cells undergo rapid proliferation, the actin cytoskeleton is reorganized completely and this process is accompanied by changes of cell shape. In flat mounts of regenerates, the staining of the longitudinal AFBs in the spindle shaped dedifferentiated cells gradually disappears and is replaced by a more intense staining of actin which is accumulated circumferentially to delineate the polygonal outlines of these cells of the lens vesicle (figure 3-4 A, B). These changes reflect the differential organization of actin filaments in different regions of the lens vesicle in which cells in the central region are more advanced than those in the lens stalk. Since the cells in these three regions are possibly at different phases of regeneration, the differential organization of F-actin may be related to changes in cell shape from elongated in the newly depigmented cell to polygonal in the redifferentiating cells. These changes in organization of actin and in the associated cell shape are accompanied by an increased proliferative activity in the lens regenerate (Eguchi & Shingai 1971) which results in a significant increase in cell numbers

(Yamada & Roesel 1971) and a temporal pseudostratification of lens vesicle (figure 3-4 E). Correspondingly, observed in sagittal sections, the punctate staining of AFBs in the normal and dedifferentiated cells (refer to figure 2-5 C, 3-2 D) is changed to become, at this level of resolution, almost like a continuous band in the cortical region of cells situated at the central region of lens vesicle (figure 3-4 E). The staining in redifferentiating cells appears to be more prevalent and intense than that in the newly dedifferentiated cells.

Starting from stage 6, the polygonal shaped cells at the central region of the internal lens vesicle undergo elongation to form lens fibers, the process continues through stages 7 to 10. The elongation of cells along their apico-basal axis is associated with the deposition of actin at the cortical regions of the cells along the same axis (Figs 3-4 C, D). Actin is also present in the apical and the basal areas (figure 3-4 C, D). In the latter regions actin staining is much more prominent than in the lateral region of the redifferentiating cells. The accumulation of actin at the apical, and more prominently at the basal regions of the elongating cells, may be important in directing the elongation of the redifferentiating lens fibers. Furthermore, from the intensity of phalloidin staining in the redifferentiating cells, one gets a strong impression that the concentration of actin increases markedly during redifferentiation.

Observations on flat mounts of iris rings stained with labelled phalloidin indicate the changes in abundance and organization of AFBs occur in all PMCs of the internal and the external P-ring iris epithelium (figure 3-3, 3-5). The changes in organization and abundance of actin filaments or AFBs also take place in PECs of the internal M and J ring, and the changes vary in different regions of IE (not shown). However, no obvious changes in organization and abundance of actin staining are observed in PECs of the external M and J ring iris (figure 3-5).

Figure 3. 4. Changes of F-actin during redifferentiation in cell-type conversion.

A, and B, are flat mounts of stage 5 regenerates showing the same lens vesicle from its internal and external faces; C, and D, are sagittal sections of stages 6 and 8 regenerates. A, and B, display the developing lens vesicle. At the lens stalk area (ls), the newly dedifferentiated cells are approximately spindle shaped (small arrow A), and their longitudinal AFBs appear to be oriented parallel to the pupillary margin (small arrow in B). In the central region (lc) of the developing lens vesicle, the cells which are at more advanced phases of redifferentiation are lacking longitudinal AFBs. Instead, these cells acquire the irregularly oriented short AFBs (large arrow in B) and the circumferentially organized AFBs; the latter can be observed as polygonal outlines of cells (large arrow in A). In the region between the lens stalk and the central region of the lens vesicle, there are short AFBs oriented parallel to the pupillary margin; these short AFBs appears like severed longitudinal AFBs (arrowhead in B). C, and D, show that in the elongating lens fiber cells, the lateral cortical AFBs appear to be organized along the apico-basal axis of the cells (long and large arrow), randomly organized AFBs are accumulated in the cytoplasm at the basal and apical regions of the cells next to the cortical actin (small arrows). E, external layer of the IE; I, internal layer of the IE.

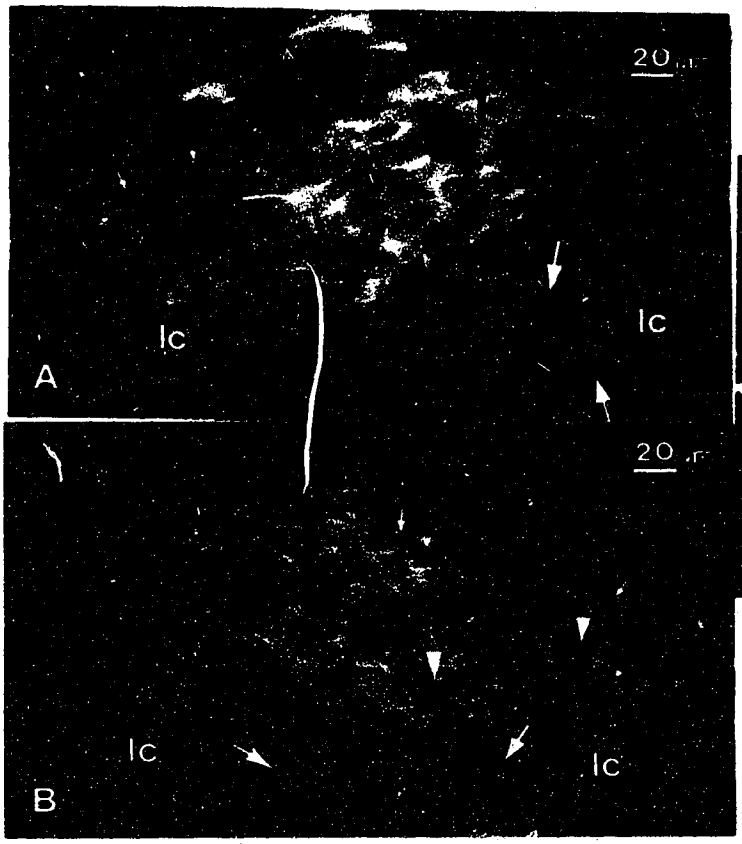
20 µm
lc
lc
A
20 µm
lc
lc
B

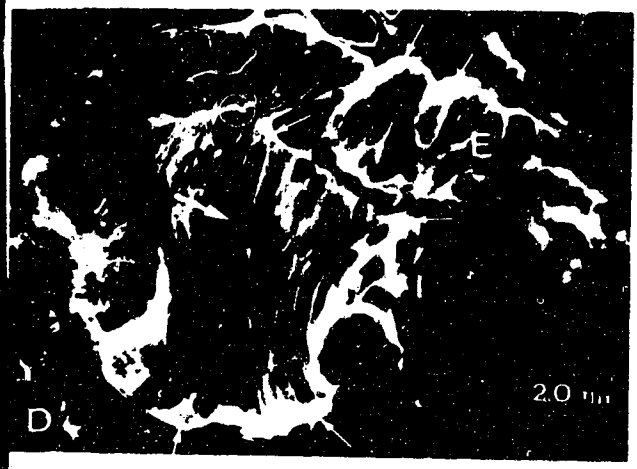
E
I
2.0 µm
D

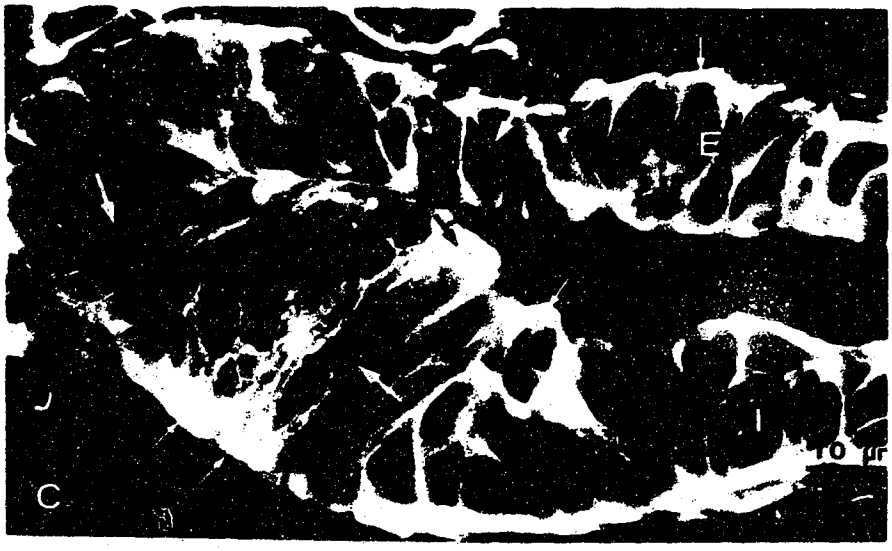
I
E
I
C

Figure 3. 4. Changes of F-actin during redifferentiation in cell-type conversion.

E, is a sagittal section of a stage 6 regenerate showing that actin staining appears like a continuous band delineating the temporally pseudostratified cells (arrow). Bar = 10 μm.

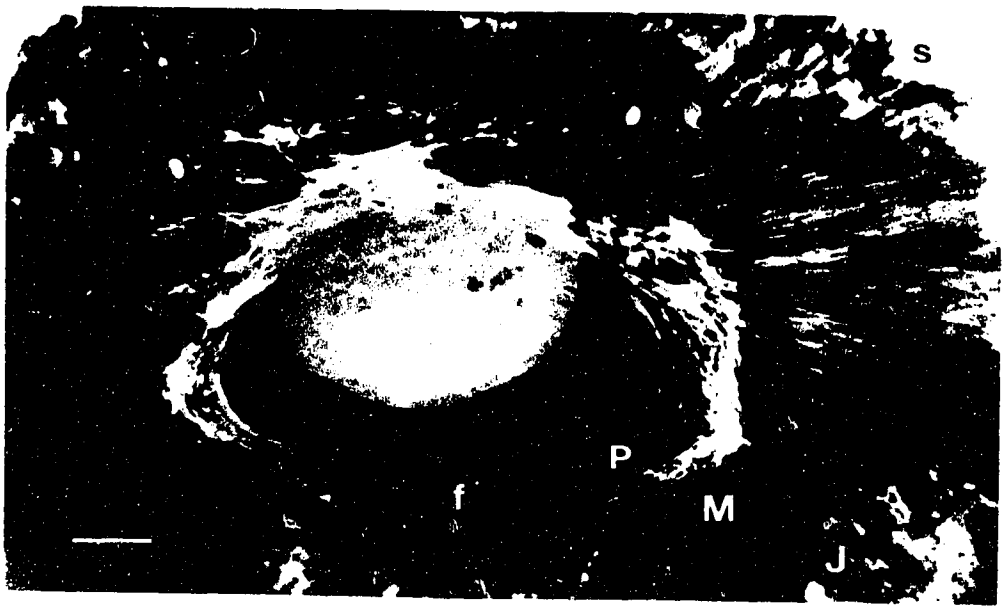

Figure 3. 5. Distribution of F-actin in a whole mount of iris tissue in a stage 8 regenerate.

This photograph shows a stage 8 regenerate visualized from its external side after removal of stroma. In the external layer of pigmented myoepithelial cells of the P-ring, the prominent staining of AFBs is observed as those thickened, clustered and branched AFBs present in the internal layer of PMC of the P-ring iris of stage 2 (figure 3-2, 3-3). In cells of the external M-and J-ring iris, the longitudinal AFBs are oriented radially along the center of the iris ring; these AFBs are thinner than those AFBs present in PMC s of the P-ring of the iris, and the staining is much less intense than that of the former. L, lens vesicle; ls, lens stalk; P, P-ring; M, M-ring; J, J-ring of iris epithelium; s, the undetached stroma tissue.

Changes in vinculin during lens regeneration.

Starting from stage 2, flat mount preparations of iris rings show the preferential accumulation of vinculin staining at the basal intercellular regions along the AFBs and at the termini of AFBs at the tips of cells (figure 3-6 A). These changes occur as the AFBs are thickened, clustered and branched at the basal region, the latter process is also accompanied by a change of cell shape, increase in cell size and expansion of the intercellular space. Sagittal sections show that vinculin is retained at the lateral, apical as well as the basal areas of the depigmenting cells (figure 3-6 B). In dedifferentiated and depigmented cells and in cells undergoing early redifferentiation, vinculin is still present at the apical, lateral and basal surfaces of the cells as punctate staining (figure 3-6 C). As differentiation into lens fibers progresses, vinculin gradually disappears from the elongating lens fiber cells at the central region of the lens vesicle (figure 3-6 D). In cells at the most advance stages of lens fiber differentiation, vinculin is absent from the apical and lateral surfaces and is retained at the basal region of the lens fibers (not shown). Vinculin, when present, always colocalizes with actin (figure 3-6 A). Due to the disappearance of vinculin, there are areas in the redifferentiating cell that are rich in actin, but do not express vinculin.

Figure 3. 6. Changes in vinculin during cell-type conversion

A, is a flat mount of the regenerate at stage 2; B, C, and D, are sagittal sections of regenerates of stages 3, 5 and 6-7 respectively. A, shows the cells of the P-ring of the dorsal iris that is double stained with rhodamine phalloidin and anti-vinculin antibodies. In this figure, the fluorescent staining of vinculin is focused displaying green colour; and actin staining is also visible as the reddish brown band because of the leakage of the rhodamine fluorescence (arrowhead). Vinculin is also shown at the basal intercellular areas (small arrow) and at the termini of the AFBs at the end of the cells (large arrow). B, shows the punctate staining of vinculin at the basal, lateral and apical regions of the partially dedifferentiated cells. C, shows that vinculin staining is present at the basal (arrowhead), lateral and apical (arrow) regions of cells at the early redifferentiation. D, shows that at the central region of the internal layer of lens vesicle, the cells that are initiating elongation have weak vinculin staining (*). Each bar = 10 μm.


A
D
C

3. 3. C. CYTOKERATIN-II

Cytokeratin in the normal iris epithelium.

As described in chapter 2, mostly in the PMC of the internal P-ring, cytokeratin II is organized as thick longitudinal fibers oriented along the long axis of cell. These fibers are oriented parallel to each other and to the pupillary margin, an organization similar to that of the AFBs. Under the electron microscope, the alignment of intermediate filaments (their thickness is in the range of 8-16 nm) with microfilaments has also been observed at the cortical region of the cell, suggesting a possible association of these two type of cytoskeletal proteins (not shown). As observed in flat mounts of the normal iris, these cytokeratin-II fibers are also interconnected by a network of finer fibers (figure 2-8 D). In sections, cytokeratin is present mostly in the internal PMCs throughout the cytoplasm, here it occurs peripheral to the nucleus as a mesh that surrounds the pigment granules (figure 3-7 A). If the tissue is fixed with methacarn and embedded in paraffin, sections show the staining present mainly in the peripheral region of cells (chapter 2-8 E). Since the PMC has abundant desmosomes scattered along the apical and lateral surfaces (chapter 2), in these regions, cytokeratin-II might be associated with these junctions.

Changes in cytokeratin during lens regeneration.

Changes in cytokeratin-II were studied in sections of iris regenerates. As the depigmenting cells form cytoplasmic projections at stage 2, this protein is present in the cytoplasm of the cells surrounding the melanosomes (figure 3-7 B, C). With the advance of the depigmentation process when the melanosomes are shed or transported into the peripheral regions of the cells, cytokeratin-II is also located in the areas close to the nucleus where the number of melanosomes is low (figure 3-7 D). This staining is more intense than that at the peripheral region where melanosome numbers are large. In the latter case, cytokeratin-II might be discharged together with cytoplasmic fragments during cytoplasmic

Figure 3. 7. Changes of cytokeratin II during dedifferentiation in cell-type conversion.

A, is a normal iris; B, C, and D, are regenerates of stages 1, 2 and 3 respectively. A, B, and C, are sagittal sections of the P-ring in the dorsal region of iris, while D, is a section of the P-ring in the ventral region of iris. A, shows that in the normal PMC, cytokeratin II is present throughout the cytoplasm surrounding the pigment granules (arrow). B, shows cytokeratin-II staining in the cells that are at the early phases of depigmentation. C, shows cytokeratin-II staining in the cells at the intermediate phases of depigmentation. D, shows cytokeratin-II staining in the cells at the advanced phases of depigmentation. The intense staining of cytokeratin-II (arrow in D) is located in the cytoplasm surrounding the nucleus (n). From the augmentation in the intensity of staining, it appears that this protein increases progressively during the process of dedifferentiation and depigmentation. E, external layer of the IE; I, internal layer of the IE; S, stroma; n, nucleus; each bar =10 μm.

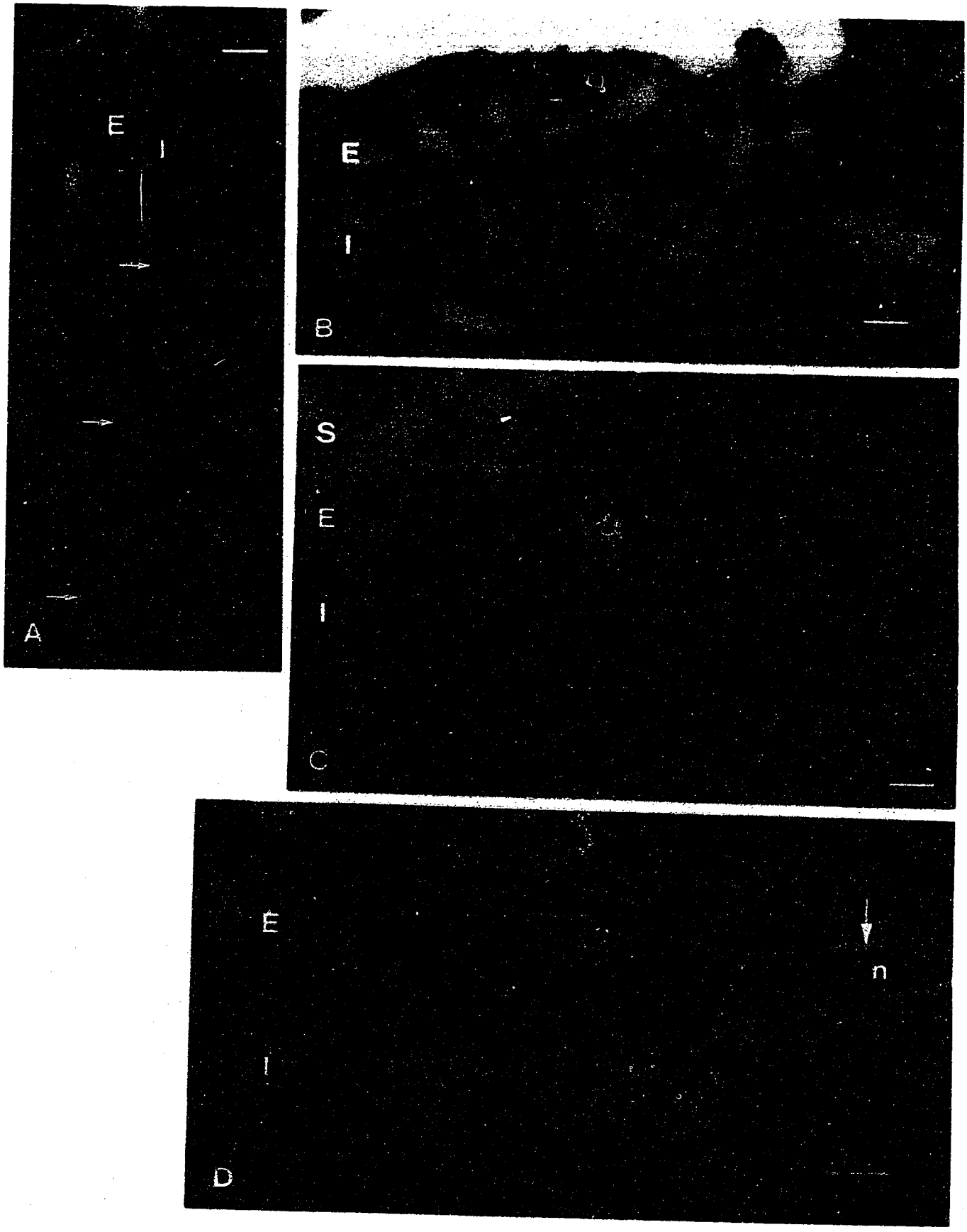
E
I
A
E
I
B
S
E
I
C
E
n
I
D

Figure 3. 8. Changes of cytokeratin II during redifferentiation in cell-type conversion.

A, and B, are sagittal sections of the dorsal iris at stages 5-6, and 7 of regeneration. A, shows the decrease of cytokeratin-II staining in the cells at the central region of lens vesicle (arrowhead). B, shows mainly the lens stalk area of a lens vesicle. To the left is the region of the lens regenerate. Observe absence of cytokeratin-II staining in the nascent lens fibers (arrowhead), and in most of the cells of the external layer of regenerate (large arrow). Only a few cells in the stalk area are stained (small arrow). E, external layer of the lens vesicle; I, internal layer of the lens vesicle; each bar =10 μm.


E
I
A


E
I
B

Figure 3. 8. Changes of cytokeratin II during redifferentiation in cell-type conversion.

C, and D, are sagittal sections of the dorsal iris at stage 8 of regeneration. These two figures show the same tissue that is double stained with anti-cytokeratin II antibodies and with DAPI for DNA. C, shows that only a few cells express cytokeratin-II at the lens stalk region (small arrow). In D, it can be observed that some of the cells in mitosis express cytokeratin -II (small arrow in C and large arrow in D). E, external layer of the lens vesicle; I, internal layer of the lens vesicle; each bar =10 μm.


E
I
C

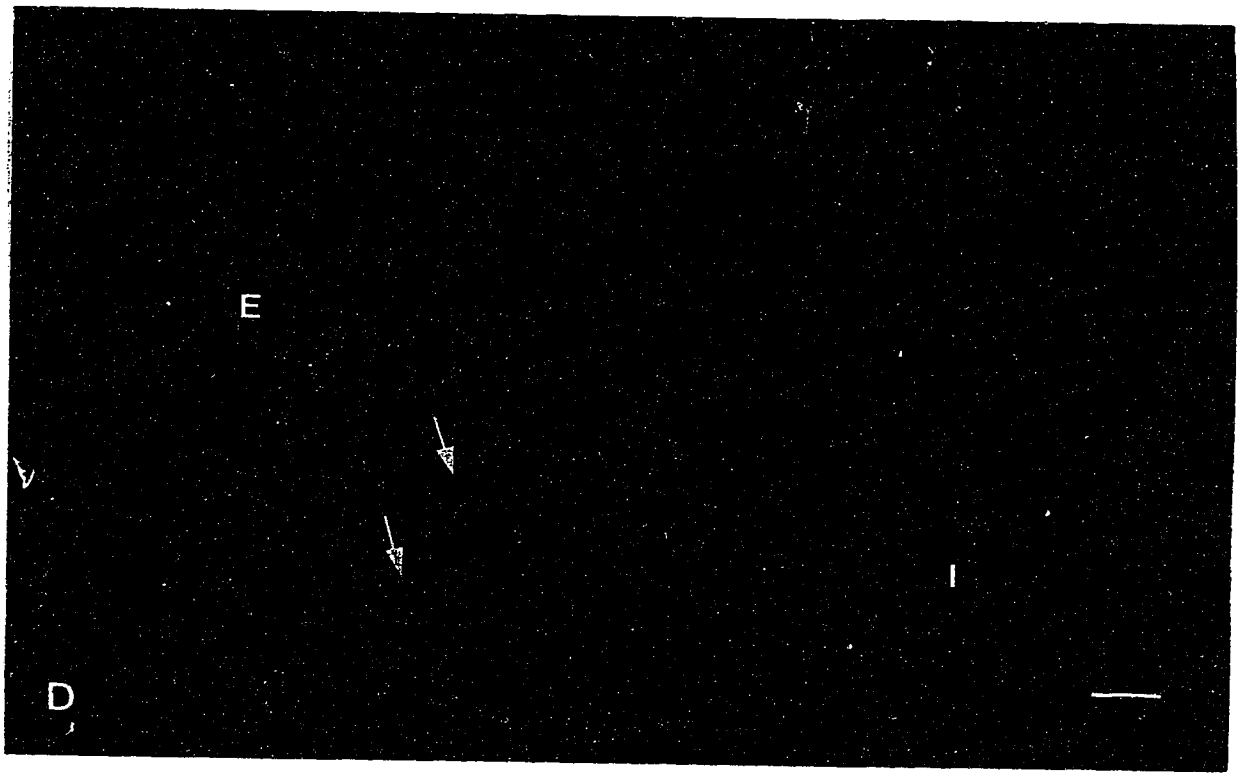
E
I
D

shedding. In the newly depigmented cells, cytokeratin II staining is seen as a thick band or network in the cytoplasm surrounding the nucleus. From the augmentation in the intensity of staining, it appears that starting from stage 2 of regeneration, this protein increases progressively, suggesting an up regulation of expression of this protein during dedifferentiation.

As redifferentiation into lens fibers occurs, cytokeratin-II disappears gradually, first from the elongating lens fiber cells in the internal layer of the lens vesicle, and subsequently from the cells of the external layer (figure 3-8 A, B). In these regenerates, some cells that express cytokeratin at stage 8 are present in the lens stalk and undergo mitosis as shown by their mitotic figures (figure 3-8 C, D). The expression of this protein is down regulated during lens fiber redifferentiation. In addition, vimentin is not detected in the regenerates up to stage 8 by immunofluorescent staining.

Table 3-1 shows the number of normal irises and of regenerates used in studies of F-actin, vinculin and cytokeratin during regeneration.

Table 3-1. Number of normal irises and of regenerates used in studies of F-actin, vinculin and cytokeratin during regeneration.

Stages of regeneration	Days of regeneration	Nº of the newts used				
		Actin		Vinculin		Cytokeratin
		F*	S*	F*	S*	S*
normal	0	8	11	6	6	4
1	1-7	6	5	3	5	2
2	6-13	12	7	2	5	4
3	7-18	8	3	1	5	2
4	14-24	5	6	3	5	8
5-6	16-24	8	4	4	4	3
7	18-24	3	3	1	2	3
8	21-23	7	3	3	2	2
9-10	24-35	6	2	1	1	2

F* = flat mounts; S* = sections.

3. 4. DISCUSSION

In these studies labelled phalloidin and immunocytochemistry were used to investigate the changes in actin, vinculin and cytokeratin during lens regeneration. Results indicate that differential changes in these proteins occur during this example of cell type conversion. In regards to the actin cytoskeleton, a reorganization of this structure occurs during dedifferentiation and redifferentiation, while the expression of actin persists throughout these processes. As judged from staining intensity, actin expression appears to be increased throughout these processes. In the normal iris, vinculin colocalizes with the AFB in the PMC, persists during dedifferentiation, and subsequently disappears from the redifferentiating lens fiber. In the PEC of the normal iris, cytokeratin II is present in filaments with a similar orientation to that of AFB. From the staining intensity, it appears that the expression of this protein increases during dedifferentiation and is down regulated in the redifferentiating lens fiber.

The findings in regards to the reorganization of F-actin during regeneration are of interest and may explain previous work of Hornsby and Zalik (1977). In these experiments, regenerates at dedifferentiation stages were exposed to cytochalasin B *in vitro* and implanted back into host lentectomized eyes. In these experiments, cytochalasin B was found to have no effect on the progression of regeneration. Functionally, cytochalasin B, resembles actin filament capping proteins which are involved in the regulation of actin filament length (Cooper 1987). Since a reorganization of the actin cytoskeleton occurs during dedifferentiation and redifferentiation which probably involves endogenous capping and severing proteins, treatment of regenerates with an exogenous actin filament capping agent would be expected either to have no effect or to stimulate lens regeneration process.

In many regenerative systems such as the neuron (Mizobuchi et al. 1990, Tashiro & Komiya 1991, Koo et al. 1988), liver (Sobczak et al. 1989) and kidney (Cowley et al. 1989)

regeneration, the expression of actin is augmented soon after the initiation of regeneration. As judged from the increase in intensity of staining with labelled phalloidin, the reorganization of the actin cytoskeleton that occurs during lens regeneration is also associated with an increase of cytoplasmic actin, the latter probably due to protein synthesis. This is also supported by electron microscopy observations indicating an increase in the microfilament system during early stages of dedifferentiation (Dumont & Yamada 1972, Reyer 1990a). In the basal and apical regions of the dedifferentiating cells, the thickening and reorganization of the cytoplasmic actin could be involved in the formation and expansion of the cytoplasmic projections that are required for cytoplasmic shedding. At the stages in which cytoplasmic shedding occurs, flat mounts of iris regenerates show the AFBs are thickened at the basal cell surface. It is possible that the contractions of these thickened AFBs could provide the driving force for separating the melanosome-laden cytoplasmic projections from the rest of the body of the depigmenting cell. In addition, changes in the organization of the actin cytoskeleton could also result in increase in the extracellular space and changes in cell shape during lens regeneration, and be associated with formation of the contractile ring in dividing cells. The fact that, in the elongating lens fibers, actin is accumulated at the peripheral region of the elongating fibers specifically in the basal and apical regions of these cells, suggest that actin could also be involved in lens fiber elongation. In other developmental systems, the reorganization of the actin cytoskeleton could involve preexisting actin as well as newly synthesized actin (Tashiro & Komiya 1991).

The changes in the actin cytoskeleton have been investigated mostly using phalloidin as a labelled ligand which binds mainly F-actin. In the PMCs of the newt iris, the F-actin was found, at the present time, to contain two isoforms, α and γ muscle and α smooth muscle actins (chapter 2). It would be of interest to determine the types of actin isoforms that are involved in the reorganization of the actin cytoskeleton. Experiments

need to be conducted using antibodies to specific actin isoforms in order to investigate this problem.

Vinculin is an actin binding protein that is involved in the association of filamentous actin with adhesive macromolecules such as adherens junctions in regions of cell to cell contact, or to regions of cell substrate contact such as focal adhesions (Geiger 1979, Geiger et al. 1980, Geiger et al. 1981, Geiger et al. 1985, Opas et al. 1985, Opas & Kalnins 1985, Drenckhahn & Franz 1986). In the PMC the localization of vinculin in areas of cell -cell contact and cell-ECM contact is consistent with both of the above -mentioned functions. Since actin colocalizes with A-CAM (Chapter 4), it is reasonable to assume that A-CAM and vinculin may also be colocalized in these areas, suggesting a membrane association of actin, vinculin and A-CAM in the normal iris epithelium. This transmembrane association has been reported in areas of intercellular contact in avian and mammalian tissue (Volk & Geiger 1986a, 1986b, Hirano et al. 1987, Miyatani et al. 1989). The colocalization of these proteins at the basal region of the cell suggests that in the newt iris epithelium, a similar association of the actin skeleton with the cell membrane also occurs in areas of cell-ECM contact. This may be a special case since, in other species, vinculin is found in association with actin and integrins in areas of cell-substrate contact (Burridge et al. 1988, Burridge & Fath 1989). During dedifferentiation vinculin accumulates differentially at the edges of the spindle-shaped cells that are dedifferentiating. At these stages there is also an increase in the intercellular space. The preferential accumulation of vinculin may be involved in maintaining the binding of actin to the cell membrane in regions where cell -cell contact is broken and A-CAM is significantly reduced (chapter 4). This case may be different from that in cultured cells in which once cell-cell contact through A-CAM is disrupted, the actin cytoskeleton collapses (Volk and Geiger 1986b, Volberg et al. 1986). During redifferentiation, vinculin disappears from the apical and lateral surfaces of the elongated lens fiber cells. A similar change also occurs to its associated A-CAM on the cell surface

(see chapter 4). In both cases, disappearance of these two molecules occurs in areas of the elongating and elongated lens fiber cells that are rich in actin, but do not express vinculin and A-CAM. This dissociation of actin from vinculin and A-CAM appears to occur mainly in the regions of the cell to cell contact.

In the normal iris cell, cytokeratin II is observed organized as longitudinal filaments aligned with the AFBs. This raises the possibility that the intermediate filament system in which this protein is localized is associated with the actin cytoskeleton as noticed in other systems (Green et al. 1987). This protein increases during dedifferentiation and is down regulated in the differentiating lens fiber. The presence of cytokeratin II in the dedifferentiated cells suggest that these cells still retain their epithelial phenotype. At the present we do not know the functional role that this increase in cytokeratin expression may have in dedifferentiation.

3. 5. LITERATURE CITED

Amsterdam A, Rotmensch S, Ben-Ze'ev A. 1989. Coordinated regulation of morphological and biochemical differentiation in steroidogenic cell: the granulosa cell model. TIBS 14:377-382.

Bacallao R, Fine L G. 1989. Molecular events in the organization of renal tubular epithelium: from nephrogenesis to regeneration. Am. J. Physiol. 257:913-924.

Ben-Ze'ev A. 1986. The relationship between cytoplasmic organization, gene expression and morphogenesis. TIBS. pp. 478-481.

Burridge K, Fath K, Kelly T, Nuckolls G, Turner C. 1988. Focal adhesions: transmembrane junctions between the extracellular matrix and the cytoskeleton . Annu. Rev. Cell Biol. 4:487-525.

Burridge K, Fath K. 1989. Focal contacts: transmembrane links between the extracellular matrix and the cytoskeleton. BioEssays. 10:104-108.

Bussolati G, Alfani V, Weber K, and Osborn M. 1980. Immunocytochemical detection of actin on fixed and embedded tissues: its potential use in routine pathology. J Histochem. Cytochem. 28:169-173.

Coleman A W, Maguire M J, Coleman J R. 1981. Nithramycin and 4'-6-Diamidino- 2-Phenylindole (DAPI)-DNA staining for fluorescence microspectrophotometric measurement of DNA in nuclei, plastids and virus particles. J. Histochem. Cytochem. 29:959-968.

Cooper J A. 1987. Effects of cytochalasin and phalloidin on actin. J. Cell Biol. 105:1473-1478.

Cowley B D Jr, Chadwick L J, Grantham J J, Calvet J P. 1989. Sequential protooncogene expression in regenerating kidney following acute renal injury. J. Biol. Chem. 264:8389-8393.

Drenckhahn D, Franz H. 1986. Identification of Actin, α-actinin, and vinculin containing plaques at the lateral membrane of epithelial cells. J. Cell Biol. 102:1843-1852.

Dumont J N, Yamada T. 1972. Dedifferentiation of iris epithelial cells. Dev. Biol. 29:385-401.

Eguchi G, Shingai R. 1971. Cellular analysis on localization of lens forming potency in the newt iris epithelium. Devel. Growth Differ. 13:337-349.

Eguchi G. 1963. Electron microscopic studies on lens regeneration. I. Mechanism of depigmentation of the iris. Embryologia. 8:47-64.

Eguchi G. 1964. Electron microscopic studies on lens regeneration. II. formation and growth of lens vesicle and differentiation of lens fibers. Embryologia. 8:247-287.

Eisenberg S, Yamada T. 1966. A study of DNA synthesis during the transformation of the iris into lens in the lentectomized newt. J. Exp. Zool. 162:353-368.

Elgert K, Zalik S E. 1989. Fibronectin distribution during cell-type conversion in newt lens regeneration. Anat. Embryol. 180:131-142.

Estes J E, Selden L A, Gershman L C. 1981. Mechanism of action of phalloidin on the polymerization of muscle actin. Biochemistry. 20:708-712.

Geiger B. 1979. A 130K protein from chicken gizzard. Its localization at the termini of microfilament bundles in cultured chicken cells. Cell 18:193-205.

Geiger B, Tokuyasu K T, Dutton A H, Singer S J. 1980 Vinculin, an intracellular protein localized at specialized sites where microfilament bundles terminate at cell membranes. Proc. Nati. Acad. Sci. USA. 77:4127-4131.

Geiger B, Dutton A.H, Tokuyasu K T, Singer S J. 1981. Immunoelectron microscope studies of membrane-microfilament interaction: distributions of α-actinin, tropomyosin, and vinculin in intestinal epithelial brush border and in chicken gizzard smooth muscle cells. J. Cell Biol. 91 614-628.

Geiger B, Volk T, Volberg T. 1985. Molecular heterogeneity of adherens junctions. J. Cell Biol. 101:1523-1531.

Geiger B. 1989. Cytoskeleton-associated cell contacts. Current Opinion in Cell Biology. 1:103-109.

Geiger B. 1991. Adherin' with cadherin. Current Biol. 1:237-238.

Gottlieb A. 1990. The endothelial cytoskeleton: organization in normal and regenerating endothelium. Toxicol. Pathol. 18:603-617.

Green K J, Geiger B, Jones J C R, Talian J C. 1987. The relationship between intermediate filaments and microfilaments before and during the formation of desmosomes and adherens-type junctions in mouse epidermal keratinocytes. J. Cell Biol. 104:1389-1402.

Hatta K, Takeichi M. 1986. Expression of N-cadherin adhesion molecule associated with early morphogenetic events in chick development. Nature, Lond. 320:447-449.

Hatta K, Okada T S, Takeichi M. 1985. A monoclonal antibody disrupting calcium-dependent cell-cell adhesion of brain tissues: Possible role of its target antigen in animal pattern formation. Proc. Natl. Acad. Sci. USA 82:2789-2793.

Hirano S, Nose A, Hatta K, Kawakami A ,Takeichi M. 1987 Calcium-dependent cell-cell adhesion (cadherins): subclass specificities and possible involvement of actin bundles. J. Cell Biol. 105: 2501-2510.

Hornsby S, Zalik S E. 1977. Redifferentiation, cellular elongation and cell surface during lens regeneration. J. Embryl. Exp. Morph. 39:23-43.

Koo E H, Hoffman P N, Price D L. 1988. Levels of neurotransmitter and cytoskeletal protein mRNAs during nerve regeneration in sympathetic ganglia. Brain Res. 449:361-363.

Kulyk W M, Zalik S E. 1982. Synthesis of sulfated glycosaminoglycans in the newt iris during lens regeneration. Differentiation 23:29-35.

Kulyk W M, Zalik S E, Dimitrov E. 1987. Hyaluronic acid production and hyaluronidase activity in the newt iris during lens regeneration. Exp. Cell Res. 172:180-191

Lazarides E, Woods C. 1989. Biogenesis of the red blood cell membrane-skeleton and the control of erythroid morphogenesis. Annu. Rev. Cell Biol. 5:427-452.

McDevitt D S. 1989. Transdifferentiation in animals a model for differentiation control. *In*: Developmental Biology: a comprehensive synthesis. Vol. 6. M. DiBerardino, L. Etkin, eds. Plenum Publ.

Miyatani S, Shimamura K, Hatta M, Nagafuchi A, Nose A. 1989. Neural cadherin: role in selective cell-cell adhesion. Science. 245: 631-635.

Mizobuchi T, Yagi Y, Mizuno A. 1990. Changes in α-tubulin and actin gene expression during optic nerve regeneration in frog retina. J. Neurochem. 55:54-59.

Nagata K, Ichikawa Y. 1984. Changes in actin during cell differentiation. *In*: Cell and muscle motility. Vol 5.J W Shay, ed. Plenum Press, New York and London.

Opas M, Kalnins V I. 1985. Light-microscopic analysis of focal adhesions of retinal pigmented epithelial cells. Invest. Ophthalmol. Vis. Sci. 27:1622-1633.

Opas M, Turksen K, Kalnins V I. 1985. Adhesiveness and distribution of vinculin and spectrin in retinal pigmented epithelial cells during growth and differentiation *in vitro*. Dev. Biol. 107: 269-280.

Osborn M, Weber K. 1982. Immumofluorescence and immunocytochemical procedures with affinity purified antibodies. Tubulin-containing structures. *In*: Methods in Cell Biology. L Wilson, ed. 24:9 .2.

Reyer R W. 1990a. Macrophage invasion and phagocytic activity during lens regeneration form the iris epithelium in newts. Am. J. Anat. 188:239-344.

Reyer R W. 1990b. Macrophage mobilization and morphology during lens regeneration form the iris epithelium in newts: studies with correlated scanning and transmission electron microscopy. Am. J. Anat. 188:345-365.

Russel W W. 1975. A simple cytochemical technique for demonstration of DNA in cells infected with mycoplasmas and viruses. Nature. 253. 461-462.

Sobczak J, Tournier M F, Lotti A M, Duguet M. 1989. Gene expression in regenerating liver in relation to cell proliferation and stress. Eur. J. Biochem. 180:49-53.

Stone L S. 1967. An investigation recording all salamanders which can and cannot regenerate a lens from the dorsal iris. J. Exp. Zool. 164: 87-104.

Takata C, Albright J F, Yamada T. 1964a. Study of lens antigens in the developing newt lens with immunofluorescence. Expl. Cell Res. 34:207-210.

Takata C, Albright J F, Yamada T. 1964b. Lens antigens in a lens-regenerating system studied by the immunofluorescent technique. Dev. Biol. 9:385-397.

Takata C, Albright J F, Yamada T. 1966. Gamma-crystallins in Wolffian lens regeneration demonstrated by immunofluorescence. Dev. Biol. 14:382-400.

Tashiro T, Komiya Y. 1991. Changes in organization and axonal transport of cytoskeletal proteins during regeneration. J. Neurochem.56:1559-1563.

Volberg T, Geiger B, Kartenbeck J, Franke W W. 1986. Changes in membrane microfilament interaction in intercellular adherens junction upon removal of extracellular Ca^{2+} ions. J. Cell Biol. 102:1832-42.

Volk T, Geiger B. 1984. A 135-kd membrane protein of intercellular adherens junctions. EMBO J. 3:2249-2260.

Volk T, Geiger B. 1986a. A-CAM: a 135-kd receptor of intercellular adherens junctions. I. immunoelectron microscopic localization and biochemical studies. J. Cell Biol. 103:1441-1450.

Volk T, Geiger B. 1986b. A-CAM: a 135-kd receptor of intercellular adherens junctions. II. antibody- mediated modulation of junction formation. J. Cell Biol. 103;1451-1464.

Wessells N K, Spooner B S, Ash J F. Bradley M O, Luduena M A, Taylor E L, Wrenn J T, Yamada KM. 1971. Microfilaments in cellular and developmental processes. Science. 171:135-143.

Wieland T. 1977. Modification of actins by phallotoxins. Naturwissenschaften. 64:303-309.

Wieland T, Faulstich H. 1978. Amatoxins, phallotoxins, phallolysin, and antamanide: the biological active components of poisonous *Amanita* mushrooms. CRC Crit. Rev. Biochem. 5:185-260.

Yamada T, Karasaki S. 1963. Nuclear RNA synthesis in newt iris cells engaged in regenerative transformation into lens cells. Dev. Biol. 7: 595-604.

Yamada T, Roesel M E. 1971. Control of mitotic activity in Wolffian lens regeneration. J. Exp. Zool. 177:119-128.

Yamada T, Takata C. 1963. An autoradiographic study of protein synthesis in regenerative tissue transformation of iris into lens in the newt. Dev. Biol. 8:358-369

Yamada T. 1967b. Cellular and subcellular events in Wolffian lens regeneration. Curr. Top. Devl. Biol. 2:247-283.

Yamada T. 1977. Control mechanisms in cell-type conversion in newts lens regeneration. *In*: Monographs in Developmental Biology. Vol.13, A. Wolsky, ed. S. Karger, Basel. pp. 1-126.

Zalik S E, Scott V. 1972. Cell surface changes during dedifferentiation in the metaplastic transformation of iris into lens. J Cell Biol.. 55:134-146.

Zalik S E, Scott V. 1973. Sequential disappearance of cell surface components during dedifferentiation in lens regeneration. Nature (New Biology). 244:212-214.

CHAPTER 4. CHANGES OF A-CAM DURING NEWT LENS REGENERATION

4. 1. INTRODUCTION

Adult urodeles, such as newts, and other species of salamanders have the capability to regenerate a new lens from their dorsal iris after removal of the original ocular lens (Stone 1967). In *Notophthalmus viridescens*, the pigmented epithelial cells (PEC) that give rise to a new lens are located in the pupillary marginal ring of the iris epithelium (IE). In chapter-2 these cells have been recently characterized as pigmented myo-epithelial cells (PMC). Being elongated spindle shaped, these cells are oriented with their long axis parallel to the pupillary margin, enclosing the pupil. As mentioned previously, the IE is organized as a ring shaped and double layered epithelium, when observed in sagittal sections, two layers of PMC adhere on each other at their apical surfaces, and adhere at their basal surfaces to a fibronectin containing extracellular matrix (Elgert & Zalik 1989). During lens regeneration, PMCs in the dorsal iris lose their pigment, dedifferentiate and then redifferentiate to form lens tissue (Yamada 1977). Triggered by lentectomy, lens regeneration is initiated with the activation and transition of PMC form the G0 to the G1 phase of cell cycle which occurs during stage 1 of lens regeneration. This is followed by a general stimulation of metabolic synthesis and cell division (Yamada & Takata 1963, Yamada & Karasaki 1963, Yamada & Roesel 1969). The latter is also associated with depigmentation via cytoplasmic shedding (Dumont and Yamada 1972, Patmore and Yamada 1982), which occurs preferentially during stages 2 and 3 (Yamada 1977). During the above mentioned processes, the intercellular space also expands as the cells undergo pronounced changes in cell shape, emit cytoplasmic projections and discard membrane and cytoplasm-enclosed melanosomes for depigmentation. As the resulting depigmented and

dedifferentiated cell undergoes redifferentiation, the cell shape changes from spindle to cuboidal or round (chapter 2); the process is also accompanied by active cell proliferation (Eguchi & Shingai 1971, Yamada & Roesel 1971). Subsequently, the cell ceases division, undergoes elongation along its apico-basal axes and synthesizes lens the specific proteins, the α, β and γ crystallins (Reyer 1977, Yamada 1977, Yamada & McDevitt 1984). As a result, the pigmented myoepithelial cell is transformed to become a transparent lens cell.

During these processes, the morphological changes of the cell coincide with changes at the cell surface, the associated actin cytoskeleton and the extracellular matrix (ECM). During dedifferentiation the cell surface charge density decreases due to the disappearance of hyaluronidase-, chondroitinase- and neuraminidase-sensitive groups (Zalik & Scott 1972, 1973). Fibronectin, a substrate adhesion molecule that in the normal iris is restricted to the basal lamina of PMC and PEC of the iris, is deposited at the lateral and apical areas of the dedifferentiating cells and subsequently disappears from the cell surface of the redifferentiating lens fibers (Elgert & Zalik 1989). The cortical actin cytoskeleton is also reorganized and the staining of actin appears increased during the whole process of the cell-type conversion (chapter-2). In addition, synthesis of sulfated glycosaminoglycans and hyaluronate in the iris PMC and PECs is increased during dedifferentiation (Kulyk & Zalik 1982, Kulyk et al. 1987). All these observations suggest an involvement of the cell surface molecules in cell-type conversion.

A-CAM (adherens-junction-specific cell adhesion molecule) (Volk & Geiger 1984, 1986a) is a member of the cadherin family of cell adhesion molecules (CAM) that mediate cell-cell binding in a calcium dependent manner. Prominent members of cadherin family also include E-cadherin (epithelial cadherin also called uvomorulin), L-CAM (liver CAM), P-cadherin (placenta cadherin), and N-cadherin (neural cadherin) (Takeichi 1988); A-CAM and N-cadherin (Hatta et al 1985, Hatta et al. 1987, Duband et al 1987, Hatta & Takeichi, 1986) are identical (Duband et al. 1988, Matsuzaki et al 1990). Cadherins are 120-140 kD

transmembrane glycoproteins that are involved in cell adhesion via homophilic interactions of their extracellular domain. Through these cell contacts, cadherins control cell-cell communication and help to maintain cellular and tissue architecture (see reviews Takeichi 1988, 1990, 1991). These functions are best illustrated in experiments performed in the non-adhesive S180 cells which lack A-CAM and L-CAM. Here, transfection with A-CAM or L-CAM genes or both induces binding of the cells, formation of adhesive junctions and gap junction and formation of epithelial-like morphology (Matsuzaki et al 1990). Through their intracellular domain, cadherins also associate with the actin cytoskeleton presumably via vinculin (Volk & Geiger 1986 a, b, Hirano et al. 1987, Nagafuchi & Takeichi 1988). Because of this association, cadherins can affect cell shape and cell motility which in turn can influence cell differentiation (Geiger 1989, Takeichi 1988). If cadherin-mediated cell adhesion is perturbed either by deletion of Ca^{2+} or treatment with antibodies, the actin cytoskeleton collapses and cell shape and cell motility are altered (Volk & Geiger 1986b, Volberg et al 1986).

A current assumption is that differential expression of members of cadherin family during embryogenesis plays an important role in the regulation of morphogenetic events and cell differentiation (Edelman 1988, Takeichi 1988, Geiger et al. 1989, Takeichi 1991). This is supported by the fact that A-CAM or N-cadherin expression is precisely organized spatio-temporally in association with morphogenetic events, involving aggregation, separation and reorganization of the cells (Hatta & Takeichi 1986, Hatta et al. 1987, Duband et al. 1988). In the *Xenopus* embryo, N-cadherin is expressed at neurulation and ectopic expression of N-cadherin in the ectoderm prior to neural induction can lead to morphological defects in neural development (Detrick et al.1990).

Studies of A-CAM or N-cadherin have been mainly carried out in the chick and mouse, and most recently in *Xenopus laevis*. This 135-kD protein is believed to be present in adherens junctions of epithelial cells (Volk & Geiger 1986 a, b, Duband et al. 1988,

Geiger et al. 1989). Although during embryogenesis this molecule is expressed in cells from all three germ layers, it is limited to only a few tissues in the adult including heart, neural tissue and lens (Duband et al. 1988, Hatta et al. 1987). During eye development in the chick and mouse embryo, this molecule is expressed independently in different ocular tissues, though both layers of iris PECs express N-cadherin (Lagunowich & Grunwald 1989). When the lens is induced from the ectoderm by the optic cup, expression of N-cadherin is turned on in the lens placode, this expression become more intense in the growing lens vesicle and is kept at a high levels up to the hatching stage (Nose & Takeichi 1986, Hatta & Takeichi 1986, Hatta et al. 1987, Lagunowich & Grunwald 1989). Recently, N-cadherin has also been detected in the amphibian *X. laevis* where it is present in extracts of early embryonic and adult tissues, among the latter, brain and heart (Detrick et al. 1990, Ginsberg et al. 1991). At the present time, no studies on the changes of this molecule have been performed in the newt system.

As mentioned before, lens regeneration in the adult newt represents a unique case of cell-type conversion. These studies were, therefore, performed to examine whether A-CAM is present in the iris tissue, and if present, to trace its changes in expression and distribution during lens regeneration. These studies could furnish important information to determine if A-CAM plays a role in cell-type conversion. Observations on A-CAM distribution were made on flat mounted iris rings and on sagittal sections of the iris in order to provide a global view on distribution of this protein in iris tissue. The results show that A-CAM is present in both cell-cell and cell-ECM contact regions in the iris PMC and PECs. This protein is reduced or eliminated locally and temporally during dedifferentiation in association with depigmentation, and it is down regulated in most of the lens fiber cells during redifferentiation.

4. 2. MATERIAL AND METHODS

Animals and Lentectomy

Adult newts, *N. viridescens*, were purchased from Lee' s Newt Farm, Oak Ridge, Tennessee. The animals were anesthetized in 0.1 % Tricaine (4-aminobenzoic acid ethyl ester, MS-222, Sigma) in distilled water. For lentectomy, a horizontal incision was made to the cornea, through this incision the lens was carefully clasped with fine forceps and removed. The lentectomized newts were held in declorinated water at room temperature with weekly feedings for different time intervals. Regenerates were staged according to Yamada (1977).

Antibodies, Ligands and Stains

Mouse monoclonal antibodies to A-CAM and to vinculin (ID: 7.2.3. and 11.5) were kindly provided by Drs. Volk and Geiger (Weizmann Inst of Science, Israel). Preliminary experiments were conducted using hybridoma supernatant, subsequently ascites fluid was used. Mouse ascites fluid (NS1) was from Sigma, anti-digoxin antibodies in ascites fluid were kindly supplied by Dr. M. Belosevic (University of Alberta, Canada), and mouse anti-N-CAM and anti-L-CAM antibodies were gifts from Dr. W. Gallin (University of Alberta, Canada). These ascites fluid and antibodies were used as controls. Fluorescein-labelled sheep anti-mouse IgG antibodies were from Amersham; DAPI (4'-6-Diamino-2-Phenylindole) and rhodamine or fluorescein-labelled phalloidin were commercially purchased from Sigma and Molecular Probes.

Immunoblot analysis

Newt hearts and lens and chick heart were homogenized with a Polytron homogenizer at medium speed for 4-5 minutes, in SDS sample buffer (0.414 M glycerol, 0.18 M SDS, 0.139 M Tris, 30 % urea in 1 liter water, pH 6.8), heated for 5 minutes at 95

°C, and centrifuged in a Centra-7R International Centrifuge at 3,000 g for 10 minutes. The supernatant was used for sodium dodecyl sulfate polyacrylamide gel electrophoresis (SDS-PAGE) which, was performed on 7 % slab polyacrylamide gels according to Laemmli (1970) using the Bio-Rad minigel system. For immunoblotting, proteins were transferred electrophoretically onto nitrocellulose sheets in 50 mM Tris-glycine buffer according to Towbin et al. (1979) at 200 mA for 1 hour and 45 minutes. This was followed by 6 to 10 washes with Tris buffered saline (TBS: 40 mM Tris-hydroxymethyl aminomethane (Bio-Rad), 1 mM NaCl, PH 7.5) for two days to remove traces of SDS.

Prior to immunoblotting, blots were blocked in 5 % dry skim milk powder in TBS for 48 hours to renature the proteins (Garlaud et al. 1990). After 3 washes in TBS 10 minutes each, the nitrocellulose was incubated overnight (18-24 hours) with antibody solutions containing mouse anti-A-CAM and anti-vinculin monoclonal antibodies diluted 1:50 in TBS with 1 % BSA (sigma). Following incubation blots were washed twice in 0.05 % Tween-20 (Bio-Rad) in TBS and three times in TBS, each wash 10 minutes. The nitrocellulose was subsequently incubated for 2 hours with peroxidase conjugated rabbit anti-mouse IgG at a dilution of 1:2000 in TBS-BSA, followed by washing as for the primary antibody. In all solutions used above, the $CaCl_2$ was added to a final concentration of 1 mM to protect A-CAM from degradation (Volk & Geiger 1986a, Volk et al. 1990), 0.01 % thimerosal (Sigma) was included as an anti-bacterial agent in the antibody solutions. The color reaction is carried out in HRP color development reagent (Bio-Rad) and hydrogen peroxide in TBS according to Hawkes (1982). Controls consisted of ascites fluid from non-immunized mice and mouse ascites fluid containing anti-digoxin antibody.

Immunofluorescence staining of flat mounted iris tissue

Fixation and manipulation of iris tissue for flat mount preparations have been described in chapter 2. The procedure for removal of iris stroma has also described in the previous section. After fixation and rinsing in A-PBS, the iris was permeabilized in acetone at -20°C for 5 minutes and rehydrated in A-PBS at room temperature for 20 minutes. The iris was incubated for 2 hours in solutions containing anti-A-CAM or anti-vinculin antibodies diluted 1:50 in antibody buffer (1% BSA, 0.1% Triton X-100 in A-PBS). The tissue was then washed with 3 changes of A-PBS, 10 minutes each with gentle shaking. This was followed by an incubation for 1 hour in fluorescein-labelled sheep anti-mouse IgG diluted 1:30 in the above mentioned antibody buffer and by washes in A-PBS as before. Tissues were mounted between two cover slips in Mowiol mounting medium (Osborn and Klaus 1982) (Mowiol 4-88, Calbiochem), modified by the addition of 0.5 g of DABCO (2,4-diazabicyclo (2,2,2) octane, Sigma) per 24 ml of Mowiol solution. Aliquots of this medium were kept in dark at - 20 °C until required. Controls consisted of non-immune mouse ascites fluid and anti-digoxin antibodies as above. To observe the colocalization of A-CAM with F-actin, sections were then incubated in 1.65 X 10^{-6}M rhodamine phalloidin in A-PBS for 30 minutes, followed by three washes in A-PBS for a total of 5 minutes. The double staining can also be achieved by dissolving the rhodamine phalloidin in the buffer containing the secondary antibodies. In some experiments, the nucleus was also stained for reference purposes using DAPI, a drug that binds to DNA (Coleman et al. 1981, Russel 1975). For this purpose, the iris tissues were further incubated for 2-5 minutes in 0.2-0.5 µg / ml DAPI in A-PBS and rinsed as above.

Immunofluorescence staining of sagittal sections of the iris.

After fixation as above, the iris tissue was washed in 3 changes of ice cold solution of 2% sucrose in A-PBS, 10 minutes each with gentle shaking. Tissue was infiltrated

overnight at 4 °C with O.C.T. Tissue Tek compound (Canlab), transferred to a plastic mold, and embedded in O.C.T. by a immediate freezing at -20 °C. Sagittal sections 6 μm in thickness were cut on model 85 (American Optical) or Tissue-TEK II (Miles) cryomicrotomes at -20 to -23 °C. Sections were melted onto microscope slides which had been previously cleaned with 70 % alcohol and coated with a thin film of rubber cement (Lepage's). For incubation with antibodies, the slides were washed in A-PBS to remove the O.C.T. medium. The antibody solutions were added to the sections with a pipette about 20-50 μl per section, incubation with the antibody solutions was carried out in a moist chamber at room temperature as above. The concentrations of the primary and secondary antibodies were as the same as described above. Before each antibody incubation, the sections were rinsed briefly in distilled water, and the remaining fluid was adsorbed with filter paper. Following each antibody incubation, the sections were washed in A-PBS three times with gentle shaking for 10 minutes. The stained sections were mounted in Mowiol and kept in the dark. For double staining of A-CAM with F-actin and triple staining of A-CAM, F-actin and nucleus, the sections were further treated with rhodamine phalloidin and DAPI as described in the above section B.

Microscopical observations were conducted using a Zeiss fluorescence Photomicroscope-III or a Zeiss Axiophot. Photographs are taken using Tri-X Pan black and white film and Kodachrome 200 color film.

4. 4. RESULTS

Immunoblot analysis

The immunoreactivity of anti-chick A-CAM antibodies to newt tissue can be observed in figure 4-1. Here it can be seen that in extracts of newt hearts, these antibodies recognize a band of an approximate relative m.w. of 135 kD that comigrated with a band also present in extracts of chick heart. In contrast, incubation with mouse ascites fluid (NS1) as well as anti-digoxin monoclonal antibodies did not result in staining of the protein bands. Newt and chick extracts were also stained by anti-vinculin antibodies. These antibodies react with a band of an approximate m.w. of 130 kD that, in the chick, runs slightly faster than A-CAM. This result strongly suggests that the antibody against chick A-CAM recognizes the corresponding protein in the newt.

A-CAM in the normal iris epithelium

The iris is mainly composed of a double layered pigment epithelium. This is the result of invagination of the optic vesicle to form the optic cup, with the iris epithelium (IE) developed from the rim of the optic cup. A consequence of this infolding is that the apical regions of the iris epithelial cells (IECs) face each other, while the basal regions of these cells face the eye chambers. The internal layer of the IE is surrounded only by a basal lamina facing the lens, while the external layer of IE has, in addition, a layer of connective tissue, the so called iris stroma apposed to the basal lamina facing the cornea. As a consequence, the epithelial cells contact each other at their apical and lateral surfaces, while they adhere to the extracellular matrix (ECM) at their basal surfaces (figure 1-2). As described in chapter 1, the iris epithelial ring can be divided into three main regions: the pupillary (P) ring, the middle (M) and the junctional (J) rings; the cells in the P-ring IE adjacent to and enclosing the pupil are myoepithelial in nature (figure 2-1 C, 2-2).

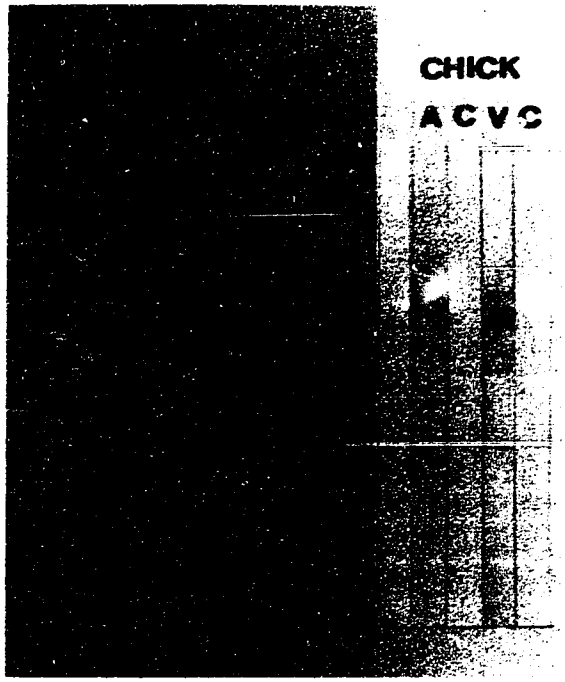

Figure 4-1. Immunoblot analysis of extracts of chick and newt hearts reacted with anti-chick A-CAM (ID 7.2.3.) and anti-chick-vinculin (ID 11.5) monoclonal antibodies, showing antibody specificity. The antibodies recognize A-CAM (A) and vinculin (V) whose molecular weights are very close to each other (approximate 135 kD and 130 kD respectively). The controls (C) were reacted with mouse ascites fluid and show no staining.

Figure 4-2 Distribution of A-CAM in the pigmented myo-epithelial cell (PMC) of the normal iris studied by immunofluorescence.

A, C and E are flat mounts; B, D and F are sagittal sections. E and F have not been stained, to show the intrinsic yellowish fluorescence of PMC. An internal (A) and external (C) view of the iris epithelium (IE), exhibiting staining at the basal and baso-lateral surfaces of the cells (arrow) is shown in the flat mount preparation. To view the external layer of IE in the flat mount shown in C, the stroma was removed manually. In sagittal sections, A-CAM staining is shown in focus at the basal (B arrow), and at the lateral cell surface (D arrow). A, also shows A-CAM staining in the M-ring cells at their basal surface delineating an irregular morphology of the cells (arrowhead). Staining at the apical surfaces of PMC was also observed but is not shown here. S, stroma; E, external; I, internal layer of the IE; P, pupillary ring; M, middle ring of IE; Each bar= 10 μm

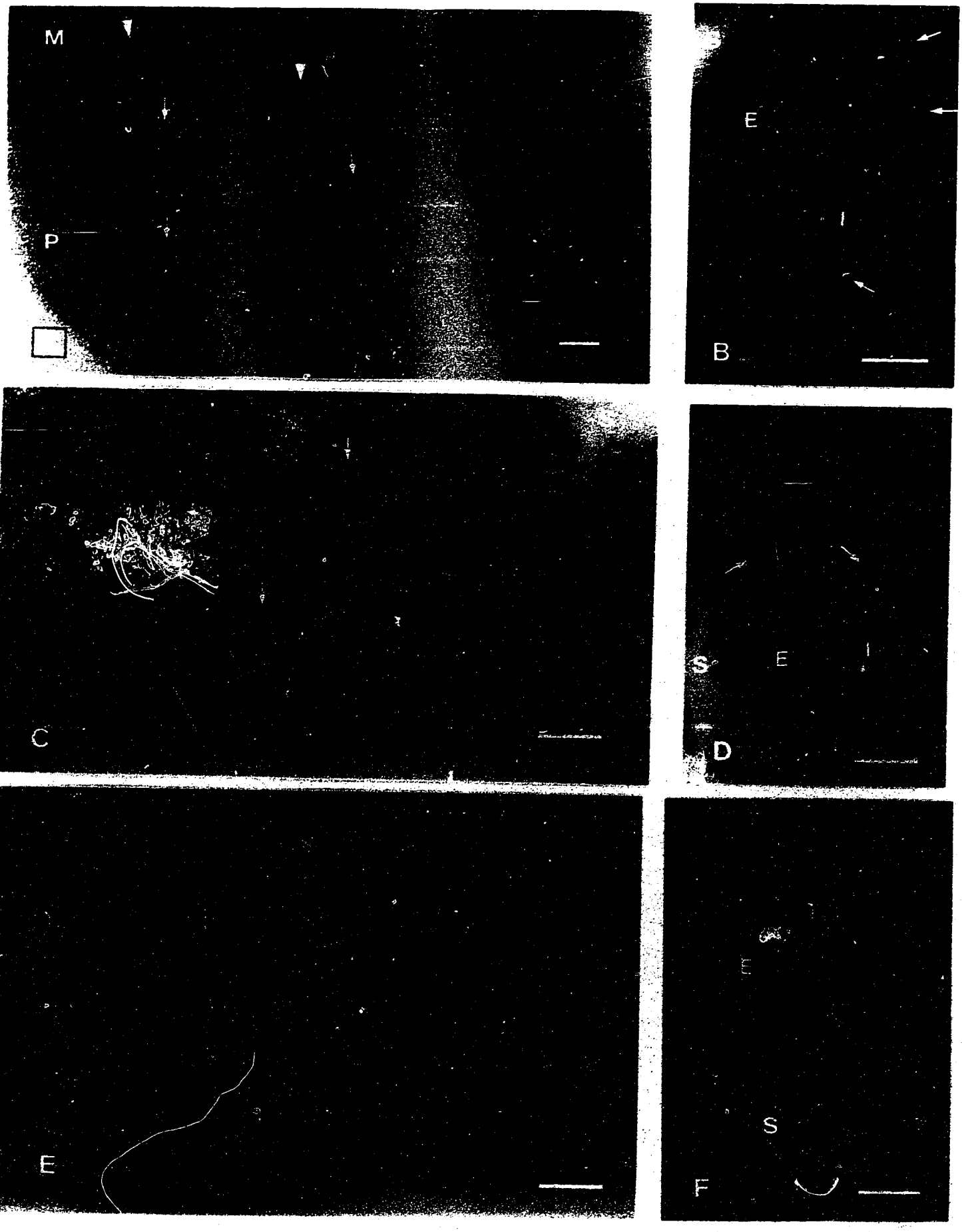
M
P
B
E
I
C
S
E
I
D
E
E
S
F

Since the main focus of my research was on the cell surface characteristics of PMC involved in lens regeneration, i .e., those present in the dorsal P-ring, this report will deal mainly with the cells present in this area.

The iris tissue has a high intrinsic autofluorescence (figure 4-2 E & F) which varies among specimens, so the immunofluorescent staining of the protein present in this tissue has to be viewed against this background. Flat mounts of iris rings when reacted with against A-CAM antibodies, show this protein present as small, round spots located at the basal cell surface and at the basal intercellular areas bordering the spindle shaped PMC (figure 4-2 A). When the stroma is removed from the external layer of IE, a similar pattern of A-CAM staining is observed at the basal surfaces of the external PMC (figure 4-2 C). In iris sections A-CAM is evident as punctate staining at the cell boundary of the basal (fig 4-2 B) and lateral (fig 4-2 D) regions of PMC, this adhesion molecule was also observed at the apical surface of the PMC, but is not shown here. In summary, A-CAM is present in both cell-cell and cell-ECM contact regions in the PMC. When the iris is reacted with mouse ascites fluid (NS1), anti-N-CAM and anti-L-CAM antibodies at the same dilution as that of A-CAM antibodies, the staining is not observed in flat mounts and in sections of the tissue (NS1 is shown in figure 4-3 A & B, others not shown). The presence of A-CAM in areas of contact between the cells and the basal lamina has not been reported previously, in most of the tissues studied so far, this cell adhesion molecule appears to be present only in areas of cell-cell adhesion (Volk & Geiger 1984, 1986 a, b, Takeichi 1988).

Changes in A-CAM during lens regeneration

According to Yamada (1977), newt lens regeneration can be divided in ten stages. Cell dedifferentiation occurs during stages 1-4, while the ensuing a process of redifferentiation during stages 5-10 (figure 1-3). At stage I, cells are first activated to enter the cell cycle, during stages 2 and 3 cells shed their melanosomes with associated

cytoplasm, dedifferentiate and become depigmented, while at stage 4 cells organize into a lens vesicle at the mid-dorsal margin of the iris. During the process of redifferentiation, the cells undergo rapid proliferation (Eguchi & Shingai 1971, Yamada & Roesel 1971) with changes in the cell shape (chapter 3), resulting in an increase in size of the lens vesicle at stages 5-6. Cell elongation and synthesis of lens specific proteins starts in the cells of the internal layer at the central region of the lens vesicle. These cells elongate to form the primary lens fibers during a process that starts at stage 5 and continues to stages 7-8. Subsequently, through stages 8-10, secondary lens fibers are formed at the periphery of the primary lens fibers, and the external layer of the lens vesicle differentiates into the lens epithelium. During these stages, cells in the lens stalk as well as in the external lens vesicle proliferate and contribute more cells to the lens, these cells will eventually cease division and undergo redifferentiation (Yamada 1977).

Dedifferentiation

At the earliest stage of regeneration when cells are activated, A-CAM staining is maintained at the apical, lateral and basal regions of the epithelial cell surfaces (figure 4-3 C, D, E). From visual inspection, the staining intensity for this molecule seems to be increased (figure 4-3 C). As cells depigment and dedifferentiate during stages 2 and 3, A-CAM is either significantly reduced or disappears from the basal, baso-lateral and apical areas of cell surface (figure 4-3 F, G: a, b), but remains in the mid-lateral area (figure 4-3 G and 4-4 A). The decrease in A-CAM is a sequential process, starting from the basal and followed by the apical regions of the cells. According to my observations, the cytoplasmic projections involved in shedding of the pigment granules with associated cytoplasm are produced in two locations, first at the basal compartment and subsequently at the apical compartment of the cells of stages 2-3 regenerates. The selective elimination of A-CAM may be important in establishing discrete areas at the cell surface free of cell adhesion molecules which may be required for depigmentation or cytoplasmic shedding.

Figure 4-3. Distribution of A-CAM in the dedifferentiating cells at stages 1 and 2 of regeneration.

A, D and F are flat mounts, while B, C, E, G and H are sagittal sections of the tissue. B, shows normal iris tissue (non-regenerate); C, D and E are the irises at stage 1; F, G and H are stage 2 regenerates. In figure C and G, a, b and L denotes respectively the apical, basal and lateral regions of the epithelial cells. A and B show the fluorescence of PMC of the normal newt reacted with non-immune mouse ascites fluid. G and H correspond to the same iris section stained for A-CAM and for actin; H is stained with rhodamine phalloidin. During early activation (stage 1), A-CAM is retained at the apical (C small arrow), lateral (C large arrow) and the basal (D arrows, the large arrow points the basal intercellular area, and L arrow) surface of the cells. In stage 2 with the onset of depigmentation, A-CAM is significantly decreased in the basal, baso-lateral, apical and apico-lateral surfaces of the cells (F arrows, the large arrow points the basal intercellular area, G: a, b), but is retained in the mid-lateral region (G curved arrow). G and H show that A-CAM and actin colocalize in the mid-lateral region (curved arrows) of the cells; however, actin is still present at the basal (H arrowhead) and apical (H arrow) regions of the cells where A-CAM is absent. S, stroma; E, external; I, internal layer of IE; Each bar = 10 μm.

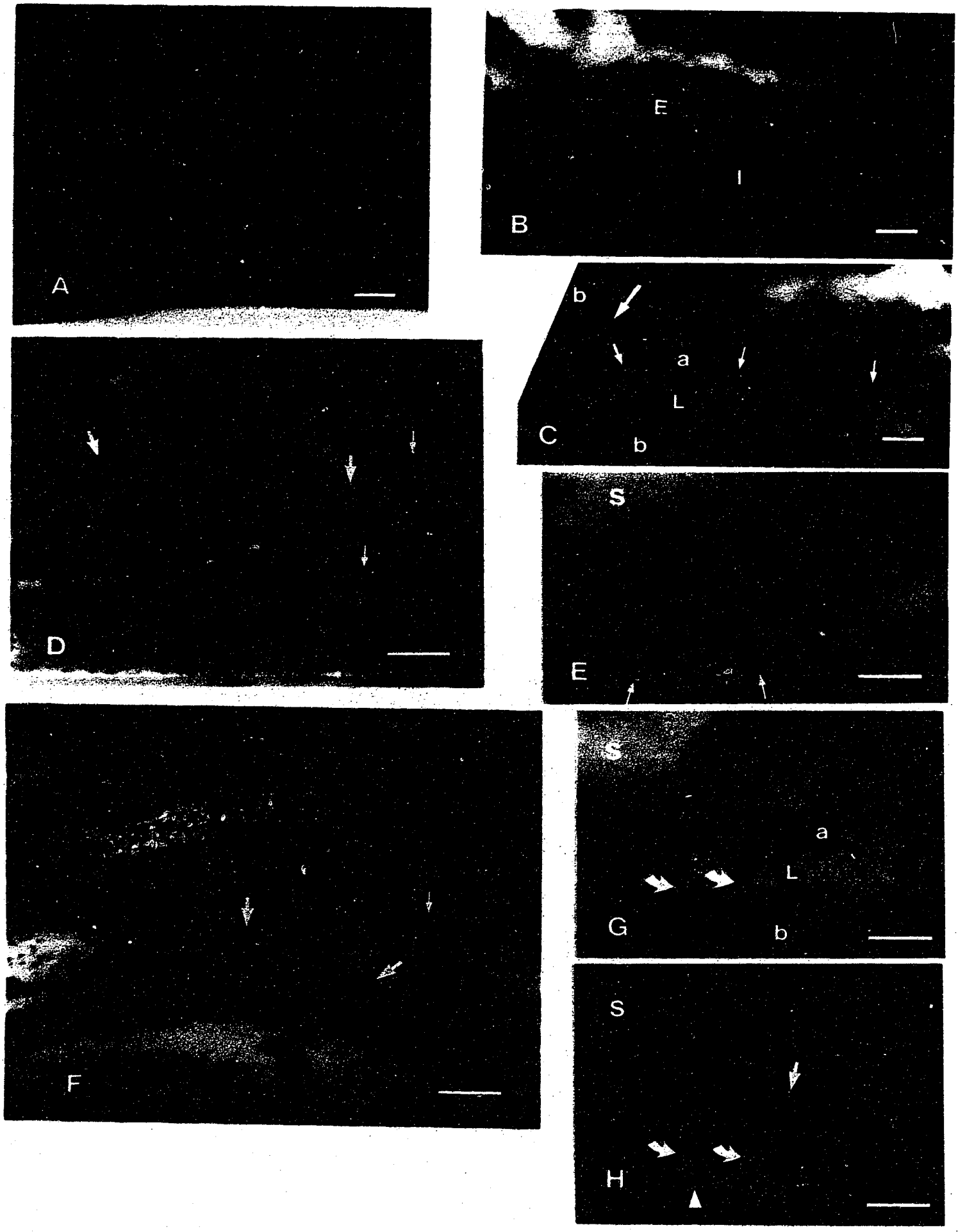
A
B
E
I
C
b
a
L
b
D
E
S
F
G
S
a
L
b
H
S

Figure 4-4. Distribution of A-CAM in lens regenerating cells during late dedifferentiation and redifferentiation.

Regenerates stages (st.): A, st 3; B, st. 4; C and D, st 4-5; E, st 7; F, st 8. C is a flat mount preparation of a regenerate, the rest are sagittal sections; a, b and l are respectively the apical, basal and lateral regions of the cell. Observe in A, the presence of A-CAM in the mid-lateral region (large arrow) and the absence of this protein in the basal regions (b) of the depigmenting cells at stage 3; A-CAM is also present between two depigmenting cells that may have recently divided (small arrow). B, shows that A-CAM surrounds the entire surface of depigmented and dedifferentiated cells at stage 4. C, D show that A-CAM staining appears to be enhanced preferentially in the early redifferentiating cells; because of the intensity of the A-CAM staining in the elongating lens fibers (D, arrow), it is assumed that the intensely stained cells in the flat mount preparation of the regenerate in C, (arrow) are also at the early stage of redifferentiation. E, is a higher magnification of area of the lens stalk in a stage 7 regenerate showing that the cells that will differentiate and contribute lens cells to the growing lens vesicle express A-CAM throughout the cell surface. As lens cells continue redifferentiation, A-CAM decreases gradually and disappears from the lateral and apical surfaces of the cells, as shown by the lack of staining in the cells of the internal layer of the lens vesicle (E and F, **), while A-CAM is maintained in some cells that are assumed to be prospective lens epithelial cells (F, arrow) because of their location. S, stroma; E, external layer; I, internal layer of the IE or lens vesicle; PEC, pigmented epithelial cells of iris; Each bar = 10 μm.

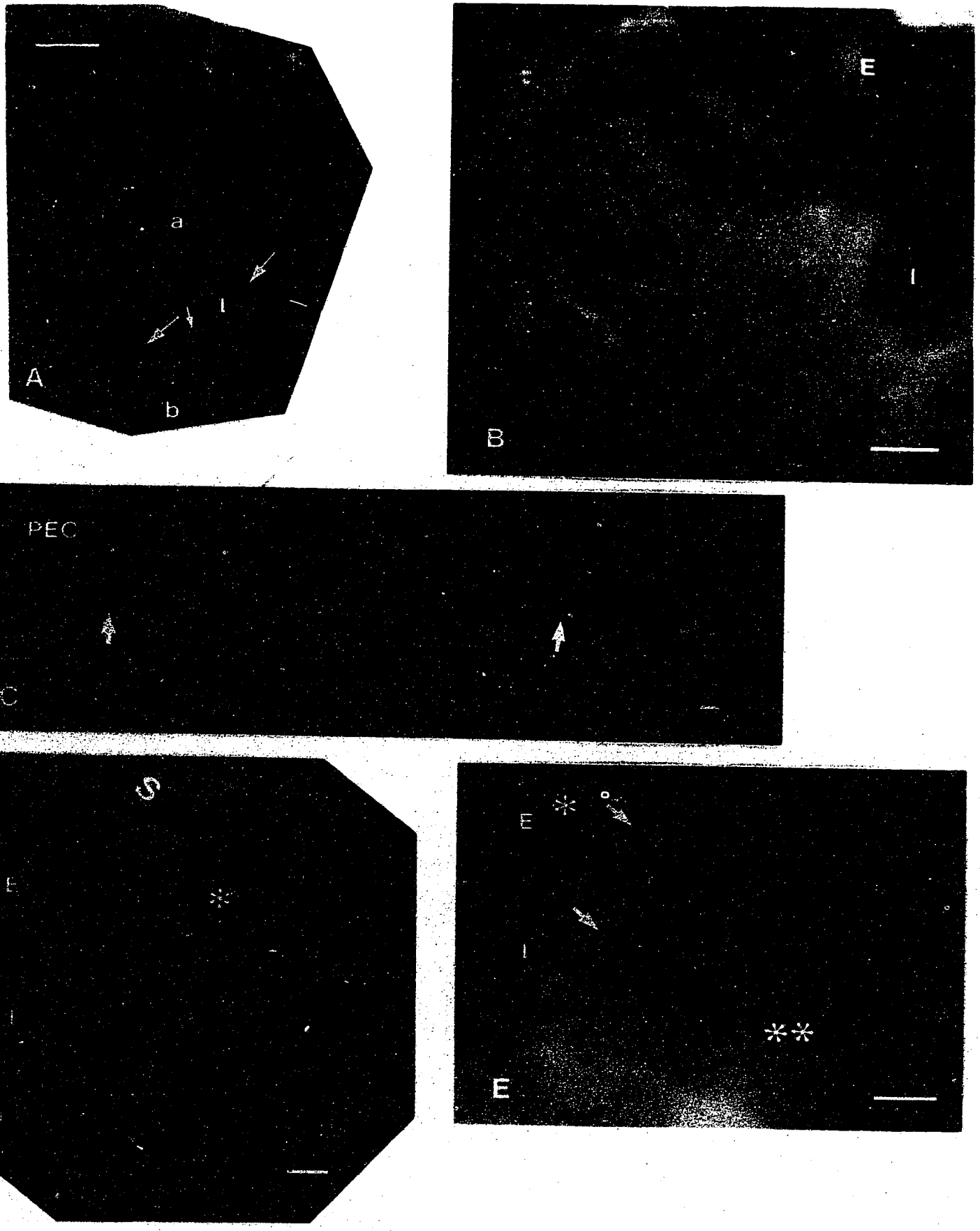
a
I
A
b
E
I
B
PEC
C
S
E
I
D
E
I
E

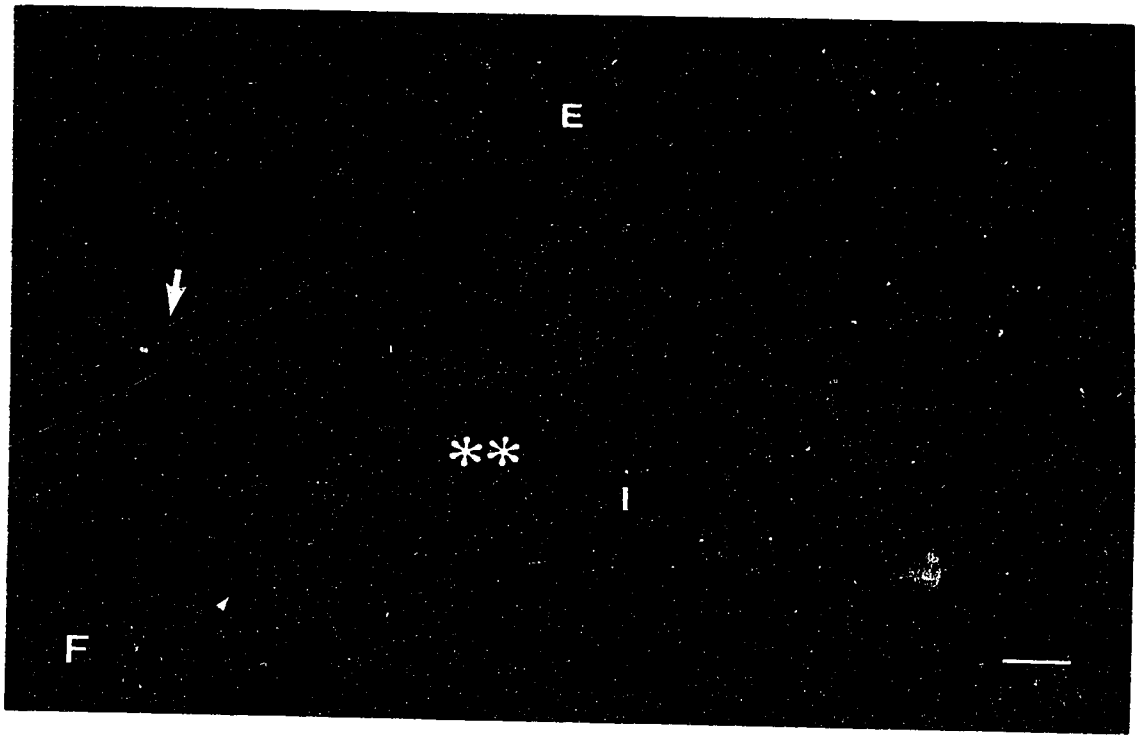

Figure 4-4. Distribution of A-CAM in lens regenerating cells during late dedifferentiation and redifferentiation.

F, a sagittal section of a regenerate at stage 8 showing lack of staining in the cells of the internal layer of the lens vesicle (**). The pattern of the staining shows that in the late stage of redifferentiation, A-CAM decreases gradually and disappears from the lateral and apical surfaces of the cells, while it is maintained in some cells that are assumed to be prospective lens epithelial cells (arrow) because of their location. Each bar = 10 μm.

As cells complete dedifferentiation, A-CAM reappears at the cell surface as punctate staining surrounding the entire surface of the depigmented and dedifferentiated cells (figure 4-4 B). At the dedifferentiation stages, cell still retains a spindle-like shape (not shown here).

Redifferentiation

Lens regenerates at stages 4 to 5, consist of a central cell population undergoing elongation into primary lens fibers, as well as a peripheral cell population continuous with the cells of the lens stalk. The cells in the latter area are also dedifferentiated cells which are gradually incorporated into the lens vesicle. Usually, the cells in the internal layer close to the central region of the lens vesicle are at the most advanced phases of regeneration. At these stages, cells that have dedifferentiated as well as the cells that are at early stages of elongation exhibit A-CAM staining at the cell surfaces, which shows the polygonal profile of the cell when observed in a flat mount (not shown). Observed in sections, the staining intensity varies in different groups of cells. As shown in figure 4-4 A-CAM staining is preferentially enhanced in those cells in the internal layer of the lens vesicle that are initiating elongation (D), and in the peripheral cell population of the stalk area of the lens vesicle at stage 7 (E). These cells may be both at early phases of redifferentiation (see also figure 4-4 C). From morphological evaluation, it appears that the depigmenting or newly depigmented cells at the less advanced phases of regeneration exhibit less intense staining of A-CAM (figure 4-4 D* and E *). As lens fiber elongation continues, A-CAM staining gradually disappears from the apical and lateral surfaces of the lens fiber cells (figure 4-4 E** and F **), and is retained at the basal surface of the lens vesicle cells (F arrowhead), and at the lateral surface of the prospective lens epithelium (F, arrow), the latter express A-CAM in the normal lens.

A-CAM in ocular tissues and Colocalization of A-CAM with Actin

A-CAM is detected at the peripheries of the iris PECs of the M- and J-ring where it is also located in areas of both cell-cell and cell-ECM contact, a distribution pattern similar to that of the PMC (figure 4-2 A, 4-6, also see chapter 2 for figure 2-1). In the lens epithelial cells, it appears as punctate staining at the cell periphery (figure 4-5), a pattern similar to that previously described in cultured chick lens epithelial cells (Volk & Geiger 1986a, Volk et al. 1990). A-CAM is also present at the cell surface of the epithelial cells of the ciliary body and the neural retina; in the internal layer of the ciliary epithelium, the staining at the basal surface of the non-pigmented cells is very strong (figure 4-6 B, C). In the cornea, this adhesion molecule is expressed in the epithelial, stroma and the presumed endothelial cells (figure 4-6 D, E, G). The expression of A-CAM in the newt cornea is different from that in the adult chick; in the latter case A-CAM is restricted to the endothelial cells of the cornea (Duband et al. 1988 and Hatta et al. 1987).

When tissues are stained with anti-A-CAM antibodies followed by labelled phalloidin to localize actin, the staining of A-CAM and actin colocalizes throughout the cell surface. This colocalization has been observed in the lens epithelium (figure 4-5 B, C), ciliary epithelium (not shown), cornea tissues (figure 4-6 J, K), and in PMC and PECs of the iris (Figure 4-6 H, I). In the PMC, the colocalization of actin and A-CAM at the cell surface is maintained during dedifferentiation (figure 4-3 G & H), although the dedifferentiating and redifferentiating cells also exhibit areas of increased actin concentration which are devoid of A-CAM. Since actin colocalizes with vinculin (chapter 3), it is assumed that A-CAM also colocalizes with vinculin. This colocalization occurs in the lateral, apical surfaces and basal surfaces of PMC and PECs of the iris. The number of normal irises and of regenerates examined in the studies reported in this chapter is shown in table 4-1.

Figure 4-5. Distribution of A-CAM (A, B) and actin (C) in lens epithelial cells of the adult newt.

All figures are flat mount preparations. A and B were stained with anti-A-CAM antibodies using fluorescein, and C with rhodamine phalloidin. A-CAM is located at the cell periphery of the epithelial cell (A and B, arrow and curved arrow) and colocalizes with actin (B and C arrow and curved arrow). Each bar = 10 μm.

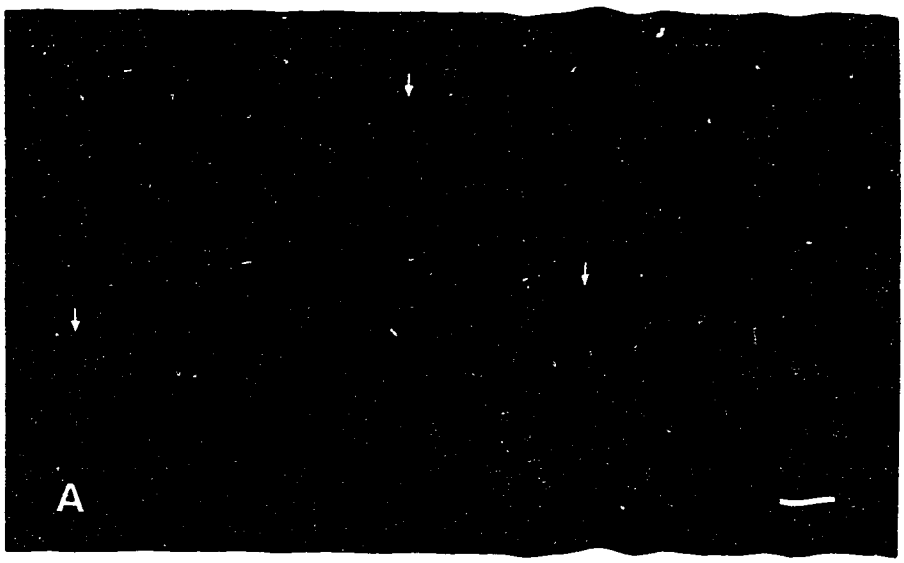
A


B

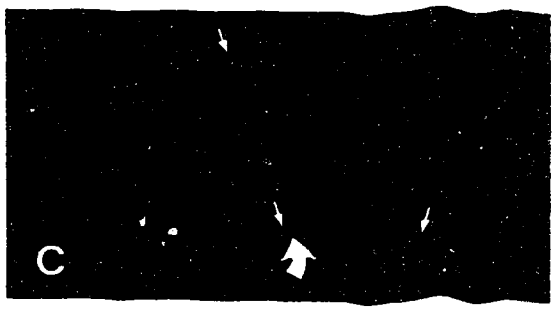
C

Figure 4-6. Immunofluorescent detection of A-CAM and actin in newt ocular tissues.

C, H and I are flat mounts; B, D, E, F, G, J and K are from sagittal sections of tissues of newt eye. H- I and J-K show the tissues double stained for A-CAM and for actin. A: the cells from the M-ring viewed from the external face of the iris after removal of the stroma exhibit staining at the cell surface. B: the cells of the internal unpigmented ciliary epithelium show A-CAM staining at the basal (arrowhead) as well as the lateral (arrow) surfaces of the cells; the external ciliary epithelium is at the top of the figure. C: the internal non-pigmented retinal epithelium showing A-CAM staining at areas of cell to cell contact. This retina tissue was attached to the periphery of the ciliary epithelium in flat tissue mounts. Since this staining pattern was observed in the internal face of the mount, it is assumed that the cells represented here correspond to the ganglion cells. D: superficial epithelium of the cornea showing A-CAM staining in areas of cell to cell contact. E: A-CAM staining in the stroma in the middle layer of the cornea. F: control cornea tissue stained with non-immune mouse ascites fluid.G: a low magnification of the cornea tissue focussed on the staining at the underlying endothelium (arrow). H and I: the dorsal internal IE showing the colocalization of A-CAM (H) with actin (I) in PMC of P-ring (small arrows) and in PEC of M-ring IE (large arrows). J and K: the same section of the corneal epithelium with double staining showing the colocalization of A-CAM (J) with actin (K) at the periphery of the cells. Each bar = 10 μm

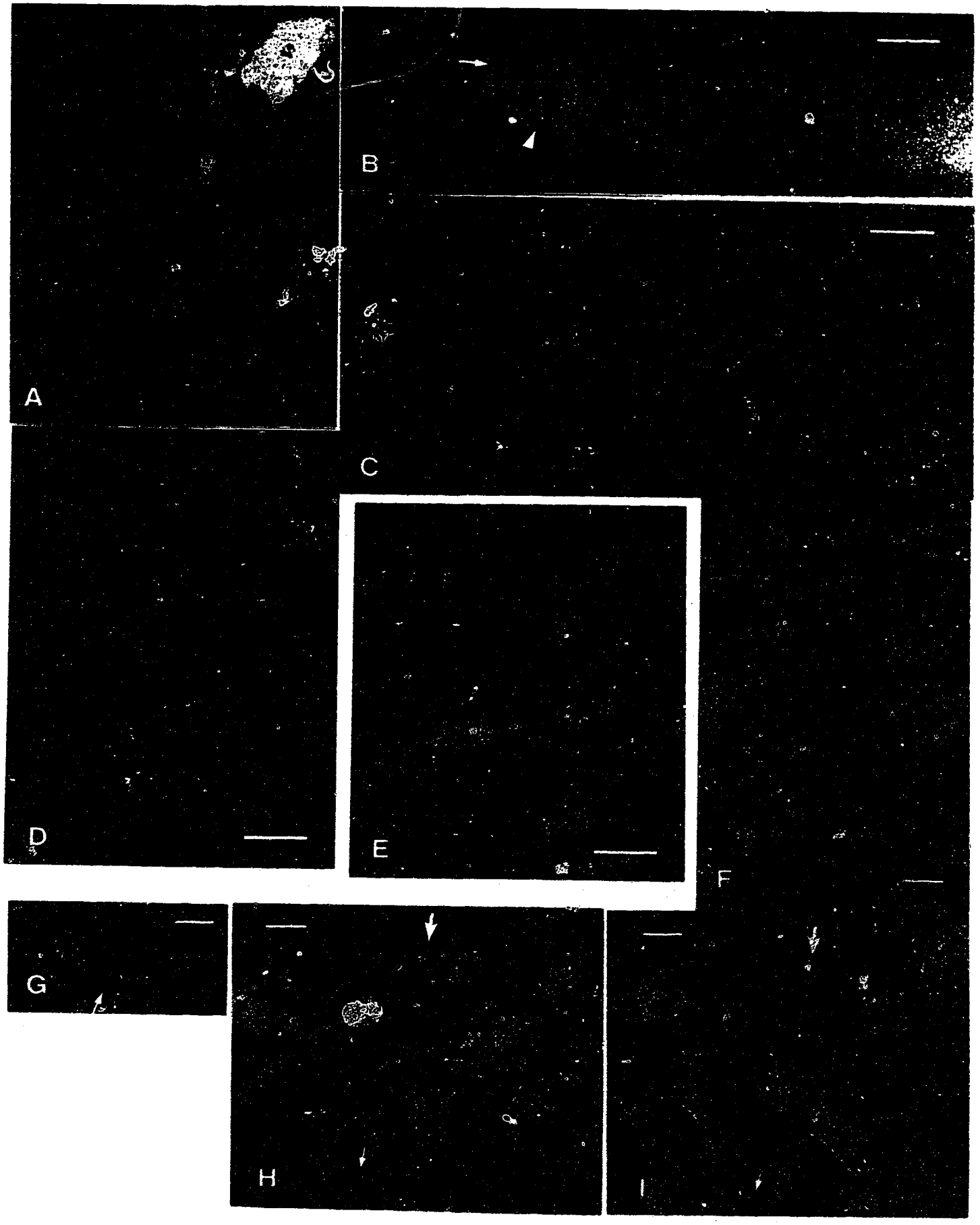
A
B
C
D
E
F
G
H
I

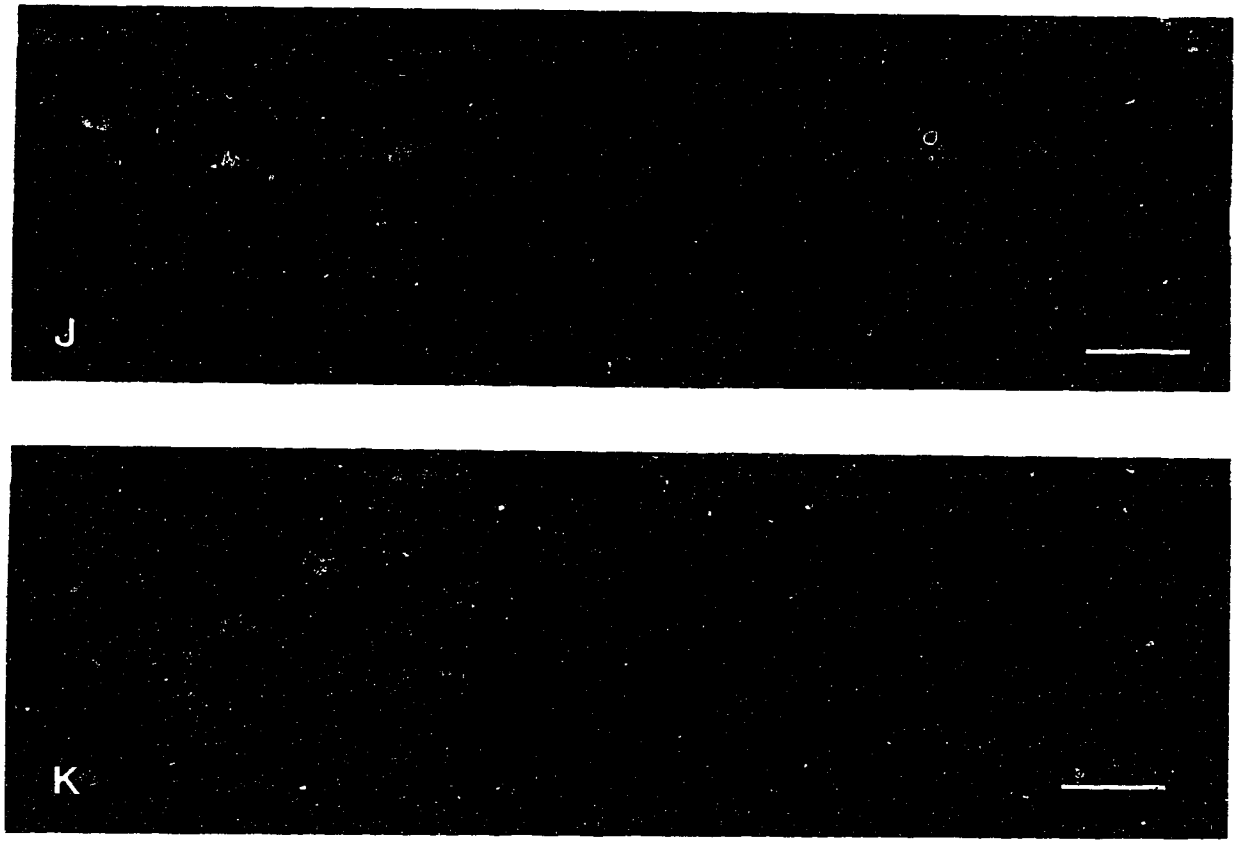

Figure 4-6. Immunofluorescent detection of A-CAM and actin in newt ocular tissues. J, and K, the same section of the corneal epithelium with double staining showing the colocalization of A-CAM (J) with actin (K) at the periphery of the cells. Each bar = 10 μm

Table 4-1. Number of normal irises and of regenerates used in studies of A-CAM during regeneration.

Stages of regeneration	Days of regeneration	No. of newts used
normal	0	21
1	3-9	10
2	6-18	11
3	10-18	7
4	15-22	10
5-6	18-28	10
7	23-28	4
8	21-30	5
9-10	28-35	4

4. 4. DISCUSSION

In this chapter, the expression and distribution of A-CAM were studied in the PMC during cell-type conversion from iris into lens tissue. Our findings are as follows. A) the PMC and PECs of iris, the epithelial cells of the ciliary bodies, the neural retina and the cornea express A-CAM. Other cell adhesion molecules such as the calcium-dependent molecule L-CAM and the calcium independent molecule, N-CAM were not detected in this system (not shown). B) A-CAM is present in areas of contact between cells and between cell and the ECM, suggesting that, in this system, this molecule not only could have a role in cell to cell adhesion but also could have an analogous role as that of integrin in mediating the adhesion of the cell to the ECM (Hynes 1987 and Ruoslahti 1991). C) the focal elimination or reduction of A-CAM from the basal and apical compartments of the cells may allow this membrane compartments to emit the cytoplasmic processes involved in depigmentation. D) A-CAM is down regulated during the lens fiber differentiation while it remains in the prospective lens epithelial cells. E) when present, A-CAM always colocalizes with actin, the latter protein always colocalizes with vinculin in regions of cell-cell and cell-ECM contact.

A-CAM is believed to be equivalent to N-cadherin; these molecules share a similar antigenic specificity (Duband et al 1988, Matsuzaki et al 1990), identical spatio-temporal distribution throughout somitogenesis (Duband et al 1987, Hatta et al 1987) and almost coincidental distribution patterns during embryogenesis (Hatta & Takeichi, 1986, Hatta, et al. 1987 and Duband et al. 1988). A-CAM or N-cadherin is a highly conserved protein, between species. As shown in transfected cells, N-cadherins from different species (ie mouse & chick) interact with each other, while in the same species N-cadherin does not interact with other cadherins (Nose & Nagafuchi 1988). Using antibodies against mouse, dog and chick antigens, E-cadherin (=uvomorulin) and L-CAM have been detected in the

amphibian, *X. laevis* (Nomura et al 1986, Choi & Gumbiner 1989, and Levi et al 1987). Recently, several amphibian cadherins have been identified by antigenic analysis and cDNA sequencing (Choi & Gumbiner 1989, Herzberg at al. 1990, Angres et al 1991, Ginsberg et al 1991). Amino acid sequence analysis shows that the Xenopus N-cadherin is 75 % identical to chick and mouse N-cadherin (Detrick et al 1990, Ginsberg et al 1991); in the later species N-cadherins share a 92 % sequence homology (Miyatani et al. 1989). According to our immunoblot analysis, the antibody against chick A-CAM (ID 7.2.3) recognizes a single protein band in the newt extract that comigrates with the chick A-CAM. As detected by immunofluorescence, the distribution pattern of this protein in the lens epithelial cells of the newt is similar to that reported in the cultured lens epithelial cells of the chick (Volk & Geiger, 1986a and Volk et al 1990). It is, therefore, likely that the anti-chick A-CAM antibody recognizes the corresponding protein in the newt.

In majority of epithelial cells of embryonic and adult animals, A-CAM is present in the subapical region of the cells where it is colocalized with adherens-junctions (Volk and Geiger,1986 a, Hatta & Takeichi, 1986, Nose & Takeichi, 1986, and Hatta, et al. 1987). In this study, at the level of resolution of the immunofluorescence technique employed, A-CAM appears to be homogeneously distributed along the lateral and apical surfaces of regions of cell to cell contact. The observed homogeneous distribution of this molecule could result from the presence of numerous adhesion junctions uniformly distributed around the cell surface. This is a possibility in this system since electron microscopic studies indicate that adhesive junctions are abundant in the lateral and apical surfaces of PMC and PECs (chapter 2). Moreover, at the site of the adhesive junction, there are fibers across the intercellular space of the junction (chapter 2 figure 2-3 B, D, E); these fibers probably correspond to A-CAM or N-cadherin since their location implies their function as cadherins. Similar ultrastructures have also been observed in the cochlear epithelium in the adherens junction in the subapical region of the cell (Raphael 1988). On the other hand,

besides having a junctional location, A-CAM could also be present extrajunctionally. An extrajunctional location of A-CAM has been reported to occur temporally in some embryonic tissues in which A-CAM or N-cadherin is homogeneously distributed along the entire lateral surface while zonula adherens junctions are only present in the subapical region of the cells (Duband et al. 1988, Raphael et al. 1988). This extrajunctional location of A-CAM is also present in the compacting cells of the segmental plate of the somite (Duband et al 1988). Further studies using immunoelectron microscopy are needed in order to determine whether A-CAM also has an extrajunctional location in the normal iris.

As discussed above, in most mammalian, avian and amphibian tissues studied so far, A-CAM and other cadherins are restricted to areas of cell to cell contact. However, in the PMC and PECs of the iris and in the ciliary epithelium, A-CAM is also located at the basal region of the cell surface (figure 4-5). This finding suggests that, in the newt, A-CAM may have a role in the association of cells with the ECM such as that of integrin (Hynes 1987 and Ruoslahti 1991). In the early embryos of chick, there are some instances in which A-CAM appears to be present at the basal regions of the cells where it could interact with the ECM (see Duband et al. 1988, figure. 6-C for A-CAM staining at the basal region of the neural tube; Hatta et al 1987, figure 7-d for staining of the lung bud; Lagunowich & Grunwald 1989, figure 9-E for staining at the basal region of PEC of retina). The basal location of A-CAM and N-cadherin was not mentioned, nor discussed by the authors. In cultured cells, A-CAM is restricted to areas of cell-cell adhesion and is not present in areas of cell substrate adhesion where fibronectin is present presumably associated with actin and integrin. In the lens regenerating system, fibronectin is detected in the basal lamina of PMC and PECs where A-CAM is also present. During dedifferentiation, fibronectin is expressed in the apical and lateral regions of the dedifferentiating cells (Elgert & Zalik 1989) where it could colocalize with A-CAM. Although, at the present time, it is not known whether other cellular matrix proteins are

present in the normal and dedifferentiating PMC, A-CAM could have an analogous role to that of integrins.

The selective elimination of A-CAM from the basal and apical compartment of dedifferentiating cells suggests that localized dissociations of cell to cell and cell to ECM contacts occur in areas involved in cytoplasmic shedding. At the basal surface of the cell in areas of cell to ECM contact, reduction or elimination of A-CAM is, on one hand, temporally accompanied by active passage of macrophages that frequently cause focal disruption of the basement membrane (Dumont & Yamada 1972, Reyer 1990 a, b). The focal dissociation of the cell to cell contact, on the other hand, is probably associated with the partial obliteration of intercellular junctions, such as desmosomes, and with the increase of intercellular space reported by Dumont & Yamada (1972). This is supported by the fact that, in cultured cells, dissociation of intercellular adhesion by depletion of extracellular Ca^{2+} results in endocytosis of the plaque-bearing, cadherin containing junctions of "adherens" category, desmosomes and zonulae adherens (Kartenbeck et al.1982, 1991, Mattey 1986). The expanded intercellular space could then provide room for protrusion of the cellular processes involved in cytoplasmic shedding. Furthermore, removal of adhesion molecules from the cell membrane could also increase membrane fluidity necessary for the formation of cytoplasmic projections. The maintenance of A-CAM mediated adhesion at the mid-lateral regions of the cells could also be necessary for maintenance of the integrity of the epithelial iris architecture during the processes of depigmentation and dedifferentiation. Since fibronectin is also deposited at the lateral region during these processes, A-CAM might not be able to directly link the neighboring cells. It is possible that during dedifferentiation this molecule helps to maintain the cell association through a mechanism similar to that involved in cell adhesion to the ECM at the basal surface of the normal IE.

Besides the colocalization of A-CAM with actin and with vinculin in PMC and PECs of normal newt iris and regenerates, the selective elimination of A-CAM from the basal and apical compartments of dedifferentiating cells occurs when AFBs are thickened, clustered, curved and branched (chapter-3). It is not known what is the relationship between the focal obliteration of A-CAM with the changes of cortical actin. According to other investigators (Geiger and Volk,1986b, Volberg et al. 1986), the dissociation of cell to cell contact by depletion of calcium or by treatment of cultured cells with anti-A-CAM antibodies could cause the detachment of cortical AFBs from the membrane, the contraction of the AFBs and the movement of AFBs from the cortical area to the perinuclear area. The dissociation of the actin cytoskeleton by cytochalasin D, on the other hand, inhibits aggregation of S180 cells transfected with N-cadherin or L-CAM, but does not disrupt the cells that are already bound (Matsuzaki et al. 1990). The changes of A-CAM and actin in the present system must be cooperative and both may be required for depigmentation.

The changes in A-CAM expression during newt lens regeneration differ from those that occur in lens development during embryogenesis of the chick and mouse. Before induction the prospective lens ectoderm expresses P- and E-cadherin, shortly after induction by the optic cup, the lens ectoderm represses the expression of P-cadherin and begin to express N-cadherin while maintaining the expression of E-cadherin. Expression of N-cadherin is increased in the growing lens vesicle and the former is kept at high levels up to hatching (Nose & Takeichi 1986, Hatta & Takeichi 1986, Hatta et al 1987, and Lagunowich & Grunwald 1989). E-cadherin, on the other hand, is coexpressed with N-cadherin in the lens epithelium, but disappears from the lens fibers (Nose & Takeichi, 1986 Hatta et al. 1987). During newt lens regeneration, the behavior of A-CAM is rather similar to that of E-cadherin during lens formation of chick embryo. Although no studies on lens development have been performed in the newt embryo, from the above mentioned studies, it appears that different adhesive molecules are employed in these two systems.

This work has centered on the study of N-cadherin during newt lens regeneration. Although I was not able to detect the presence of L-CAM using monoclonal antibodies, it is possible that other cadherins are present in the iris and are differentially expressed during lens regeneration. In the cultured chick lens cells, one of the lens polypeptides that co-migrates with the liver cadherin but does not react with L-CAM antibodies has been detected in the chick (Volk et al 1987), and an unidentified band of lower molecular weight that is recognized by pan-cadherin antibodies has also been noticed in the chick lens (Geiger et al. 1990). Further studies need to be done to determine if other cadherins are differentially expressed during lens regeneration.

4. 5. LITERATURE CITED

Angres B, Muller A H J, Kellermann J and Hausen P. 1991. Differential expression of two cadherins in *Xenopus laevis* Development. 111:829-844.

Choi Y S and Gumbiner B. 1989. Expression of cell adhesion molecule E-cadherin in *Xenopus* embryos begins at gastrulation and predominates in the ectoderm. J Cell Biol. 108:2449-58.

Coleman A W, Maguire M J and Coleman J R. 1981. Nithramycin- and 4'-6-Diamidino- 2-Phenylindole (DAPI)-DNA staining for fluorescence microspectrophotometric measurement of DNA in nuclei, plastids and virus particles. J. Histochem. Cytochem. 29:959-968.

Detrick R J, Dickey D and Kintner C R. 1990. The effects of N-cadherin misexpression on morphogenesis in *Xenopus* embryos. Neuron. 4:493-506.

Duband J L, Dufour S, Hatta K, Takeichi M, Edelman GM and Thiery J P. 1987. Adhesion molecules during somitogenesis in the avian embryo. J. Cell Biol. 104:1361-1374.

Duband J L, Volberg T, Sabanay I, Thiery J P and Geiger B. 1988. Spatial and temporal distribution of the adherens-junction-associated adhesion molecule A-CAM during avian embryogenesis. Development. 103:325-344.

Dumont J N and Yamada T. 1972. Dedifferentiation of iris epithelial cells. Dev. Biol. 29:385-401.

Edelman G M. 1988. Morphoregulatory molecules. Biochemistry. 27:3533-43.

Eguchi G and Shingai R. 1971. Cellular analysis on localization of lens forming potency in the newt iris epithelium. Devel. Grow. Differ. 13:337-349.

Elgert K and Zalik S E. 1989. Fibronectin distribution during cell-type conversion in newt lens regeneration. Anat. Embryol. 180:131-142.

Geiger B. 1989. Cytoskeleton-associated cell contacts. Current Opinion in Cell Biology. 1:103-109.

Geiger B, Volberg T, Sabanay I and Volk T. 1989. A-CAM: an adhesion junction-specific cell adhesion molecule. *In*: Morphoregulatory molecules.G M Eldeman, B A Cunningham, J P Thiery, eds. Neurosci. Inst. Pub. pp.57-79.

Geiger B, Volberg T, Ginsberg D, Bitzur S and Sabanay I. 1990. Broad spectrum pan-cadherin antibodies, reactive with the C-terminal 24 amino acid residues of N-cadherin. J Cell Sci 97:607-614.

Ginsberg D, DeSimone D and Geiger B. 1991. Expression of a novel cadherin (EP-cadherin) in unfertilized eggs and early *Xenopus* embryos. Development. 111:315-325.

Hatta K, Okada T S and Takeichi M. 1985. A monoclonal antibody disrupting calcium-dependent cell-cell adhesion of brain tissues: Possible role of its target antigen in animal pattern formation. Proc. Natl. Acad. Sci. USA 82:2789-2793.

Hatta K and Takeichi M. 1986. Expression of N-cadherin adhesion molecule associated with early morphogenetic events in chick development. Nature, Lond. 320:447-449.

Hatta K, Takagi S, Fujisawa H and Takeichi M. 1987. Spatial and temporal expression pattern of N-cadherin cell adhesion molecules correlated with morphogenetic processes of chicken embryos. Dev. Biol. 120:215-227.

Hawkes R, Niday E and Gordon J. 1982. A dot immunobinding assay for monoclonal and other antibodies. Anal. Biochem. 119:142-147.

Herzberg F, Potting A and Wedlich D. 1990. Identification of Ca^{2+}-dependent cell adhesion molecules in *Xenopus* by the use of interspecies homology. Differentiation. 44:1-7.

Hirano S, Nose A, Hatta K, Kawakami A and Takeichi M. 1987. Calcium-dependent cell-cell adhesion molecules (cadherins): subclass specificities and possible involvement of actin bundles. J Cell Biol. 105:2501-2510.

Hynes R O. 1987. Integrins: a family of cell surface receptors. Cell. 48:549-554.

Kartenbeck J, Schmelz M, Franke W W and Geiger B. 1982. Different models of internalization of proteins associated with adherens junctions and desmosomes: experimental separation of lateral contacts induces endocytosis of desmosomal plaque material. EMBO. J. 1:725-732.

Kartenbeck J, Schmelz M, Franke W W and Geiger B. 1991. Endocytosis of junctional cadherins in bovine kidney epithelial (MDBK) cells cultured in low Ca^{2+} ion medium. J Cell Biol. 113:881-892.

Kulyk W M and Zalik S E. 1982. Synthesis of sulfated glycosaminoglycans in the newt iris during lens regeneration. Differentiation 23:29-35.

Kulyk W M, Zalik S E and Dimitrov E. 1987. Hyaluronic acid production and hyaluronidase activity in the newt iris during lens regeneration. Exp Cell Res. 172:180-191

Lagunowich L A and Grunwald G B 1989. Expression of calcium-dependent cell adhesion during ocular development: a biochemical, histochemical and functional analysis. Dev. Biol. 135:158-171.

Laemmli U K. 1970. Cleavage of structural proteins during the assembly of the head of bacteriophage T4. Nature 227:680-685.

Levi G, Crossin K L and Edelman G M. 1987. Expression sequences and distribution of two primary cell adhesion molecules during embryonic development of *Xenopus laevis*. J. Cell Biol. 105:2359-72.

Mattey D L and Garrod D R. 1986. Splitting and internalization of the desmosomes of cultured kidney epithelial cells by reduction in calcium concentration. J. Cell Biol. 85:113-124.

Matsuzaki F, Miaege R M, Jaffe S H, Friedlander D R, Gallin W J, Goldberg J I, Cunningham B A and Edelman G M. 1990. cDNA of cell adhesion molecules of different specificity induce changes in cell shape and border formation in cultured S180 cells. J. Cell Biol. 110:1239-52.

Miyatani S, Shimamura K, Hatta M, Nagafuchi A and Nose A. 1989. Neural cadherin: role in selective cell-cell adhesion. Science. 245: 631-35.

Nagafuchi A and Takeichi M. 1988. Cell binding function of E-cadherin is regulated by the cytoplasmic domain. EMBO. J. 7:2679-2684.

Nomura K, Uchida M, Kageura H, Shiokawa K and Yamana K. 1986. Cell to cell adhesion system in *Xenopus laevis*, the south African clawed frog I. detection of Ca^{2+}dependent and independent adhesion system in adult and embryonic cells. Develop. Growth and Differ. 28:311-319.

Nose A and Nagafuchi A. 1988. Expressed recombinant cadherins mediate cell sorting in a model system. Cell. 54:993-1001.

Nose A and Takeichi M. 1986. A novel cadherin cell adhesion molecule: its expression patterns associated with implantation and organogenesis of mouse embryos. J. Cell Biol. 103:2649-2658

Osborn M and Weber C. 1982. Immunofluorescence and immunocytochemical procedures with affinity purified antibodies: tubulin-containing structures. In: Methods in Cell Biology, Vol. 24. L Wilson, ed. Academic press, New York. pp. 97-132 .

Patmore M and Yamada T. 1982. The role of calcium in depigmentation of iris epithelial cells during cell-type conversion. Dev. Biol. 92:266-274

Raphael Y, Volk T, Crossin K L, Edelman G M and Geiger B. 1988. The modulation of cell adhesion molecule expression and intercellular junction formation in the developing avian inner ear. Dev. Biol. 128:222-235.

Reyer RW. 1977. The Amphibian Eye: Development and Regeneration, Handbook of Sensory Physiology. Vol VII/5 F.Crescitelli, ed. Springer Verlag. pp 309-360.

Reyer R W. 1990a. Macrophage invasion and phagocytic activity during lens regeneration form the iris epitheliun in newts. Am. J. Anat. 188:239-344.

Reyer R W. 1990b. Macrophage mobilization and morphology during lens regeneration form the iris epithelium in newts: studies with correlated scanning and transmission electron microscopy. Am. J. Anat. 188:345-365.

Ruoslahti E. 1991. Integrins. J. Clin. Invest. 87:1-5.

Stone L S. 1967. An investigation recording all salamanders which can and cannot regenerate a lens from the dorsal iris. J. Exp. Zool. 164: 87-104.

Takeichi M. 1988. The cadherins: cell-cell adhesion molecules controlling animal morphogenesis. Development. 102:639-655.

Takeichi M. 1990. Cadherins: a molecular family important in selective cell-cell adhesion. Ann. Rev. Biochem. 59:237-252.

Takeichi M. 1991. Cadherins, cell adhesion receptors as a morphogenetic regulator. Science. 251:1452-1455.

Towbin H, Staehelin T and Gordon J. 1979. Electrophoretic transfer of proteins from polyacrylamide gels to nitrocellulose sheets: procedure and some applications. Proc. Natl. Acad. Sci. USA. 76:4350-4354.

Volberg T, Geiger B, Kartenbeck J and Franke W W. 1986. Changes in membrane microfilament interaction in intercellular adherens junction upon removal of extracellular Ca^{2+} ions. J. Cell Biol. 102:1832-42.

Volk T and Geiger B. 1984. A 135-kd membrane protein of intercellular adherens junctions. EMBO. J. 3:2249-2260.

Volk T and Geiger B. 1986a. A-CAM: a 135-kd receptor of intercellular adherens junctions. I. Immunoelectron microscopic localization and biochemical studies. J. Cell Biol. 103:1441-1450.

Volk T and Geiger B. 1986b. A-CAM: a 135-kd receptor of intercellular adherens junctions. II. antibody- mediated modulation of junction formation. J. Cell Biol. 103:1451-1464.

Volk T, Cohen O and Geiger B. 1987. Formation of heterotypic adherens-type junctions between L-CAM-containing liver cells and A-CAM containing lens cells. Cell. 50:987-994.

Volk T, Volberg T, Sabanay L and Geiger B. 1990. Cleavage of A-CAM by endogenous proteinases in cultured lens cells and in developing chick embryos. Dev. Biol. 139:314-326.

Yamada T and Karasaki S. 1963. Nuclear RNA synthesis in newt iris cells engaged in regenerative transformation into lens cells. Dev. Biol. 7:595-604.

Yamada T. 1977. Control mechanisms in cell-type conversion in newt lens regeneration. *In*: Monographs in Developmental Biology. Vol.13. A Wolsky, ed. S Karger, Basel. pp 1-126.

Yamada T and McDevitt D S. 1984. Conversion of iris epithelial cells as a model of differentiation control. Differentiation. 27:1-12.

Yamada T and Roesel M E. 1969. Activation of DNA replication in the iris epithelium by lens removal. J. Exp. Zool. 171:425-432.

Yamada T and Roesel M E. 1971. Control of mitotic activity in Wolffian lens regeneration. J. Exp. Zool. 177:119-128.

Yamada T and Takata C. 1963. An autoradiographic study of protein synthesis in regenerative tissue transformation of iris into lens in the newt. Dev. Biol. 8:358-369

Zalik S E and Scott V. 1972. Cell surface changes during dedifferentiation in the metaplastic transformation of iris into lens. J. Cell Biol. 55:134-146.

Zalik S E and Scott V. 1973. Sequential disappearance of cell surface components during dedifferentiation in lens regeneration. Nature (New Biology). 244:212-214.

CHAPTER 5. GENERAL DISCUSSION

5. 1. SUMMARY OF RESULTS

In this thesis I have studied the expression of cytokeratin, actin cytoskeletal proteins and the associated cell surface molecule, A-CAM (N-cadherin) in the PECs of the newt iris, and traced changes of these proteins in the PEC of the dorsal iris during lens regeneration. Studies were carried out in flat mount preparations and serial sections of iris rings using labeled phalloidin that binds to filamentous actin and a number of monoclonal antibodies specific for cytokeratin and actin isoforms, vinculin and A-CAM. When flat iris tissue mounts are stained with phalloidin and anti-A-CAM antibodies, three distinct regions can be observed in the iris epithelium: the pupillary marginal (P), middle (M) and the more external junctional (J) rings. The P-ring cells of the both internal and the external iris epithelium, the internal M- and J-ring cells and the external M- and J-ring cells differ from one another in regards to their location, cell morphology and expression of various cytoskeletal proteins (table 2-1, 2-2). The elongated spindle shaped cells of the P-ring iris exhibit an elaborate cytoskeleton of actin filament bundles (AFBs) and cytokeratin-II oriented along the longitudinal axis of cells, reminiscent of that of myoepithelial or smooth muscle cells. These cells also express smooth muscle specific α and γ muscle actins, a smooth muscle actin, and cytokeratin-14, the latter also a myoepithelial marker. Therefore, the PECs at the P-ring iris that give rise to a new lens have now been characterized as pigmented myoepithelial cells (PMCs) (chapter 2). In contrast, other PECs in M- and J-ring of the iris that do not regenerate a lens do not express those markers. These findings suggest a possible relationship between the myoepithelial phenotype and the ability of certain cells to undergo cell type conversion in this system. This hypothesis is also favored by the fact that in the anthomedusa *Podocoryne carnea* , myoepithelial cells are able to

undergo transdifferentiation to form neuron cells while the epithelial cells can't (Schmid et al.1982, Schmid and Alder 1984, Alder and Schmid 1987).

In all iris epithelial cells, F-actin, vinculin and A-CAM colocalize in areas of both cell to cell and cell to extracellular matrix contacts. This extracellular matrix has been shown to contain fibronectin (Elgert & Zalik 1989). The colocalization of A-CAM with fibronectin also occurs in the dedifferentiating cells at the lateral cell surface in areas of intercellular contact. These observations suggest that in this system A-CAM, in addition to mediating cell to cell adhesion, may be possibly involved in cell adhesion to the extracellular matrix.

During depigmentation and dedifferentiation, actin staining increases considerably as AFBs are preferentially thickened and clustered at the basal and apical cortical regions of the cell, these regions are sites where cells emit and shed cytoplasmic projections. Corresponding to the changes of F-actin, vinculin is also reorganized in those areas and colocalizes with actin suggesting that the attachment of actin to the membrane is maintained through this protein. Also, as judged from the intensity and prevalence of vinculin staining, it is that vinculin is possibly increased at the basal region at early stages of depigmentation. A-CAM, on the other hand, is preferentially reduced or eliminated from those sites, suggesting the dissociation of cell to cell and cell to extracellular matrix contact in these areas. The latter could be one of the causes for the increase in the intercellular space in those areas. However, actin, vinculin and A-CAM are maintained at the mid-lateral region of the cells where fibronectin is also deposited. This suggests that the transmembrane association of the actin cytoskeleton with the cell surface is possibly maintained at the mid-lateral region of cells. This association possibly plays some role in maintaining the polarity, integrity and communication of the PMCs, which may be important for the coordination of dedifferentiation.

During the early stages of redifferentiation, AFBs also reorganize as cells change in cell shape from spindle to polygonal. At these stages vinculin is still present and remains colocalized with actin. The staining of A-CAM that has been restored in all areas of cell surface after depigmentation is also delineating the polygonal outlines of the cells. The changes of cell shape are followed by elongation of the cells along their apico-basal axes to form lens fibers. At this stage A-CAM is observed to be preferentially increased in some polygonal shaped cells and in some cells that initiate elongation. This enhancement of A-CAM is also accompanied by intensification of actin staining in these cells (not shown). At least temporally, it appears that the enhancement of A-CAM and actin staining is associated with changes of cell shape or initiation of elongation for lens fiber redifferentiation.

Accompanied with elongation of the cells, actin is preferentially accumulated in the cytoplasm at the basal and apical regions. Although at this stage treatment with cytochalasin D, a drug that breaks down actin filaments (Cooper 1987), has no significant effect on lens fiber redifferentiation (Hornsby and Zalik 1977), the preferential accumulation of actin suggest its involvement in lens fiber formation possibly in the way that can't be affected by this drug. It would be interesting to see if treatment of cells with phalloidin that stabilizes actin filaments could result in any disruption of lens fiber redifferentiation. During the processes of lens fiber redifferentiation, vinculin and A-CAM, however, gradually disappear from the regions of cell to cell contact at the apical and lateral areas of the redifferentiating lens fiber cells, with some remaining at the basal regions of the cells.

In the normal PMCs of the newt iris, cytokeratin-II, is organized as longitudinal fibers, aligned together with the AFBs at the basal cortical region of cells. This alignment has also been observed under the electron microscope. In other systems cytokeratin filaments has been found to be associated with actin filaments (Green et al. 1987). Here the alignment of these two filaments raises a possibility of their interconnection in the

PECs. Staining of cytokeratin-II is also progressively increased during dedifferentiation, and gradually disappears during lens fiber formation.

In summary, the PECs that give rise to a new lens are myoepithelial in nature. Colocalized with actin and vinculin, A-CAM is also present in the newt iris epithelial cells in areas of both cell to cell and cell to extracellular matrix contacts. This protein is preferentially reduced during depigmentation and disappears from the lens fiber cells during redifferentiation. Also during cell-type conversion some proteins of the cytoskeleton are up regulated and reorganized while others are down regulated during lens fiber differentiation. Changes in the cytoskeletal proteins and cell surface molecules appear to be cooperative in their association with morphogenetic events for lens regeneration. The results are also summarized in figure 5-1.

Since in our laboratory we do not have the equipment that can detect the quantitative changes of immunofluorescent staining, the increase and decrease in the staining intensity of proteins observed during regeneration, are based on subjective observations of the changes in intensity and the prevalence of the staining. These results reporting changes in staining intensity using labelled antibodies and ligands need to be subjected to more quantitative analysis.

According to Dumont and Yamada (1972), depigmentation was shown to occur in all areas of cell surface. However these investigators noticed that the cytoplasmic extensions are formed mostly at the basal region of the cells. Based on my observation, depigmentation occurs mainly to the basal, baso-lateral, apical and apico-lateral regions of cells, since the cell fragments that contain concentrated pigment granules are mainly observed in these locations where the cell to cell and cell to ECM contacts are disrupted. Some of my observations are consistent with those of Reyer (1990) in which he has also observed cellular projections at the apical region that protruded into a cleft created by

Figure 5-1 A. Summary of changes of actin and A-CAM in the iris epithelial cells during cell-type conversion.

A-B-C-D, pathway of dedifferentiation; **D-E-F-G**, pathway of redifferentiation; A-B-C"-D", retrieval pathway. In these pathways, cells are observed in sagittal sections, the pigment granules are illustrated as black spots and the cortical region of cells are emphasized. A'-B'-C'-D'-E'-F'-G', pathway of dedifferentiation followed by redifferentiation in which cells are viewed from their basal surfaces as observed in flat mounts. The staining of actin and A-CAM is shown in red and green colour.

A and A' show the pigmented myoepithelial cells (PMCs) of the normal iris in which the actin filament bundles (AFBs) are colocalized with A-CAM. **B** and B' show the PMCs that are activated and start growing at stage 1 of lens regeneration. In these cells A-CAM staining is enhanced slightly. **C** and C' depict the cells that, in the early stage 2, are sending cellular processes toward basal region of the cells for depigmentation. At the basal and the baso-lateral regions, actin staining increases considerably while A-CAM is significantly reduced or eliminated; from a basal view, the AFBs appear to have a random orientation. **D** and D' show cells at the later phases of depigmentation, which are sending cellular processes towards their apical region. In the apical region actin staining is enhanced and A-CAM staining is eliminated, while in the mid-lateral region A-CAM staining persists and colocalizes with actin. **E** and E' show the newly dedifferentiated and depigmented cells in which A-CAM staining is restored to all regions of cell surface and actin staining appears to be enhanced. **F** and F' show cells at an early stage of redifferentiation when A-CAM staining is temporarily enhanced in these cells, and actin staining is increased further and display a different organization. **G** and G' depict that elongating lens fiber cells at stages 7-9. In these cells A-CAM disappears from the apical and lateral regions of the cells, but actin remains in the cortical region of cells and is accumulated in the basal and apical regions of the fibers.

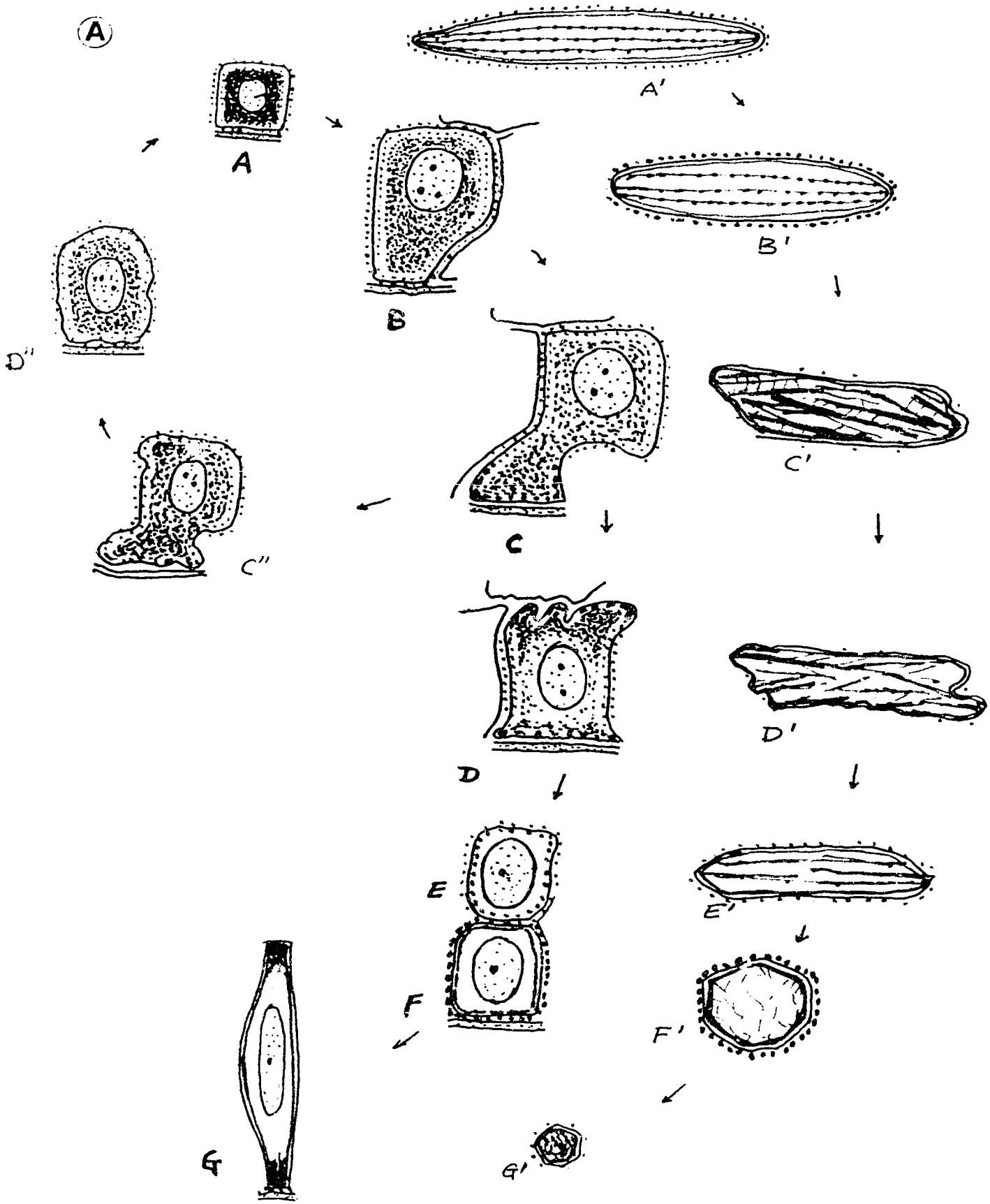
A
A'
B
B'
C
C'
C''
D
D'
D''
E
E'
F
F'
G
G'

Figure 5-1 B. Summary of changes of vinculin and A-CAM in the iris epithelial cells during cell-type conversion.

A-B-C-D, pathway of dedifferentiation; **D-E-F-G**, pathway of redifferentiation; A-B-C"-D", retrieval pathway. In these pathways, cells are observed in sagittal sections, the pigment granules are illustrated as black spots and the cortical region of cells are emphasized. A'-B'-C'-D'-E'-F'-G', pathway of dedifferentiation followed by redifferentiation in which cells are viewed from their basal surfaces as observed in flat mounts. In most cells, staining of vinculin and A-CAM is shown in yellow and green colour. In **A, B** and **C** the staining of cortical actin is shown in red for reference purposes.

A and A' show the pigmented myoepithelial cells (PMCs) of the normal iris in which vinculin staining is colocalized with A-CAM staining. **B** and B' show the PMCs that are activated and start growing at stage 1 of lens regeneration. In these cells A-CAM staining is enhanced slightly. **C** and C' depict the cells that at the early stage 2, are sending cellular processes towards the basal region of the cell to undergo depigmentation. Vinculin staining is increased preferentially at the baso-lateral regions of the cells, at the same time that actin staining is increased, A-CAM is significantly reduced or eliminated from the basal and the basal lateral regions. **D** and D' show cells at later phases of depigmentation that are sending cellular processes towards the apical region of the cell. In these cells, A-CAM staining is eliminated from the apical region of the cells, while vinculin staining appears to be retained at all regions of the cell cortex. In D' vinculin is not drawn since the distribution pattern of this protein at this stage is not known at the present time. **E** and E' show the newly dedifferentiated and depigmented cells in which A-CAM staining is restored to all regions of cell surface and vinculin is also present. **F** and F' show cells at early stages of redifferentiation when A-CAM staining is temporarily enhanced in these cells, while vinculin staining is not changed appreciably. **G** and G' depict that elongating lens fiber cells at stages 7-9. In these cells A-CAM and vinculin disappear from the apical and lateral regions of the cells.

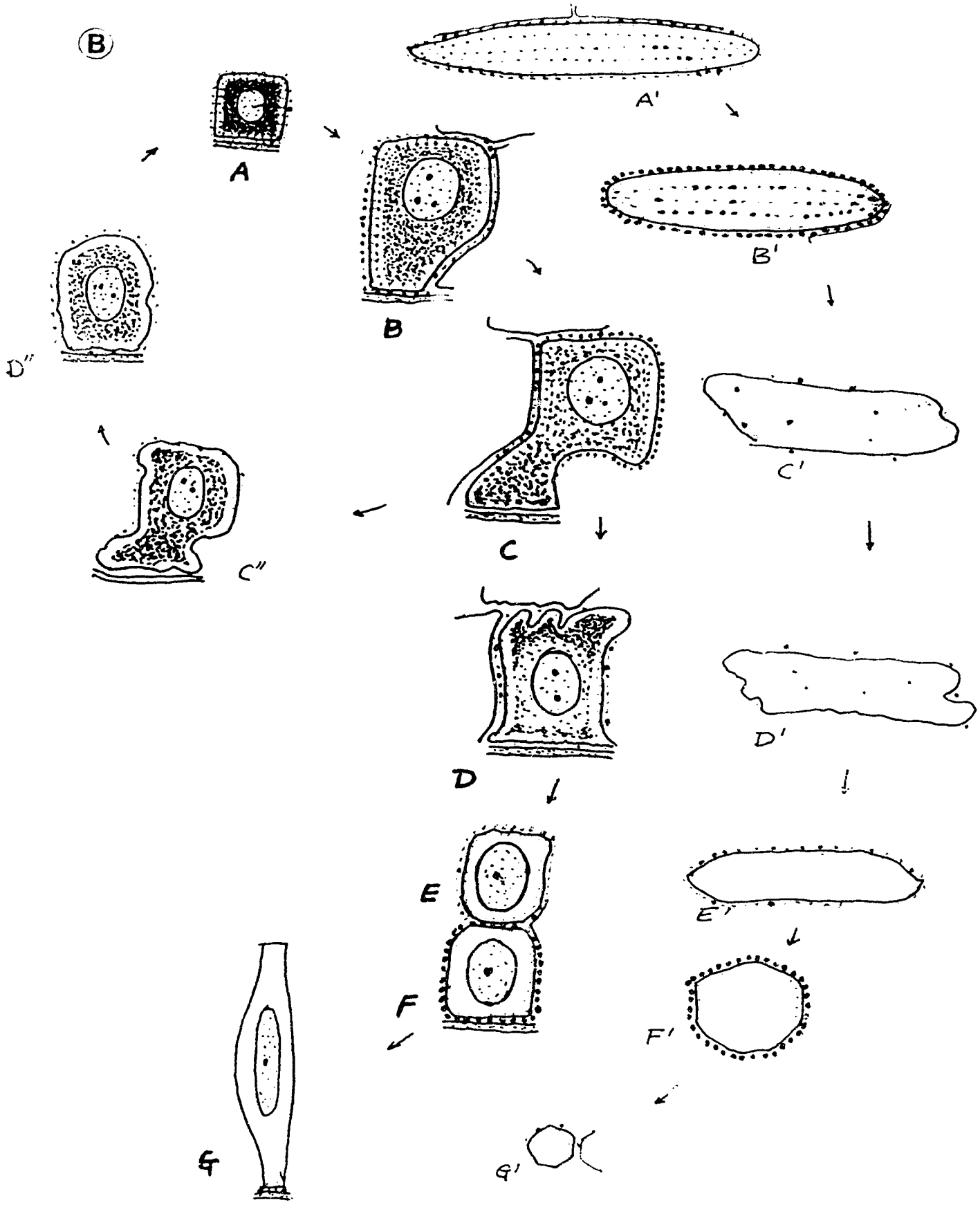
B
A
A'
B
B'
C
C'
C''
D''
D
D'
E
E'
F
F'
G
G'

dissociated cells. In between cells at the mid-lateral region of cells, few pigment granules have been observed.

As described above, the P-ring cells of both layers of the dorsal iris accomplish depigmentation to form a new lens during the processes of lens regeneration. But depigmentation also occurs in other cells of the iris epithelium, and these cells enter the retrieval pathway (Yamada 1977). According to my observations, the cells that reach the partially depigmented state during lens regeneration include the rest of the P-ring cells of both internal and external iris epithelium, the internal M- and J-ring cells. The cells in the external M- and J-ring iris appear not undergo depigmentation. Th.. is judged based on my observations in both sagittal sections and flat mounts of regenerates. In sagittal sections, the cytoplasmic projections with concentrated pigment granules are usually observed in the P-ring cells and the internal M- and J-ring cells, but not in the external M and J-ring cells. In the latter, their pigment granules remain uniformly packed in their cytoplasm during lens regeneration. In a flat mounted regenerate, nuclei of the cells of the internal iris epithelium become visible, these nuclei are obscured by pigment granules tightly packed in the cytoplasm of the cells of the normal iris. However, nuclei of external M- and J-ring cells have never been visualized in flat mounted regenerates even after removal of the stroma. It is possible that the latter group of cells is quiescent in regards to depigmentation during newt lens regeneration. The distribution of DAPI stained nuclei also suggests a possible wave of depigmentation activity that starts from the mid-dorsal iris and spreads to other regions of P-ring and internal M-and J-ring iris epithelium. This is reflected by my observations that nuclei of cells become visible first in the dorsal P-ring iris, then this activity spreads to the dorsal M-ring iris, to the entire P-ring, the entire M-ring and the J-ring iris respectively. In studies of tangential sections of iris, Eguchi and Shingai (1971) also noticed the autoradiographic labelling of DNA precursors in all areas of the

presumably internal iris epithelium with the number of labelled cells being much higher in the dorsal than in the ventral iris.

In addition, changes of actin cytoskeleton also suggest a change of cell shape from spindle to polygonal and a temporal pseudostratification (or stratification) of the lens vesicle cells at early stages (stages 4-6) of redifferentiation. I also noticed that the iris in the left eye is always at the more advanced stage of regeneration than the iris in the right eye of the same newt.

5. 2. PROPOSALS FOR FUTURE EXPERIMENTS

Further experiments need to be done to determine if the myoepithelial cell phenotype is consistently associated with cells that can undergo transdifferentiation in cell-type. These experiments can be done in several systems. In salamanders, there are 17 species that can undergo lens regeneration (Stone 1967). It would be helpful to study species that regenerate and don't regenerate using the same probes used in these present studies to determine if the myoepithelial phenotype is displayed by other cells that can regenerate a lens. Lens regeneration can also be induced in cultured and embryonic pigmented retina cells of the chick. In jellyfish the myoepithelial cells can undergo transdifferentiation, while the epithelial cells can not (Schmid et al.1982, Schmid and Alder 1984, Alder and Schmid 1987). It would be very interesting to see whether or not the chick glial cells and jellyfish myoepithelial cells that transdifferentiate also express myoepithelial markers or if the myoepithelial markers are expressed temporally in these cells.

In addition, to characterize myoepithelial cells, some other markers, such as α–smooth muscle myosin, can also be used.

5. 3. LITERATURE CITED

Alder H, Schmid V. 1987. Cell cycles and *in vitro* transdifferentiation and regeneration of isolated, striated muscle of jellyfish. Dev. Biol. 124:358-369.

Cooper J A. 1987. Effects of cytochalasin and phalloidin on actin. J. Cell Biol. 105:1473-1478.

Dumont J N, Yamada T. 1972. Dedifferentiation of iris epithelial cells. Biol. 29:385-401.

Eguchi G, Shingai R. 1971. Cellular analysis on localization of lens forming potency in the newt iris epithelium. Devel. Grow. Differ. 13:337-349.

Green K J, Geiger B, Jones J C R, Talian J C. 1987. The relationship between intermediate filaments and microfilaments before and during the formation of desmosomes and adherens-type junctions in mouse epidermal keratinocytes. J. Cell Biol. 104:1389-1402.

Hornsby S, Zalik S E. 1977. Redifferentiation, cellular elongation and the cell surface during lens regeneration. J. Embryol. Exp. Morph. 39:23-43.

Reyer R W. 1990. Macrophage invasion and phagocytic activity during lens regeneration form the iris epithelium in newts. Am. J. Anat. 188:239-344.

Schmid V, Wydler M, Alder H. 1982. Transdifferentiation and regeneration *in vitro*. Dev. Biol. 92:476-488.

Schmid V, Alder H. 1984. Isolated, mononucleated, striated muscle can undergo pluripotent transdifferentiation and form a complex regenerate. Cell. 38:801-809.

Stone L S. 1967. An investigation recording all salamanders which can and cannot regenerate a lens from the dorsal iris. J. Exp. Zool. 164: 87-104.